Copyright Warning & Restrictions

The copyright law of the United States (Title 17, United States Code) governs the making of photocopies or other reproductions of copyrighted material.

Under certain conditions specified in the law, libraries and archives are authorized to furnish a photocopy or other reproduction. One of these specified conditions is that the photocopy or reproduction is not to be "used for any purpose other than private study, scholarship, or research." If a, user makes a request for, or later uses, a photocopy or reproduction for purposes in excess of "fair use" that user may be liable for copyright infringement,

This institution reserves the right to refuse to accept a copying order if, in its judgment, fulfillment of the order would involve violation of copyright law.

Please Note: The author retains the copyright while the New Jersey Institute of Technology reserves the right to distribute this thesis or dissertation

Printing note: If you do not wish to print this page, then select "Pages from: first page # to: last page #" on the print dialog screen

INFORMATION TO USERS

This reproduction was made from a copy of a document sent to us for microfilming. While the most advanced technology has been used to photograph and reproduce this document, the quality of the reproduction is heavily dependent upon the quality of the material submitted.

The following explanation of techniques is provided to help clarify markings or notations which may appear on this reproduction.

1. The sign or "target" for pages apparently lacking from the document photographed is "Missing Page(s)". If it was possible to obtain the missing page(s) or section, they are spliced into the film along with adjacent pages. This may have necessitated cutting through an image and duplicating adjacent pages to assure complete continuity.

2. When an image on the film is obliterated with a round black mark, it is an indication of either blurred copy because of movement during exposure, duplicate copy, or copyrighted materials that should not have been filmed. For blurred pages, a good image of the page can be found in the adjacent frame. If copyrighted materials were deleted, a target note will appear listing the pages in the adjacent frame.

3. When a map, drawing or chart, etc., is part of the material being photographed, a definite method of "sectioning" the material has been followed. It is customary to begin filming at the upper left hand corner of a large sheet and to continue from left to right in equal sections with small overlaps. If necessary, sectioning is continued again—beginning below the first row and continuing on until complete.

4. For illustrations that cannot be satisfactorily reproduced by xerographic means, photographic prints can be purchased at additional cost and inserted into your xerographic copy. These prints are available upon request from the Dissertations Customer Services Department.

5. Some pages in any document may have indistinct print. In all cases the best available copy has been filmed.

University Microfilms International
300 N. Zeeb Road
Ann Arbor, MI 48106

Cunningham, Peter Edward

BROADBAND BASE ISOLATED ASYMMETRICALLY FED VHF ANTENNA

New Jersey Institute of Technology D.ENG.SC. 1983

BROADBAND BASE ISOLATED ASYMMETRICALLY FED VHF ANTENNA

by

PETER EDWARD CUNNINGHAM

Dissertation submitted to the faculty of the Graduate School of the New Jersey Institute of Technology in partial fulfillment of the requirements for the degree of

Doctor of Engineering Science

APPROVAL

TITLE OF THESIS: BROADBAND BASE ISOLATED
ASYMMETRICALLY FED
VHF ANTENNA

NAME OF CANDIDATE: PETER EDWARD CUNNINGHAM
Doctor of Engineering Science, 1983

Thesis and
Abstract approved: _____ ,
DR GERALD WHITMAN DATE

ELECTRICAL ENGINEERING DEPARTMENT

SIGNATURE OF OTHER
MEMBERS OF THE
THESIS COMMITTEE

_____
DATE

_____
DATE

_____
DATE

_____
DATE

TABLE OF CONTENTS

ABSTRACT

TITLE OF THESIS: BROADBAND BASE ISOLATED
ASYMMETRICALLY FED
VHF ANTENNA

PETER EDWARD CUNNINGHAM
DOCTOR OF ENGINEERING SCIENCE, 1983

THESIS DIRECTED BY: DR. GERALD WHITMAN
ELECTRICAL ENGINEERING DEPARTMENT

Antennas presently being used for vehicular military VHF communications are narrowband. New generation frequency hopping radios, however, require broadband antennas. The antenna must be base isolated in order to reduce undesirable pattern nulls and impedance variations caused by currents induced on the support structure. Physical constraints limit the antenna length to three meters while operating from a frequency of 30 MHz to 88 MHz.

To satisfy the above requirements a model of a broadband, base isolated, cylindrical antenna less than three meters long was analyzed and built. Equations for the current distribution as a function of the physical parameters were formulated and solved. The antenna selected as most optimum, i.e., maximum gain on the horizon, was 2.5 meters in length and fed 1.0 meters above the mounting surface. The most optimum base isolation network consisted of a coaxial cable choke wound on a ferrite toroid. The cable choke was made resonant at 25 MHz with minimum distributed capacity.

The equalizer network for this antenna was located at the feed-point. Several network configuration were examined before selecting a two-pole T-network and autotransformer. The equalizer network reduced

the antenna VSWR to 7:1. A 2 dB attenuator is required to reduce this VSWR to an acceptable 3.5:1.

LIST OF FIGURES

CHAPTER 1

OVERVIEW

1.1 Statement of Problem

The military vehicular VHF antenna must have predictable performance and operating characteristics. This antenna is used on a large variety of military vehicles. The first VHF vehicular antennas were base fed whips [1]. Antenna characteristics were greatly influenced by vehicular size and shape since the antenna used the vehicle as a counterpoise. The antenna far field patterns and input impedance varied greatly from one vehicle type to another. Pattern nulls were common [2]. The impedance variations affected communication range and transmitter life (via overheating). Base isolated antennas, introduced later, reduced much of the vehicular dependance. This type of antenna has been used successfully for many years.

Broadband antennas will be required in the future. The present military vehicular VHF communications antenna is a narrowband whip [3]. Communications are conducted on a single frequency basis. Total coverage of the 30 MHz to 76 MHz band is accomplished by dividing the band into 10 subbands and mechanically switching bands when changing frequency. The new generation of military radios will change operating frequency many times per second over a frequency range of 30 MHz to 88 MHz. A new antenna will be necessary for these radios. This antenna must be broadband.

Other requirements placed on the antenna by the military environment include the following. The physical antenna structure must be rugged enough to withstand abnormal abuse. The antenna must be capable of surviving collisions with trees and immovable objects. The antenna

must be unobtrusive, i.e., the antenna must be less than three meters high and less than three centimeters wide.

Previous experience and the physical constraints indicate a solution consisting of a broadband, base isolated whip antenna less than three meters in height. The physical structure is shown in Figure 1.1 and consists of the following parts. The base isolation choke is used to reduce the currents on the supporting structure or vehicle. It is a coaxial cable wound on a ferrite toroid. The coaxial cable continues to the feedpoint. A matching network is located at the feedpoint. The output of this network is connected to the upper antenna element. This thesis determines the optimum values for the antenna length, feedpoint height, base isolation choke and matching network. A patent for the antenna is currently being processed.

1.2 Previous Work

Much of the previous work on linear antennas has been directed toward the loading of monopole or dipole antennas to achieve large impedance bandwidth [4]. By impedance bandwidth we mean that the VSWR remains independent of frequency over a given bandwidth. A few authors have considered the effect of loading on the radiation pattern [24]. Asymmetrical antennas or antennas with ground systems have not been analyzed.

A method of analyzing cylindrical antennas with distributed impedance loading is presented by B. D. Popovic [5]. The loading is assumed to be an arbitrary but differentiable function of position along the antenna. In a continuing effort, Popovic [6] presented an analysis of a thin symmetrical cylindrical antenna with lumped impedance loadings

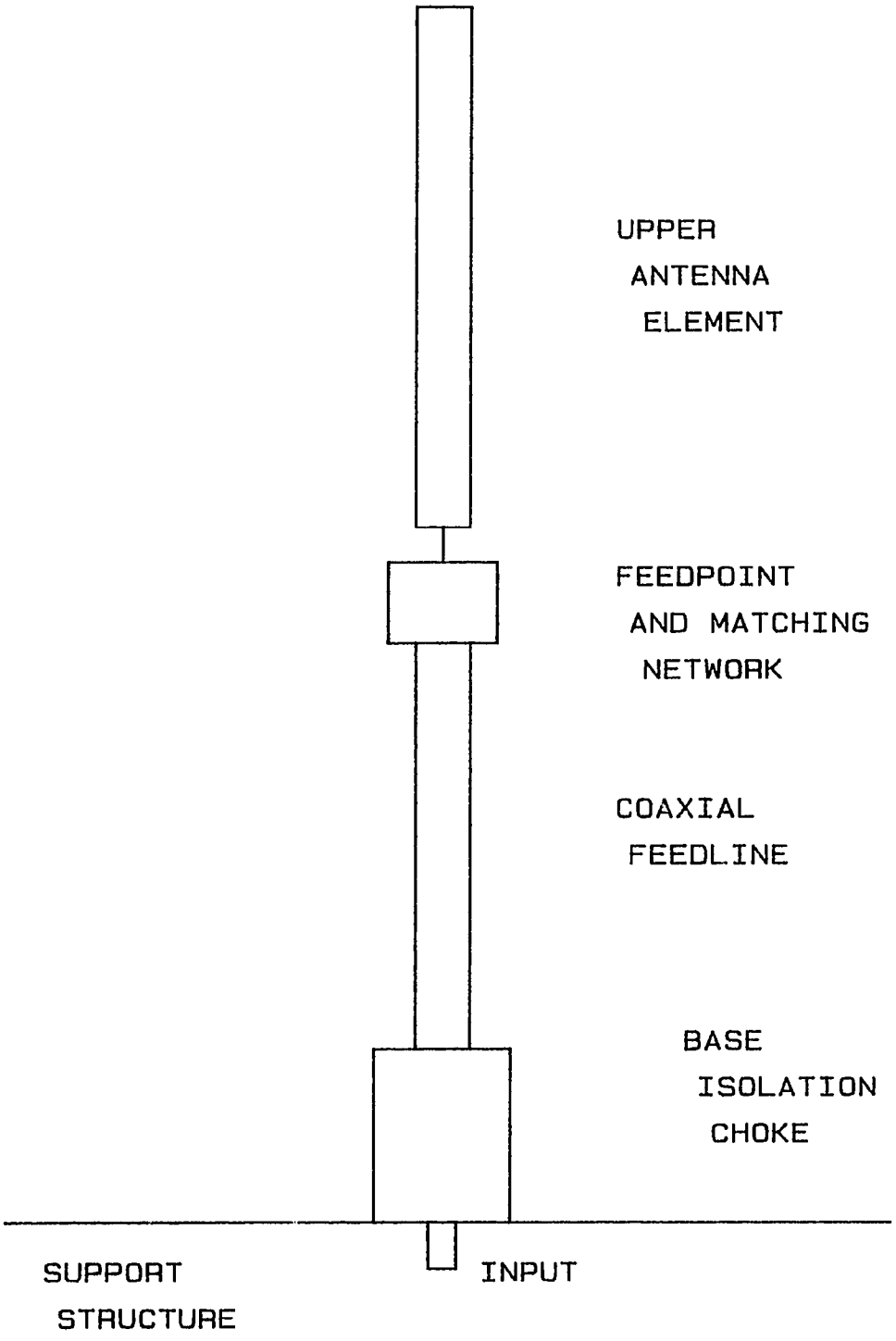

FIGURE 1.1 WHIP ANTENNA

along its length. The loading could be resistive, inductive, capacitive, or mixed.

The current distribution of a symmetrical cylindrical antenna with continuous resistive loading is analyzed by Wu and King [7]. A solution is obtained specifically when the current is represented by an outward traveling wave with no reflected wave.

Experiments by Rao and Ferris [8] show the electrical characteristics of a cylindrical antenna loaded with capacitive elements whose reactance increases exponentically with distance from the free end. Results indicate good impedance bandwidth and radiation patterns.

A cylindrical antenna with one and two lumped capacitive loadings is presented by Popovic [9]. The antenna structure is optimized for broadband admittance. Experiments are in good agreement with theory.

A method is presented by Paunovic [4] for the theoretical synthesis of an RC loaded broadband cylindrical antenna. The antenna synthesized and realized has minimum input susceptance and good radiation pattern in a 3:1 bandwidth.

Although the literature on linear antennas is extensive, asymmetrical antennas and antennas with ground systems have not been analyzed. This thesis develops the theory for a base isolated asymmetrically fed antenna and determines optimum parameters for a military vehicular whip antenna.

1.3 Method of Approach

A model of a broadband, base isolated, cylindrical antenna will be developed. The equations describing the electrical behavior of the model will be formulated. These equations will be solved for the current distribution on the antenna as a function of the physical

parameters. Once the current distribution is known all other important characteristics of the antenna can be calculated. The antenna impedance will be studied to determine the difficulty of matching. The field pattern will be studied with particular interest in the field strength on the horizon. Antenna gain on the horizon with respect to a quarter wave monopole will be plotted as a function of frequency. The antenna with the best over all gain on the horizon will be selected as the most optimum. The physical dimensions of this antenna will be used to build a model. Similar antennas will be built and experiments conducted to verify the theoretical results.

A broadband matching network will be designed for the most optimum antenna. Matching network synthesis is a multivariable nonlinear problem not solvable by ordinary methods. A best possible characteristic function for the matching network will be developed. Given the load impedance and network complexity desired a best possible tolerance of match will be determined.

CHAPTER 2

THEORY OF LINEAR ANTENNA

2.1 Introduction

The theory of the linear broadband base isolated asymmetrically fed antenna is presented in this chapter. A dipole above a ground plane is modeled by the antenna and its image. An equation is developed describing the current distribution on the antenna. This integral equation has no closed form solution. An approximate solution is obtained by a point matching method. The current is assumed to be a power series with unknown complex coefficients. The complex coefficients are determined by solving a number of linear equations derived from the integral equation at several points along the antenna. Once the complex coefficients are known, the current distribution, input impedance, and radiation pattern can be calculated. The theory closely follows that of Popovic [6].

2.2 Formal Solution

The linear base isolated antenna and its image are shown in Figure 2.1. The antenna is a perfectly conducting cylinder of radius a ($a/\lambda << 1$) and a length of h ($h >> a$). The antenna and its image are driven by generators of rms voltage V_g and angular frequency ω at positions $z = \pm z_g$. Assume the antenna to be loaded at points $z_1, z_2, \ldots, z_n$ with loads $Z_1, Z_2, \ldots, Z_n$. At the surface of the antenna the following equation must be satisfied.

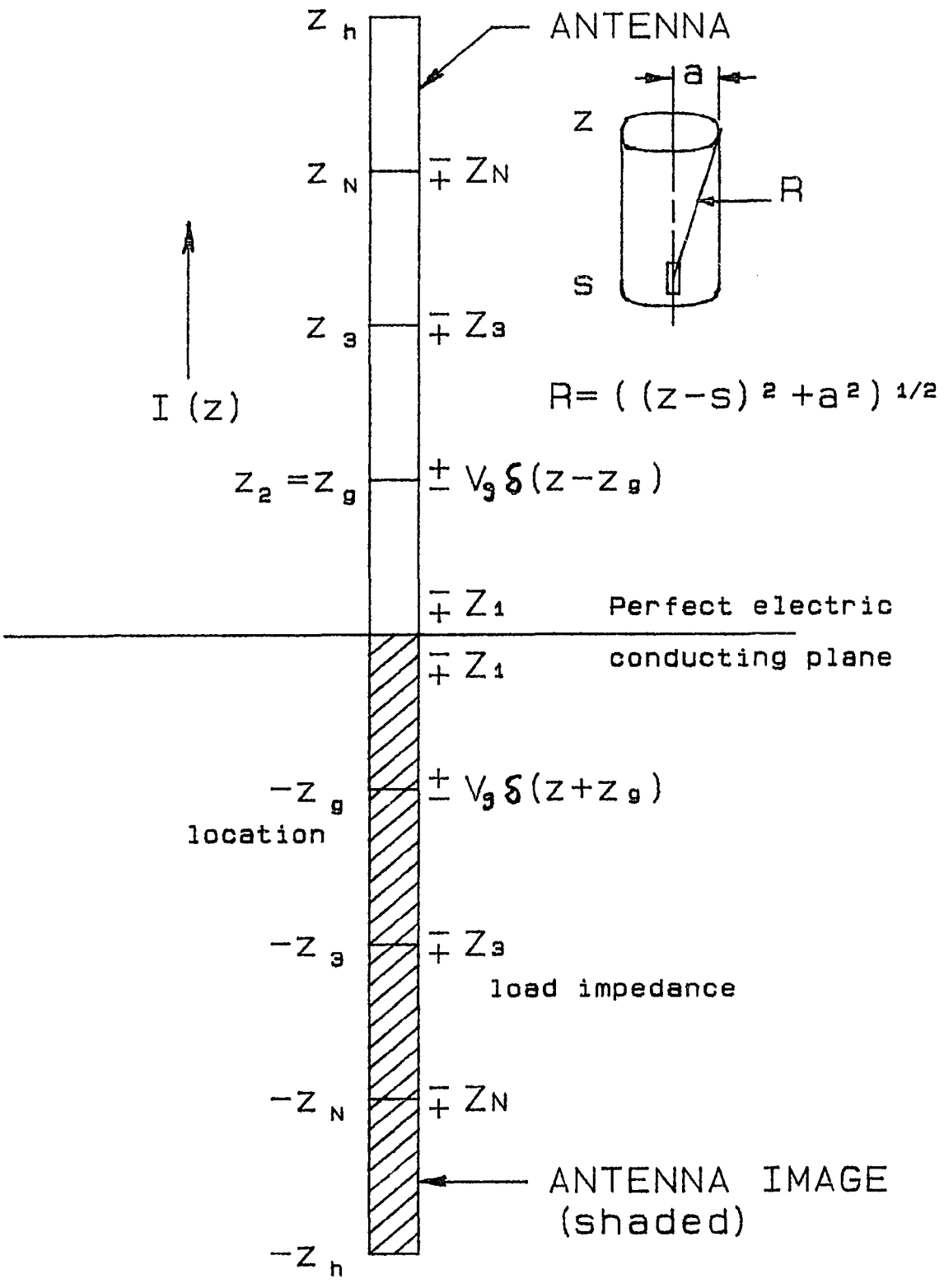

FIGURE 2.1 ANTENNA MODEL

$$E_z(z) = - V_g\{\delta(z-z_g) + \delta(z+z_g)\} + \sum_{i=1}^{N} Z_i I(z_i)\{\delta(z-z_i) + \delta(z+z_i)\}. \quad (1)$$

In this equation, $E_z(z)$ is the z-component of the electric field on the antenna surface, $\delta(z)$ is the Dirac delta function, and $I(z)$ is the current on the antenna. The electric field can also be expressed in terms of the magnetic vector potential as follows

$$E_z(z) = -j\omega(1 + \frac{1}{\beta^2}\frac{\partial^2}{\partial z^2})A_z(z) \quad (2)$$

where $\beta = \omega(\varepsilon_o\mu_o)^{1/2}$. (3)

In this equation, β is the free space propagation coefficient, ε_o is the permittivity and μ_o is the permeability of a vacuum. Substituting equation (2) into equation (1) gives

$$j\omega(1 + \frac{1}{\beta^2}\frac{\partial^2}{\partial z^2})A_z(z) = V_g\{\delta(z-z_g) + \delta(z+z_g)\} - \sum_{i=1}^{N} Z_i I(z_i)\{\delta(z-z_i) + \delta(z+z_i)\}. \quad (4)$$

Since the antenna model is symmetric, $I(z)=I(-z)$. Therefore, the magnetic vector potential $A_z(z)$ is symmetric, i.e.,

$$A_z(z) = A_z(-z) \quad (5)$$

The solution of equation (4) is broken up into the homogeneous and

particular solutions. The solution of the homogeneous equation has the following form

$$A_{zh}(z) = C\cos\beta z + D\sin\beta z. \tag{6}$$

In this equation C and D are unknown complex constants. Since $A_z(z)=A_z(-z)$ for all z, D must equal zero which leaves C as a complex constant to be determined. The particular solution of equation (4) is broken into N+1 parts. The left hand side of equation (4) is first set equal to the driving function $V_g\{\delta(z-z_g) + \delta(z+z_g)\}$ and a solution is determined. Similar solutions apply by superposition for the load functions $Z_iI(z_i)\delta(z-z_i)$ and $Z_iI(z_i)\delta(z+z_i)$. A partial particular solution is assumed for equation (4) of the following form for the driving function $V_g\{\delta(z-z_g) + \delta(z+z_g)\}$

$$A_{zp}(z) = D_p\{\sin\beta|z-z_g| + \sin\beta|z+z_g|\}. \tag{7}$$

The Lorentz condition states that the electric scalar potential is related to the magnetic vector potential by the following relationship

$$\phi(z) = \frac{j\omega}{\beta^2}\frac{\partial}{\partial z}A_z(z). \tag{8}$$

The partial derivative of the magnetic vector potential is:

for $z>z_g$

$$\frac{\partial}{\partial z}A_{zp}(z) = \beta D_p\{\cos\beta(z-z_g) + \cos\beta(z+z_g)\} \quad , \tag{9a}$$

for $-z_g < z < z_g$

$$\frac{\partial}{\partial z} A_{zp}(z) = \beta D_p\{-\cos\beta(z-z_g) + \cos\beta(z+z_g)\} \quad , \tag{9b}$$

and for $z < -z_g$

$$\frac{\partial}{\partial z} A_{zp}(z) = \beta D_p\{-\cos\beta(z-z_g) - \cos\beta(z+z_g)\} \quad . \tag{9c}$$

Combining equations (8) and (9) gives

for $z > z_g$

$$\phi(z) = (j\omega/\beta)D_p\{\cos\beta(z-z_g) + \cos\beta(z+z_g)\} \quad , \tag{10a}$$

for $-z_g < z < z_g$

$$\phi(z) = (j\omega/\beta)D_p\{-\cos\beta(z-z_g) + \cos\beta(z+z_g)\} \quad , \tag{10b}$$

and for $z < -z_g$

$$\phi(z) = (j\omega/\beta)D_p\{-\cos\beta(z-z_g) - \cos\beta(z+z_g)\} \quad . \tag{10c}$$

The difference in the electric scalar potential at $z=z_g$ across the generator is equal to V_g; hence,

for $z=+z_g$

$$\phi(z_g+\varepsilon) - \phi(z_g-\varepsilon) = V_g \quad , \tag{11}$$

and for $z=-z_g$

$$\phi(-z_g+\varepsilon) - \phi(-z_g-\varepsilon) = V_g \quad . \tag{12}$$

Using equation (10a) at $z=z_g+\varepsilon$ and equation (10b) at $z=z_g-\varepsilon$ to evaluate equation (11) gives the following result

$$(j\omega/\beta)D_p\{\cos\beta(z_g+\varepsilon-z_g) + \cos\beta(z_g+\varepsilon+z_g)\}$$

$$- (j\omega/\beta)D_p\{-\cos\beta(z_g-\varepsilon-z_g) + \cos\beta(z_g-\varepsilon+z_g)\} = V_g \qquad (13)$$

$$(j\omega/\beta)D_p\{\cos\beta\varepsilon + \cos\beta(2z_g+\varepsilon) + \cos\beta(-\varepsilon) - \cos\beta(2z_g-\varepsilon)\} = V_g. \qquad (14)$$

Now allowing ε to go to zero ($\varepsilon=0$) results in the following

$$D_p = \frac{\beta V_g}{2j\omega} \quad . \qquad (15)$$

The same result can be obtained by using equation (10b) at $z=-z_g+\varepsilon$ and equation (10c) at $z=-z_g-\varepsilon$ in equation (12). Substituting equation (15) back into equation (7) gives the following particular solution for equation (4)

$$A_{zp}(z) = \frac{\beta V_g}{2j\omega}\{\sin\beta|z-z_g| + \sin\beta|z+z_g|\}. \qquad (17)$$

The contributions of the load functions $Z_iI(z_i)\delta(z-z_i)$ and $Z_iI(z_i)\delta(z+z_i)$ can be considered in a similar manner. The particular solution of equation (4) resulting from the load functions is the following

$$A_{zp}(z) = \frac{\beta Z_i I(z_i)}{2j\omega}\{\sin\beta|z-z_i| + \sin\beta|z+z_i|\}. \tag{18}$$

By superposition the particular solution of equation (4) is the sum of the contributions of equations (17), and (18). Combining these solutions with the homogeneous solutions in equation (6) results in the following total solution to equation (4)

$$A_z(z) = C\cos\beta z + \frac{\beta V_g}{2j\omega}\{\sin\beta|z-z_g| + \sin\beta|z+z_g|\}$$

$$- \frac{\beta}{2j\omega}\sum_{i=1}^{N} Z_i I(z_i)\{\sin\beta|z-z_i| + \sin\beta|z+z_i|\}. \tag{19}$$

The magnetic vector potential can also be expressed in terms of the current on the antenna. For z-directed line sources the magnetic vector potential has the following form

$$A_z(z) = \frac{\mu_o}{4\pi}\int_{-h}^{h} \frac{I(s)e^{(-j\beta R)}}{R}\, ds \tag{20}$$

where $R = [(z-s)^2 + a^2]^{1/2}$ (see Figure 2.1). (21)

Combining equations (19) and (20) results in an equation for the current on the antenna

$$\int_{-h}^{h} \frac{I(s)e^{(-j\beta R)}}{R}\, ds = C_1\cos\beta z + \frac{2\pi V_g}{j\xi_o}\{\sin\beta|z-z_g| + \sin\beta|z+z_g|\}$$

$$- \frac{2\pi}{j\xi_o}\sum_{i=1}^{N} Z_i I(z_i)\{\sin\beta|z-z_i| + \sin\beta|z+z_i|\}. \tag{22}$$

where $C_1 = 4\pi C/\mu_o$, $\xi_o = (\mu_o/\varepsilon_o)^{1/2}$. This equation must be satisfied for any z and thus also for z=0. At z=0 equation (22) can be written in the following form

$$\int_{-h}^{h} \frac{I(s)e^{(-j\beta r)}}{r}\,ds = C_1$$

$$+ \frac{2\pi V_g}{j\xi_o}\{2\sin\beta|z_g|\} - \frac{2\pi}{j\xi_o}\sum_{i=1}^{N} 2Z_i I(z_i)\sin\beta|z_i| \qquad (24)$$

where $r = (s^2 + a^2)^{1/2}$. (25)

Expression (24) can be solved for the constant C_1, in the terms of the current

$$C_1 = \int_{-h}^{h} \frac{I(s)e^{(-j\beta r)}}{r}\,ds$$

$$- \frac{2\pi V_g}{j\xi_o}\{2\sin\beta|z_g|\} + \frac{2\pi}{j\xi_o}\sum_{i=1}^{N} 2Z_i I(z_i)\sin\beta|z_i|. \qquad (26)$$

Substituting the value of C_1, into equation (22) results in the following expression for the current on the antenna

$$\int_{-h}^{h} I(s)\{\frac{e^{(-j\beta R)}}{R} - \cos\beta z\frac{e^{(-j\beta R)}}{r}\}ds =$$

$$+ \frac{2\pi V_g}{j\xi_o}\{\sin\beta|z-z_g| + \sin\beta|z+z_g| - 2\cos\beta z\sin\beta|z_g|\}$$

$$- \frac{2\pi}{j\xi_o}\sum_{i=1}^{N} Z_i I(z_i)\{\sin\beta|z-z_i| + \sin\beta|z+z_i| - 2\cos\beta z\sin\beta|z_i|\} \qquad (27)$$

This equation can be written in the more concise form

$$\int_{-h}^{h} I(s)F(z,s)ds + \sum_{i=1}^{N} I(z_i)H(z,z_i) = G(z) \tag{28}$$

where

$$F(z,s) = \frac{e^{(-j\beta R)}}{R} - \cos\beta z \frac{e^{(-j\beta r)}}{r} \tag{29}$$

$$H(z,z_i) = \frac{j2\pi Z_i}{\xi_o}\{2\cos\beta z\sin\beta|z_i| - \sin\beta|z-z_i| - \sin\beta|z+z_i|\} \tag{30}$$

$$G(z) = \frac{j2\pi V_g}{\xi_o}\{2\cos\beta z\sin\beta|z_g| - \sin\beta|z-z_g| - \sin\beta|z+z_g|\}. \tag{31}$$

A closed form solution for equation (28) does not exist. However, an approximate solution can be obtained by a point matching method. In this method a power series expansion with unknown complex coefficients is chosen as an approximation to the current on the antenna. Equation (28) is then required to be satisfied at several points along the antenna. A system of complex linear equations results. These equations are solved for the complex coefficients of the power series expansion. A different power series expansion is required for each segment (i) of the antenna and is expressed in the following form

$$I(z) = \sum_{k=1}^{K} I_{i,k}\left|\frac{z}{z_{i+1}}\right|^{k-1} \tag{32}$$

where $z_i < z < z_{i+1}$, $i=1,2, \ldots, M$.

In equation (32) M is the number of antenna segments from the perfect electric conducting plane to the end of the antenna (see Figure 2.1), $I_{i,k}$ are the unknown complex coefficients, K-1 is the order

of the power series approximation, and z is the position on the ith segment. Substituting equation (32) into equation (28) gives the following result

$$\int_{-h}^{h} \sum_{k=1}^{K} I_{i,k} \left| \frac{s}{z_{i+1}} \right|^{k-1} F(z,s)ds +$$

$$\sum_{i=1}^{N} \sum_{k=1}^{K} I_{i,k} \left| \frac{z}{z_{i+1}} \right|^{k-1} H(z,z_i) = G(z). \qquad (33)$$

Recall from equation (1) that N is the number of loads on the antenna. The first term of equation (33) can be broken into two integrals for each segment. Equation (33) can then be expressed in the following form

$$\sum_{i=1}^{M} \left[\int_{z_i}^{z_{i+1}} - \int_{-z_i}^{-z_{i+1}} \right] \sum_{k=1}^{K} I_{i,k} \left| \frac{s}{z_{i+1}} \right|^{k-1} F(z,s)ds +$$

$$\sum_{i=1}^{N} \sum_{k=1}^{K} I_{i,k} \left| \frac{z}{z_{i+1}} \right|^{k-1} H(z,z_i) = G(z). \qquad (34)$$

Setting N=M, equation (34) can be written in the more compact form

$$\sum_{i=1}^{M} \sum_{k=1}^{K} I_{i,k} P(z,i,k) = G(z). \qquad (35)$$

Equation (35) is a linear complex matrix equation. It can be written at as many points z along the antenna as is necessary to solve explicitly for the unknown complex coefficients $I_{i,k}$. In equation (35) matrix elements P(z,i,k) can be expressed in the following form

$$P(z,i,k) = Q(z,i,k) + \left|\frac{z}{z_{i+1}}\right|^{k-1} H(z,z_i). \tag{36}$$

By replacing s by -s in the second integral of equation (34) the Q term of equation (36) can be expressed in the following form

$$Q(z,i,k) = \frac{1}{(z_{i+1})^{k-1}} \int_{z_i}^{z_{i+1}} s^{k-1}\{F(z,s) + F(z,-s)\}ds. \tag{37}$$

The current on the antenna must be continuous from one segment to another. This condition can be expressed in the following manner from equation (32) at $z=z_i$

$$\sum_{k=1}^{K} I_{i-1,k} = \sum_{k=1}^{K} I_{i,k}\left|\frac{z_i}{z_{i+1}}\right|^{k-1} \qquad i=2, \ldots, M. \tag{38}$$

At $z=\pm h$, the current must go to zero ($I(\pm h)=0$). In terms of equation (32), this condition can be expressed in the following manner

$$\sum_{k=1}^{K} I_{m,k} = 0 \tag{39}$$

The total number of complex coefficients $I_{i,k}$ to be determined is M x K. Equation (38) can be written M-1 times and equation (39) only once. This leaves M x K - M equations to be written using equation (35) in order to have sufficient information to solve for the complex coefficients $I_{i,k}$.

Equation (35) will be written and satisfied at the end of each segment except at z=0, which was used to find the constant C_1 (see equation (24)). A number of additional points within each segment may be selected depending on the degree of the polynomial approximation (K)

for the current. These points can be selected by the following relationship

$$z_p = z_i + \frac{(z_{i+1} - z_i)t}{k-1} \qquad \begin{matrix} t=1,2, \ldots, K-1 \\ i=1,2, \ldots, g, \ldots, M \end{matrix} \tag{40}$$

Thus equation (35) can be written (K-1) x M times in the following form

$$\sum_{i=1}^{M} \sum_{k=1}^{K} I_{i,k} P(z_p, i, k) = G(z_p). \tag{41}$$

Equations (38), (39), and (41) constitute a set of M x K linear complex equations in M x K unknowns $I_{i,k}$.

The integrals Q(z,i,k) cannot be evaluated in closed form, however, they can be integrated numerically. It will be noted that these integrals depend on frequency and geometry only, not on the loads Z_i.

When the coefficients $I_{i,k}$ are known, the current distribution on the antenna is given by equation (32). All other antenna parameters including the driving point admittance, field pattern, and gain can be calculated. The antenna driving point admittance can be expressed in the following form

$$Y = \frac{I(z_g)}{V_g} = \sum_{k=1}^{K} I_{g,k} \tag{42}$$

where V_g equals unity and the subscript g on $I_{g,k}$ is the segment number just below the generator (e.g., if $z_g = z_2$ then below the generator is segment 2 and above the generator is segment 3).

2.3 Field Pattern

The field pattern of the antenna is a function of the observation

point. The field pattern can be calculated from the magnetic vector potential as shown in equation (41)

$$A_z(r,\theta) = \frac{\mu_o}{4\pi}\int_{-h}^{h}\frac{I(s)e^{(-j\beta R)}}{R}\,ds \tag{43}$$

with R defined in equation (21). Recall that R is the distance form the source point on the antenna to the observation point. This distance may be approximated by

$$R \sim r - s\cos\theta \tag{44}$$

The denominator of equation (43) affects only the amplitude of A_z. In the far field R is very large compared to the antenna size ($R>>s>s\cos\theta$). Thus in the denominator R can be approximated by only r. In the term $(-j\beta R)$ more accuracy is necessary in computing the distance from the antenna to the observation point. Substituting equation (44) into equation (43) and approximating the integral by a summation results in the following equation

$$A_z(r,\theta) = \frac{\mu_o}{4\pi}\sum_{m=1}^{M}\frac{I(z_m)\Delta z}{r}e^{(-j\beta r+j\beta z_m\cos\theta)}$$

$$= \frac{\mu_o\Delta z e^{(-j\beta r)}}{4\pi r}\sum_{m=1}^{M}I(z_m)e^{(j\beta z_m\cos\theta)} \quad . \tag{45}$$

In equation (45), I can be expressed as magnitude and phase and $\exp(j\beta z_m\cos\theta)$ can be expanded in terms of sines and cosines.

$$A_z(r,\theta) = C\sum_{m=1}^{M}|I(z_m)|\{\cos(\theta_m+\beta z_m\cos\theta) + j\sin(\theta_m+\beta z_m\cos\theta)\} \tag{46}$$

where $C = \dfrac{\mu_o \Delta z e^{(-j\beta r)}}{4\pi r}$.

For z-directed sources the electric field vector potential can be expressed in the following manner

$$\underline{E}_\theta = j\omega \sin\theta A_z \underline{\theta} \quad . \tag{47}$$

Substituting equation (46) into equation (47) and including both the antenna and its image results in the following expression for the far electric field as a function of the angle θ

$$\underline{E}_\theta = \underline{C}_1 \sin\theta \sum_{m=1}^{M} |I(z_m)| \{\cos(\theta_m + \beta z_m \cos\theta) + \cos(\theta_m - \beta z_m \cos\theta) + j\sin(\theta_m + \beta z_m \cos\theta)\} + j\sin(\theta_m - \beta z_m \cos\theta)\} \tag{48}$$

where $\underline{C}_1 = \dfrac{j\omega\mu_o \Delta z e^{(-j\beta r)}}{4\pi r} \underline{\theta}$. (48a)

The magnitude of the electric field vector can be expressed in the following manner

$$|E_\theta| = |C_1 \sin\theta| \Big[\{ \sum_{m=1}^{M} |I(z_m)| \{\cos(\theta_m + \beta z_m \cos\theta) + \cos(\theta_m - \beta z_m \cos\theta)\}\}^2 + \{ \sum_{m=1}^{M} |I(z_m)| \{\sin(\theta_m + \beta z_m \cos\theta) + \sin(\theta_m - \beta z_m \cos\theta)\}\}^2 \Big]^{1/2} \quad . \tag{49}$$

The magnitude of the electric field vector potential on the horizon is determined by allowing θ to be 90 degrees. In this case, the magnitude

of the electric field vector can be expressed in the following manner

$$|E_\theta| = 2|C_1| \left[\{ \sum_{m=1}^{M} |I(z_m)|\cos\theta_m \}^2 + \{ \sum_{m=1}^{M} |I(z_m)|\sin\theta_m \}^2 \right]^{1/2}. \quad (50)$$

Equation (50) shows the field strength for an input of one volt (V_g=1). In order to determine the antenna with the greatest field strength on the horizon, the antennas must be compared relative to input power. The input power to the antenna is given by

$$P_{in} = V_g^2 G_a \quad (51)$$

where G_a is the antenna input conductance. This equation can be solved for V_g.

$$V_g = (P_{in}/G_a)^{1/2} \quad . \quad (52)$$

Equation (52) expresses the input voltage in terms of the input power. If the input power is set to one watt, equation (52) then represents a normalization factor. Then we can write

$$|E_\theta| = \frac{2|C_1|}{(G_a)^{1/2}} \left[\{ \sum_{m=1}^{M} |I(z_m)|\cos\theta_m \}^2 + \{ \sum_{m=1}^{M} |I(z_m)|\sin\theta_m \}^2 \right]^{1/2}. \quad (53)$$

Equation (53) shows the normalization factor multiplied by the previously calculated field strength of equation (50) in order to compare the antennas at equal input power.

CHAPTER 3

CALCULATED AND MEASURED RESULTS

3.1 Introduction

Several computer programs are used to calculate and plot antenna characteristics. These programs are presented and discussed in Appendix A. The results and conclusions based on these calculations are explained in this chapter. The calculated data includes antenna impedance, current distribution, field pattern, and gain on the horizon relative to a quarter wave monopole. These important antenna characteristics are the result of the antenna geometry. The physical parameters investigated are base isolation, feed point height, and antenna length. Figure 3.1 shows these physical properties of the antenna.

3.2 Base Isolation Choke

As a preliminary exercise the antenna feedpoint height and the antenna length were fixed. The resonant frequency and distributed capacity of the base isolation choke were varied. It was immediately apparent that the resonant frequency must be lower than the lowest operating frequency and that the distributed capacity be as low as possible. These results are shown in more detail in Appendix B.

3.3 Feedpoint Height and Antenna Length

The primary criteria for selecting the optimum antenna is gain on the horizon. It is this characteristic of the antenna that determines the effective range for a given communication system. Complete plots and discussions of gain on the horizon for various feedpoint heights and antenna lengths are included in Appendix C. Concise results are described below.

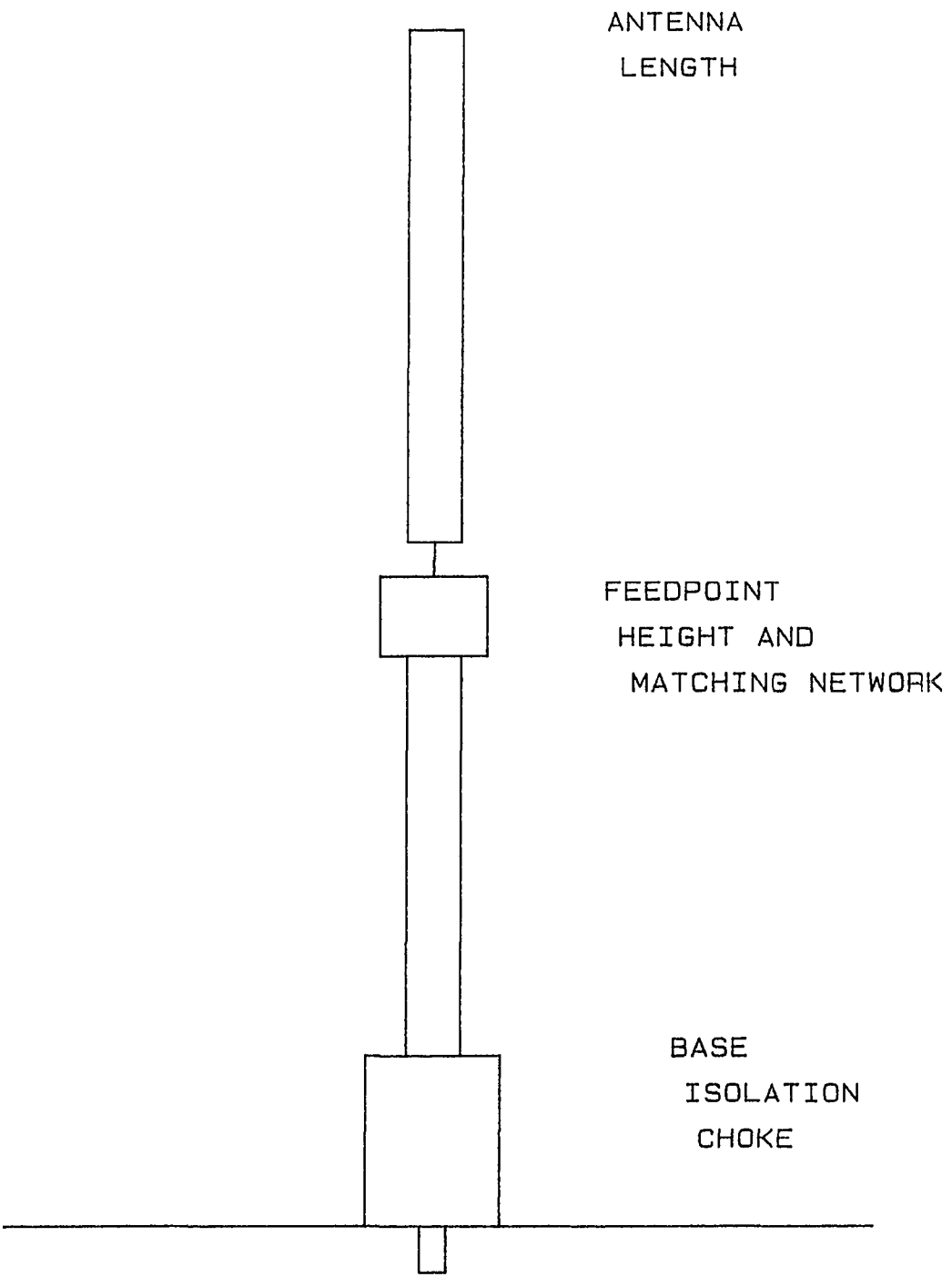

FIGURE 3.1 ANTENNA PARAMETERS

Appendix C shows the gain curves to be rather smooth functions of frequency. It is only necessary to examine the end points to determine the most optimum antenna configuration. Figure 3.2 shows the gain on the horizon at 30 MHz and 90 MHz. At 30 MHz, the most gain is obtained from the longest antenna (3.0 meters) regardless of feedpoint height. At 90 MHz the most gain from a 3.0 meter long antenna is obtained with the feedpoint located at 1.4 meters. This then is the most optimum antenna given the constraint that the antenna be no longer than 3.0 meters.

However, an additional constraint must be added at this point. An equalizer network must be added to the antenna to match the antenna to a 50 ohm transmitter at all operating frequencies without bandswitching. The equalizer network is discussed in Chapter 4. In order to be effective the matching network must be located at the feedpoint. Since the feedpoint is elevated, a lump will be necessary in the whip antenna to house the equalizer network. This lump will have two undiserable affects. First, it will increase the visibility of the antenna. Second, the lump will create a discontinuity in the physical construction of the antenna envelope, thus weakening it. For these two reasons, a feedpoint height no higher than 1 meter is desirable. The height of the antenna can now be optimized for a feedpoint height of one meter. Figure 3.2 shows that at 90 MHz the antenna with a feedpoint at one meter and the most gain on the horizon is 2.5 meters long.

The calculated current distribution, field patterns, and input impedance of this optimal antenna are shown in Figures 3.3, 3.4, and 3.5. Two antenna segments (M=2) and a three term expansion for the current (K=3) are used.

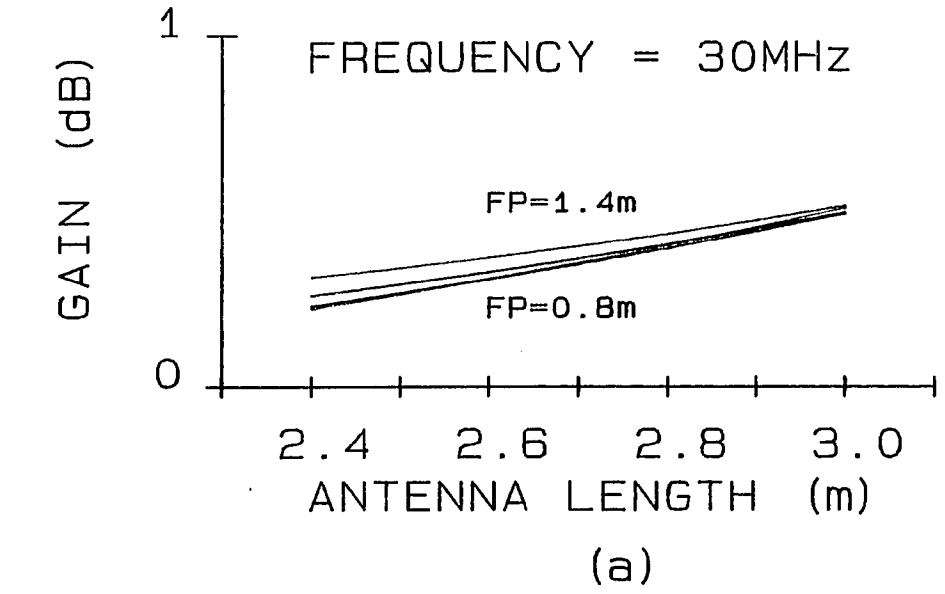

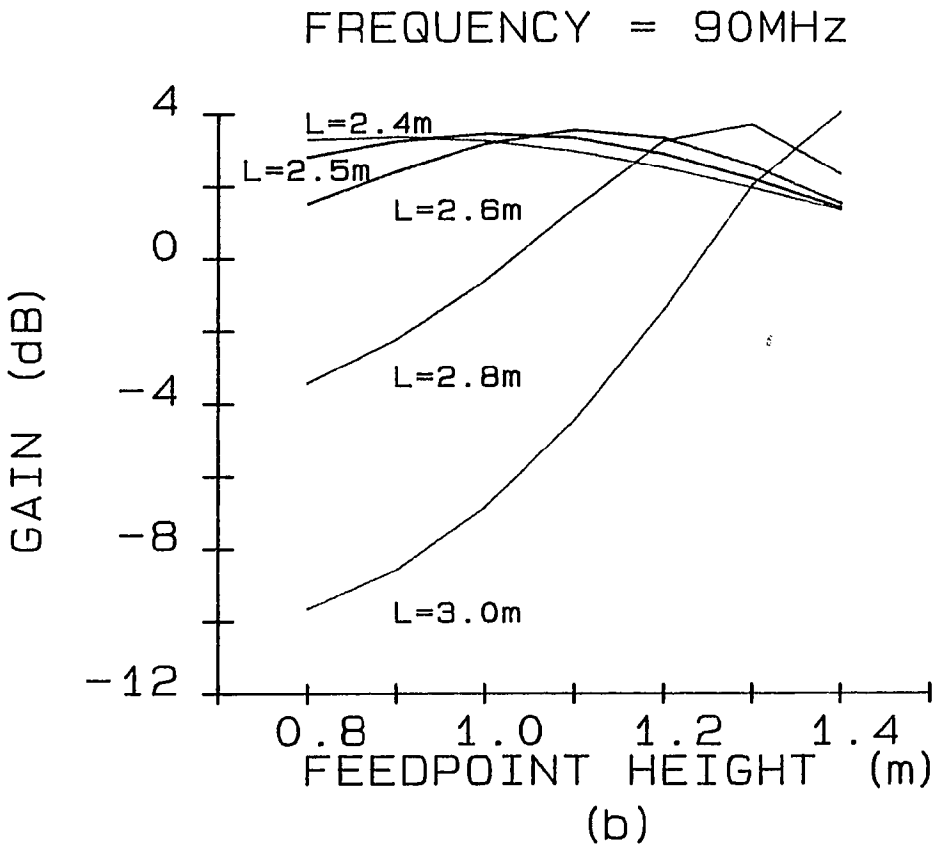

FIGURE 3.2 GAIN AT 30 MHZ AND 90 MHZ VERSUS FEEDPOINT HEIGHT AND ANTENNA LENGTH

The current distribution (Figure 3.3) shows that the base isolation choke has minimized the current at the base of the antenna at all frequencies. The phase of the current is reasonably constant over the entire length of the antenna at all frequencies. This is desirable to create good field patterns.

The field pattern (Figure 3.4) shows that there is no frequency where a major portion of the radiated energy is being transmitted into the sky. This is necessary to create the maximum field intensity on the horizon.

The input impedance (Figure 3.5) shows an antenna that will be difficult to broadband match. At 30 MHz, the antenna has very high capacitive reactance and very little resistance. At 50 MHz, the antenna has a reasonable resistance and little reactance. At 90 MHz, the antenna presents a high resistance. Matching of the antenna is discussed in Chapter 4.

3.4 Measured Results

Measurements were made of antenna gain, current distribution and impedance. These measurements are in good agreement with calculated values.

The measured current distribution of an antenna of length L=2.5 meters and feed point height FP= 1.0 meter is shown in Figure 3.6. Only the magnitude of the current is shown as measurements of phase are extremely difficult to make. The magnitudes of the calculated results are depicted in Figure 3.3. A comparison (Figures 3.3-3.5 calculated and Figures 3.6-3.8 measured) shows that the measurements are in good agreement with the calculations.

The relative gain of antennas of various heights are shown in

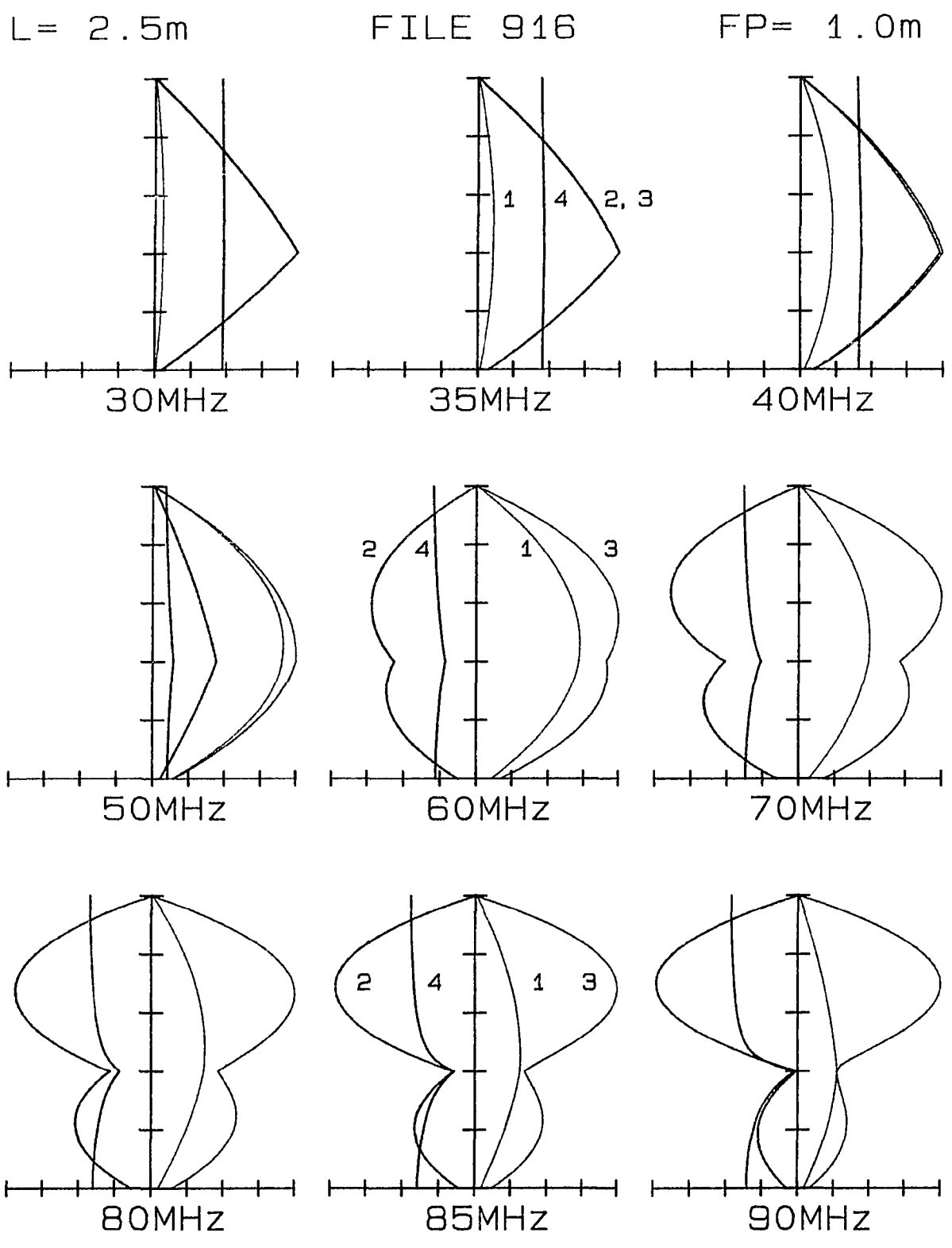

FIGURE 3.3 CALCULATED NORMALIZED CURRENT DISTIBUTIONS

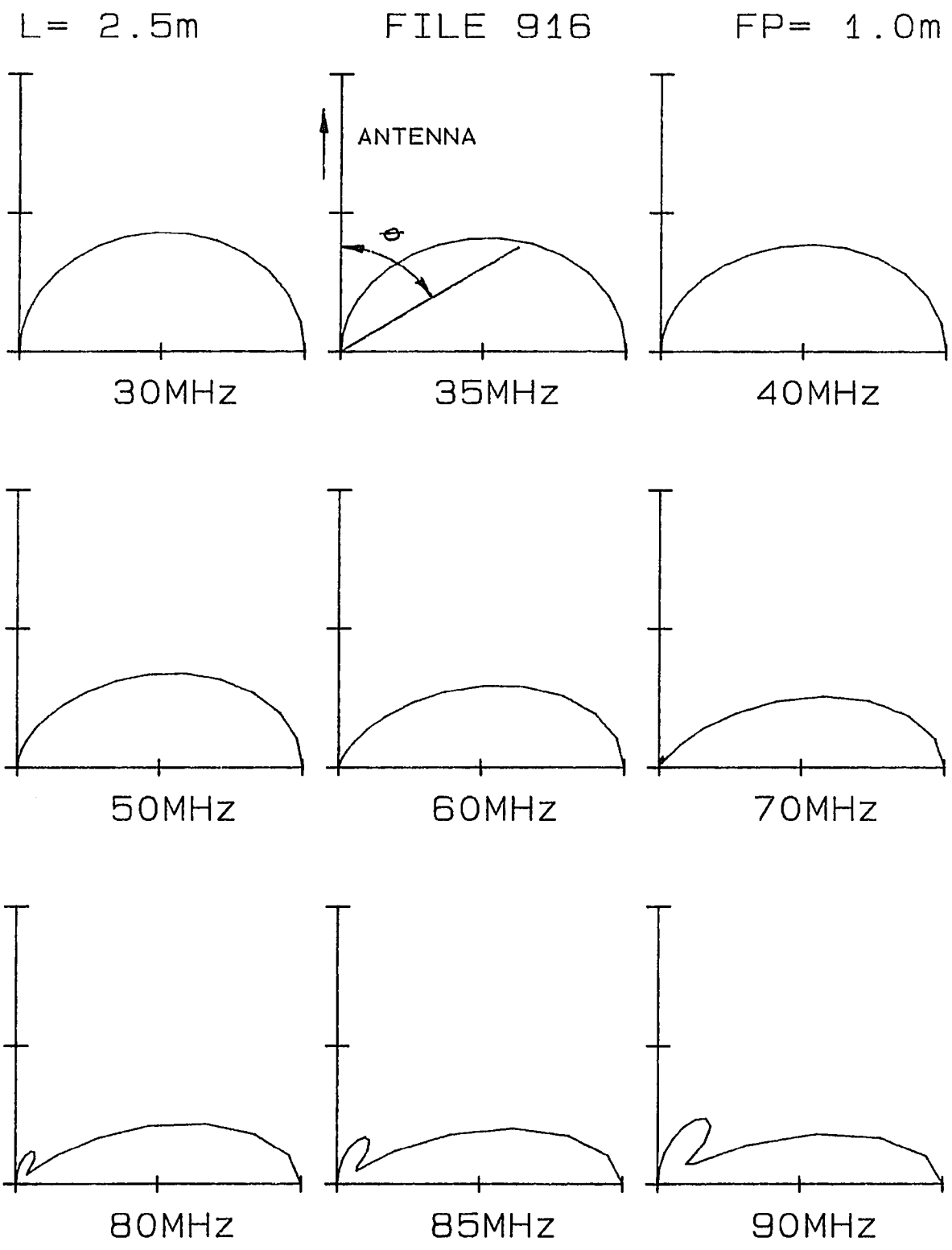

FIGURE 3.4 CALCULATED NORMALIZED FIELD PATTERNS

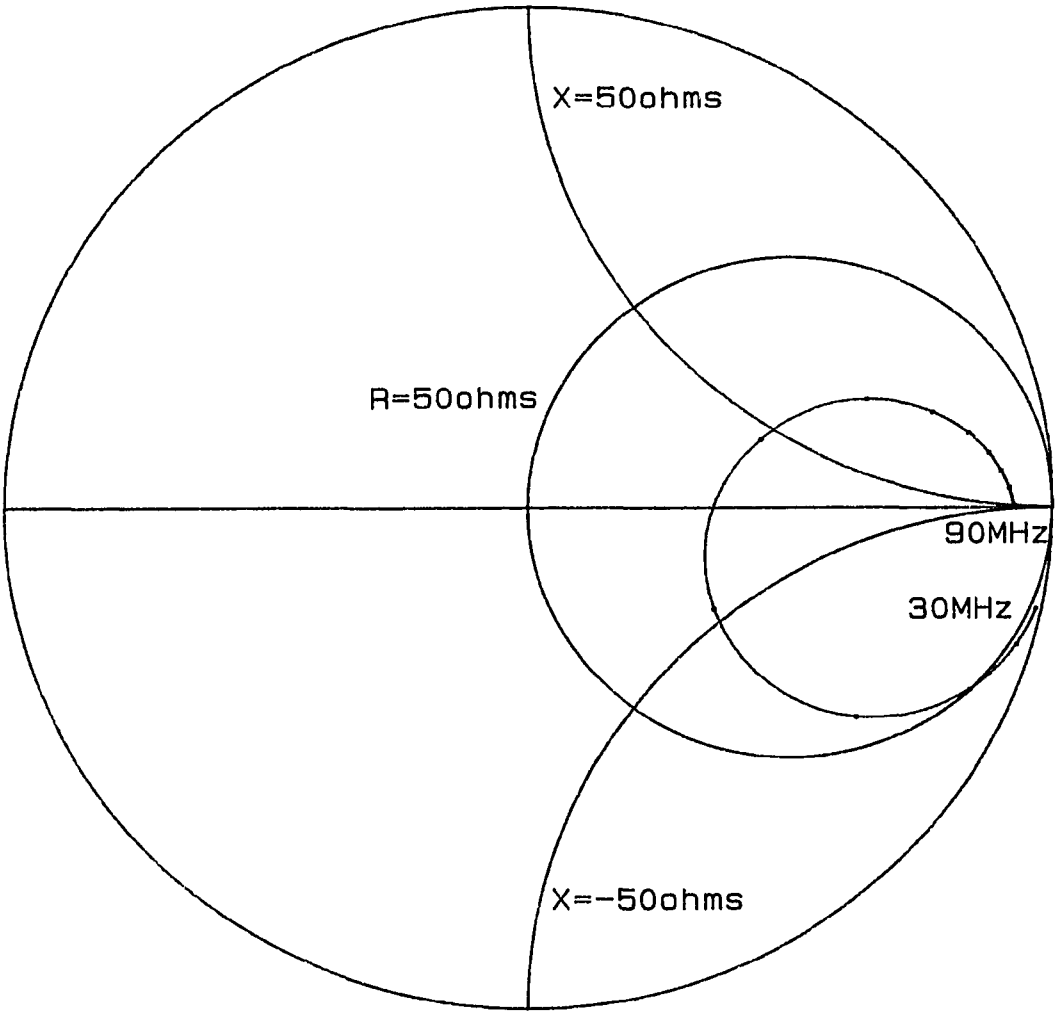

FREQUENCY STEPS OF 5MHz
FROM 30MHz TO 90MHz

FIGURE 3.5 CALCULATED IMPEDANCE NORMALIZED TO 50 OHMS

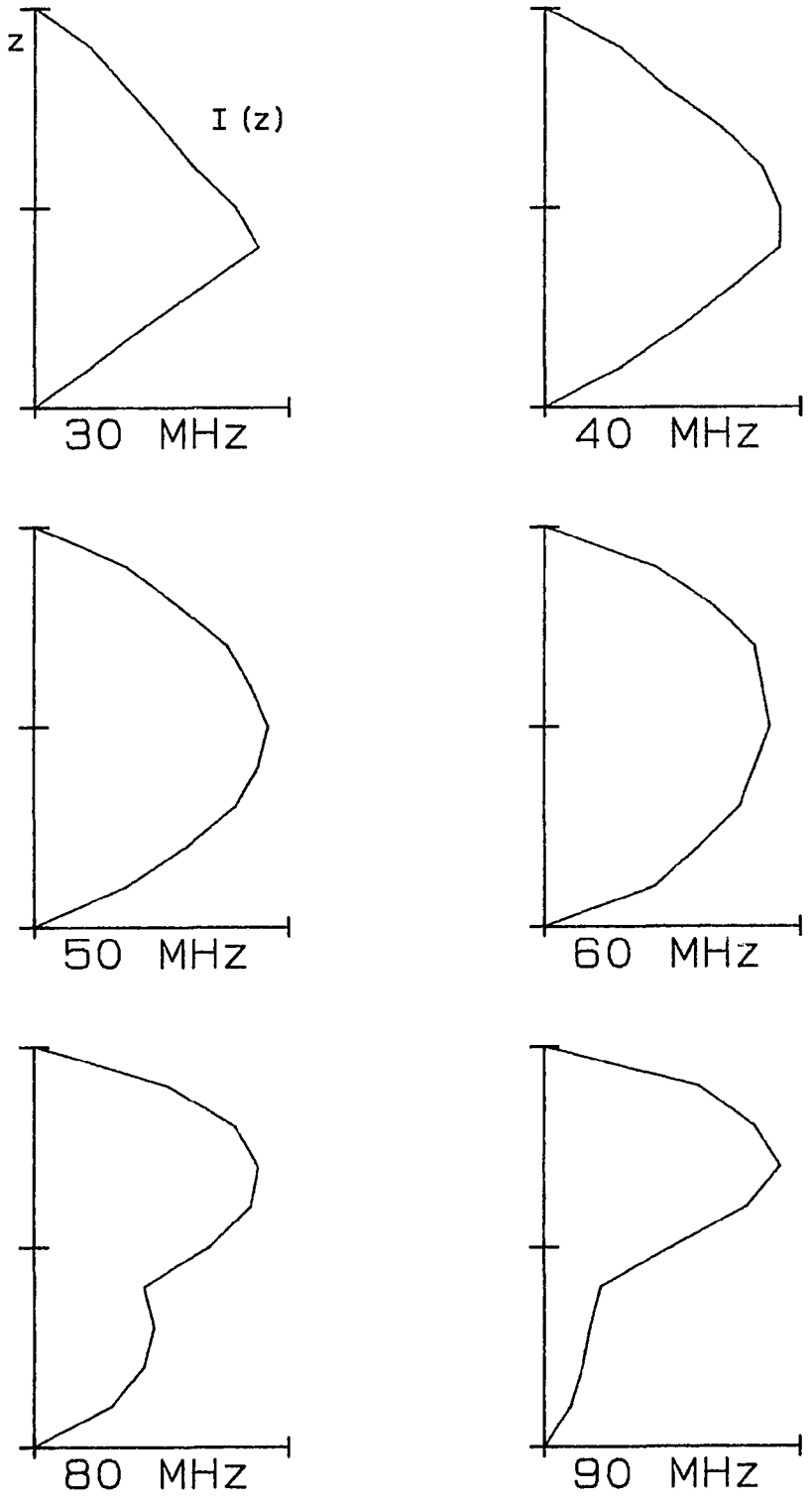

FIGURE 3.6 MEASURED CURRENT MAGNITUDE DISTRIBUTION

Figure 3.7. This plot is made at 90 MHz for an antenna with a feedpoint located at one meter. The plot indicates the best antenna is 2.5 meters in length.

The measured impedance of the antenna is plotted normalized to 50 ohms in Figure 3.8. The calculated impedance of Figure 3.5 is included for comparison.

The current distribution, impedance and gain measurements were made on a 10 feet by 10 feet copper ground sheet located 10 feet above the ground. The current distribution measurements of Figure 3.6 were made with a lab built and calibrated current probe. The impedance measurements of Figure 3.8 were made with a Hewlett Packard HP8505A Network Analyzer. The gain measurements of Figure 3.7 were made with a Hewlett Packard HP8568A Spectrum Analyzer. Account was made in the gain measurements for varying impedance levels while changing antenna lengths and feedpoint heights.

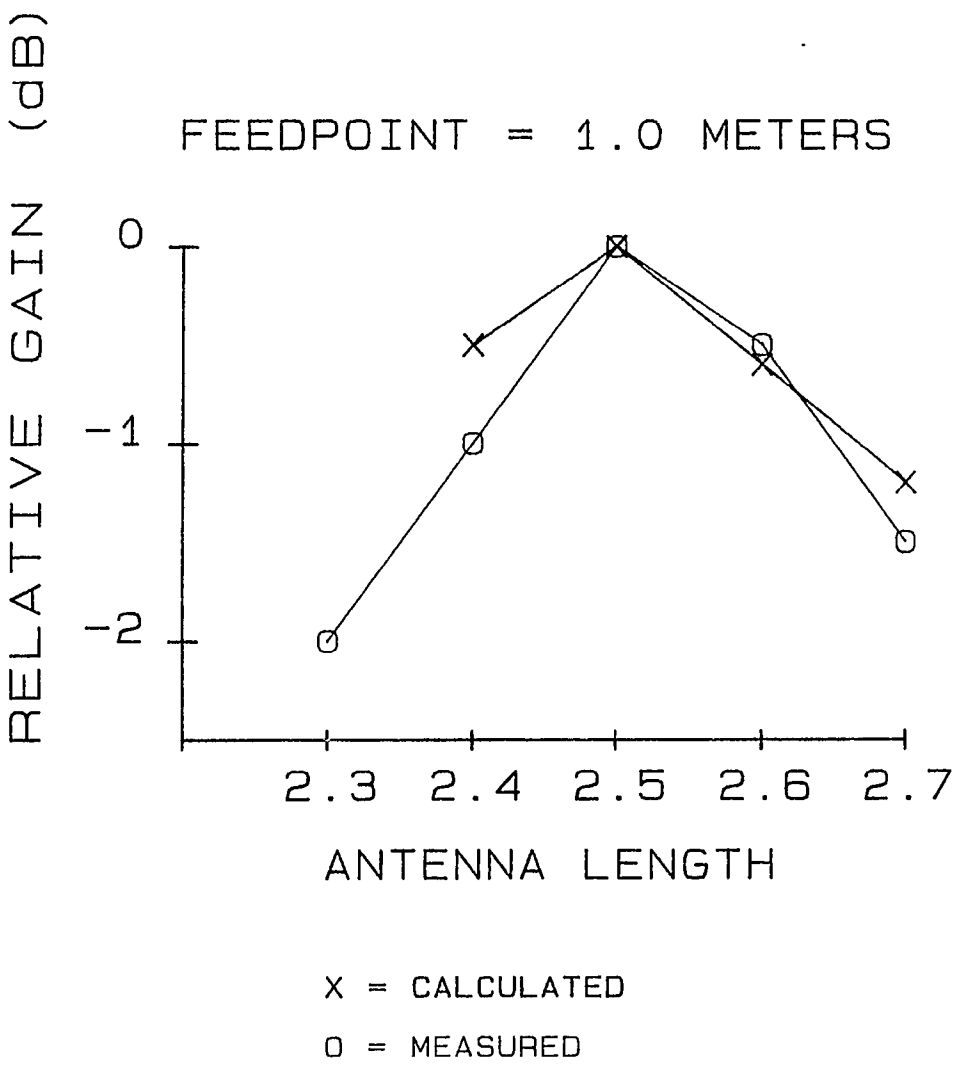

FIGURE 3.7 MEASURED AND CALCULATED GAIN AT 90 MHZ

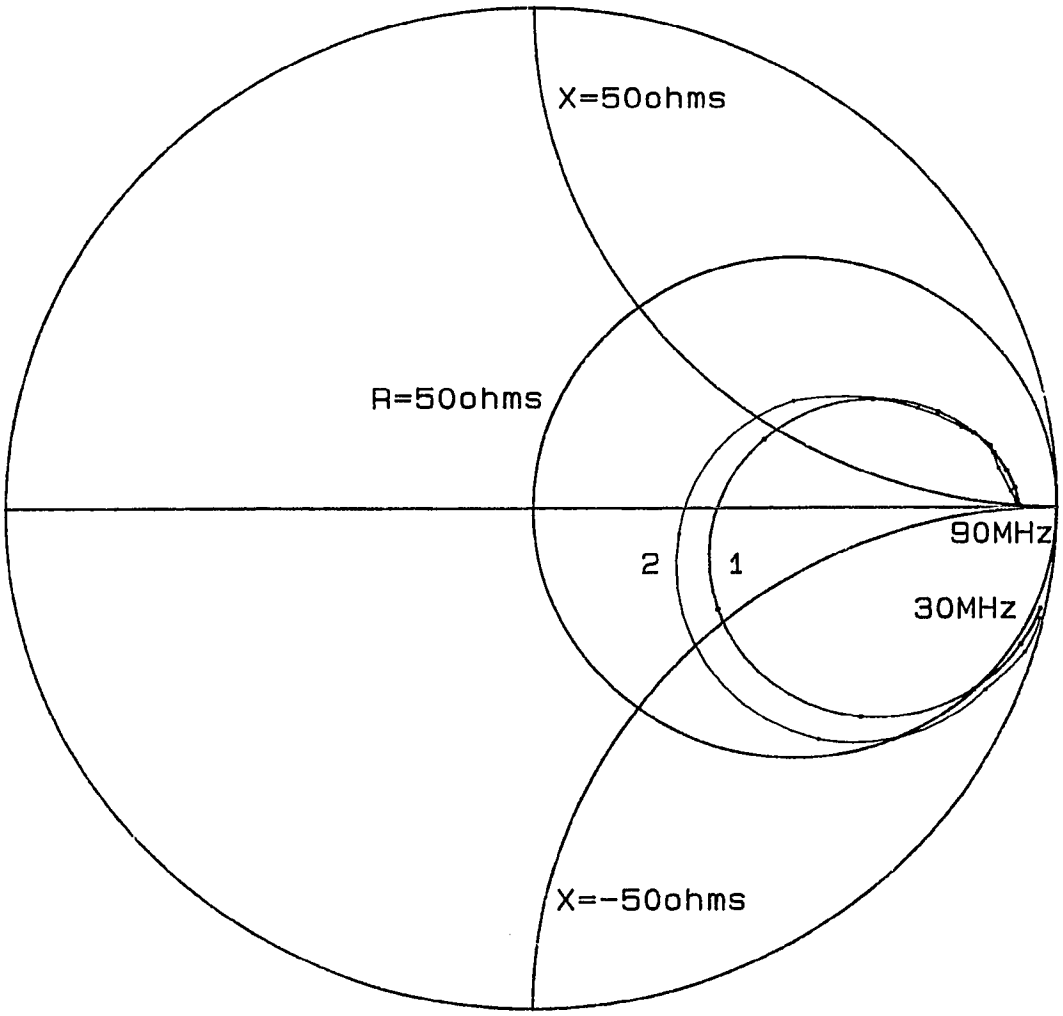

FREQUENCY STEPS OF 5MHz
FROM 30MHz TO 90MHz
CALCULATED (1) MEASURED (2)

FIGURE 3.8 MEASURED AND CALCULATED IMPEDANCE NORMALIZED TO 50 OHMS

CHAPTER 4

EQUALIZER NETWORK

4.1 Introduction

A matching network is required between the antenna and the generator. The purpose of this matching network is to reduce the VSWR of a given load. High VSWR values cause overheating of the transmitter by reflections from the load (antenna). A matching network is used to equalize and reduce these mismatch losses within a particular frequency band.

The gain of the antennas investigated in this thesis were all compared on the basis of equal input power. This would require a matching network to present the transmitter with equal VSWR values for each frequency. The most difficult load impedance to match occurs at 30 MHz. In Figure 4.1 we see that the longest antenna is the least difficult to match because the input resistance is the greatest while the input reactance is the smallest. The characteristic impedance of the generator and transmission lines are 50 ohms. Observe further that the longest antenna has the most gain. Hence the best choice antenna is the longest one. Fortuitously, therefore, an antenna gain and mismatch tradeoff does not have to be made. However, we are restricted to a feedpoint height of one meter.

It is sufficient to provide the best possible equalizer for the antenna with the best broadband gain. Since this antenna is to be used without band-switching networks on both transmit and receive, a passive linear equalizer network is required. This chapter will discuss network configurations and describe the rationale for the network selected. Appendix D describes a procedure for determining the best possible

IMPEDANCE at 30MHz

for FP=1.0m

LENGTH	RESISTANCE	REACTANCE
2.4m	23.7ohms	-508ohms
2.6m	28.3ohms	-455ohms
2.8m	33.7ohms	-408ohms
3.0m	40.0ohms	-365ohms

GAIN at 30MHz

for FP=1.0m

LENGTH	GAIN
2.4m	.230dB
2.6m	.307dB
2.8m	.395dB
3.0m	.494dB

FIGURE 4.1 IMPEDANCE AND GAIN DATA AT 30 MHZ

tolerance of match for a given input impedance.

4.2 Network Types

A physically realizable equalizer network must be limited to a reasonable number of components or independent variables. A network of many components will be extremely difficult to produce and align on a consistent basis. Also a large number of components usually increases the insertion loss of an equalizer.

Consider an equalizer configured as a ladder network as shown in Figure 4.2(a). A series branch ($Z_s=jX_s$, $X_s=X_1+X_c$) must consist only of a series LC component ($L_s<\infty$, $C_s>0$) because a parallel component would introduce an undesirable high reactance. Also note that if series branch was resonant out of band, the series branch would be more effective without one of the components (L_s or C_s). The parallel branch (Y_p) consists only of a parallel LC component ($L_p>0$, $C_p<\infty$) since a series components would cause an undesirable high reactance. An equalizer network of three branches is triple tuned. This network can be configured as a T or a pi network. The load impedance (i.e.,the antenna impedance) will determine which configuration provides the best match.

A transformer is a very useful equalizer component. An ideal transformer will allow the renormalization of impedances. The best match is not affected by where the ideal transformer is located. An autotransformer can sometimes produce a better overall match since it can be tailored to have frequency variations.

4.3 Network Selection

A pi type network was first investigated. The series and parallel

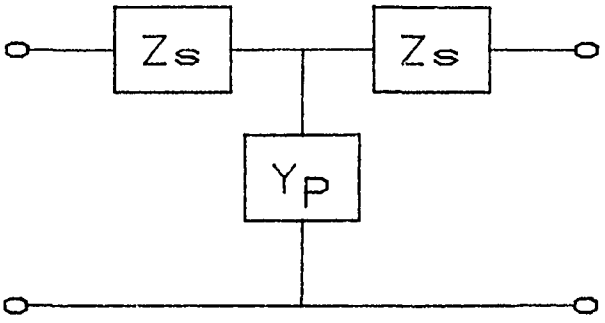

(a) LADDER NETWORK

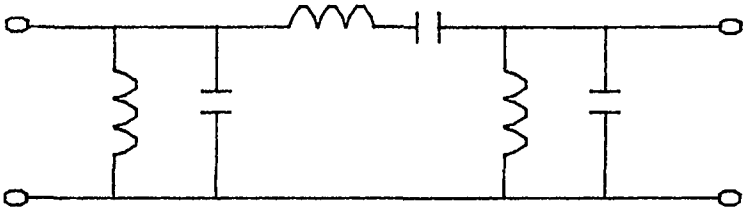

(b) PI NETWORK

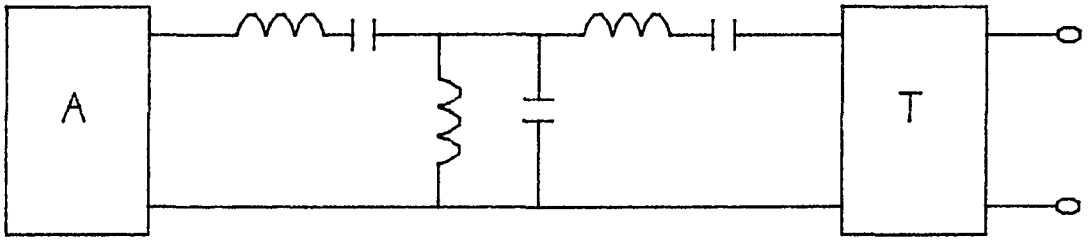

(c) T NETWORK AND TRANSFORMER

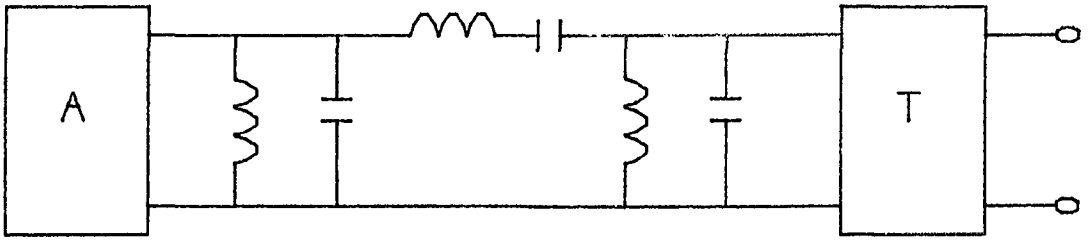

(d) PI NETWORK AND TRANSFORMER

FIGURE 4.2 NETWORK TYPES

branches each were assumed to contain an inductance and a capacitance as shown in Figure 4.2(d). An ideal transformer was also included. In the frequency range from 30 MHz to 90 MHz, reasonable values of inductance are .05 to 2 microhenries. Reasonable values of capacitance are 5 to 200 picofarads. A computer program (see Appendix A.9) was written to step through these values at 50 percent increments (i.e.,C=5,10,20,50,100,200 picofarads). Also included in these increments were 0 and 10^{30} where appropriate to effectively remove the contribution of each component in the network. The transformation ratio was varied from 1:1 to 7:1. For the input impedance associated with an antenna of length L=2.5 meters and feedpoint height FP=1.0 meter, the best VSWR found at the input of the network configuration as shown in Figure 4.2(d) was 18.6:1.

The same procedure was repeated for a T network shown in Figure 4.2(c) (see Appendix A.10). In this configuration, the best network did not contain a capacitor in the branch nearest the antenna. For the input impedance associated with an antenna of length L=2.5 meters and a feedpoint height of FP=1.0 meter the best VSWR found at the input of the network configuration as shown in Figure 4.2(c) was 14.3:1.

The equalizer was then configured as a T network as above but with an autotransformer used instead of an ideal transformer as shown in Figure 4.3. A computer program (see Appendix A.11) was written to step through component values and coupling coefficients first with large steps and then with smaller increments. The final network is shown in Figure 4.3.

The network of Figure 4.3 reduced the maximum VSWR of the antenna to approximately 7:1 (see Figure 4.4(a)). This value was still too

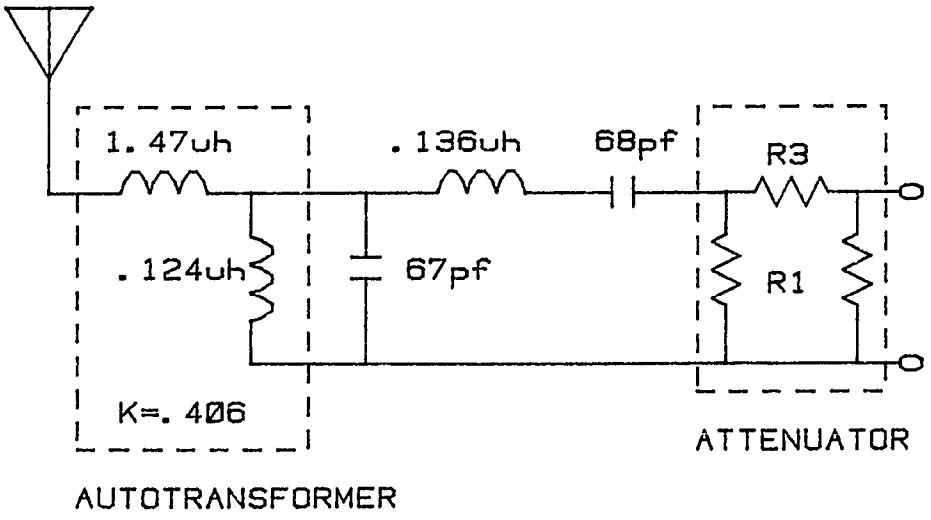

R1= 436ohms R3=11.6ohms

K= coupling coefficient

FIGURE 4.3 FINAL EQUALIZER NETWORK

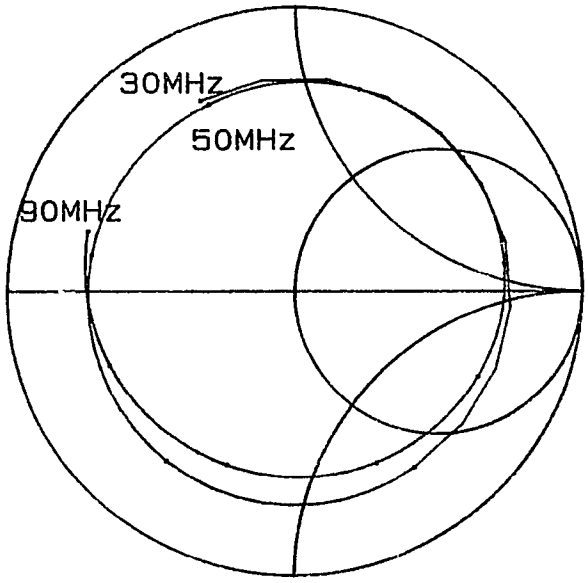

(a) ANTENNA AND NETWORK

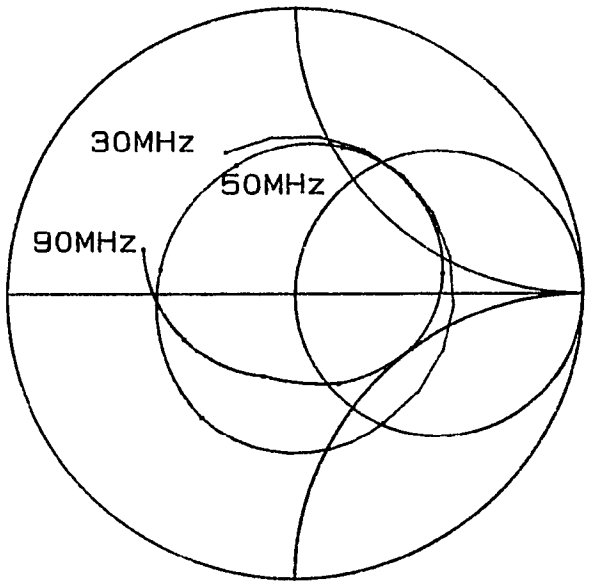

(b) ANTENNA, NETWORK & ATTENUATOR

FIGURE 4.4 IMPEDANCE OF ANTENNA AND EQUALIZER NETWORK

high. An attenuator was used at the base of the antenna to further reduce the VSWR to 3.5:1. The impedance of the antenna after the equalizer network and after the attenuator is shown in Figure 4.4(b). The value of the attenuator is obtained by calculating the mismatch loss for a given VSWR

$$\text{loss} = 10\log\{1 - (\frac{\text{VSWR}-1}{\text{VSWR}+1})^2\}\text{db}$$

-1.6dB for VSWR=3.5
-3.6dB for VSWR=7

The difference of these two values of loss is 2dB. From [36] the values of the resistors making up the attenuator are required to be R = 436 ohms and R = 11.6 ohms.

APPENDIX A

COMPUTER PROGRAMS

A.1 Introduction

Seven computer programs are used to determine the optimum broadband base isolated asymmetrically fed VHF antenna. The programs were written in HPL to run on a HP9825 calculator. The computer system configuration is shown in Figure A.1. These programs are included in their entirety at the end of this appendix. Each of these programs will be explained in moderate detail in the following paragraphs.

A.2 Main Program - CALCUR

The main program is used to calculate the current distribution on the antenna. Lines 2 and 3 are dimension statements defining arrays. Line 4 establishes the angular notation as radians and the antenna radius A. Lines 5 and 6 vary the feedpoint height and antenna length. Line 7 denotes the points (equation 40) at which a solution to equation (35) will be required. Line 8 varies the frequency of study. Line 10 calls a subroutine to calculate the matrix Q of equation (37). Lines 12 and 13 calculate the reactance of the base isolation choke with a resonant frequency of 25 MHz and a distributed capacity of 2pf. Lines 16, 17, and 18 calculate the load function of equation (30) and the driving function of equation (31).

Matrices A and C are the real and imaginary solution matrices respectively. They both have the following construction. Each row is an equation to be satisfied. Columns 1, 2 and 3 correspond to $I_{1,1}$, $I_{1,2}$, $I_{1,3}$. Columns 4, 5, and 6 correspond to $I_{2,1}$, $I_{2,2}$, $I_{2,3}$. Column 7 corresponds to the driving function. Row 1 corresponds to equation (39). Rows 4 through 6 correspond to equation (35).

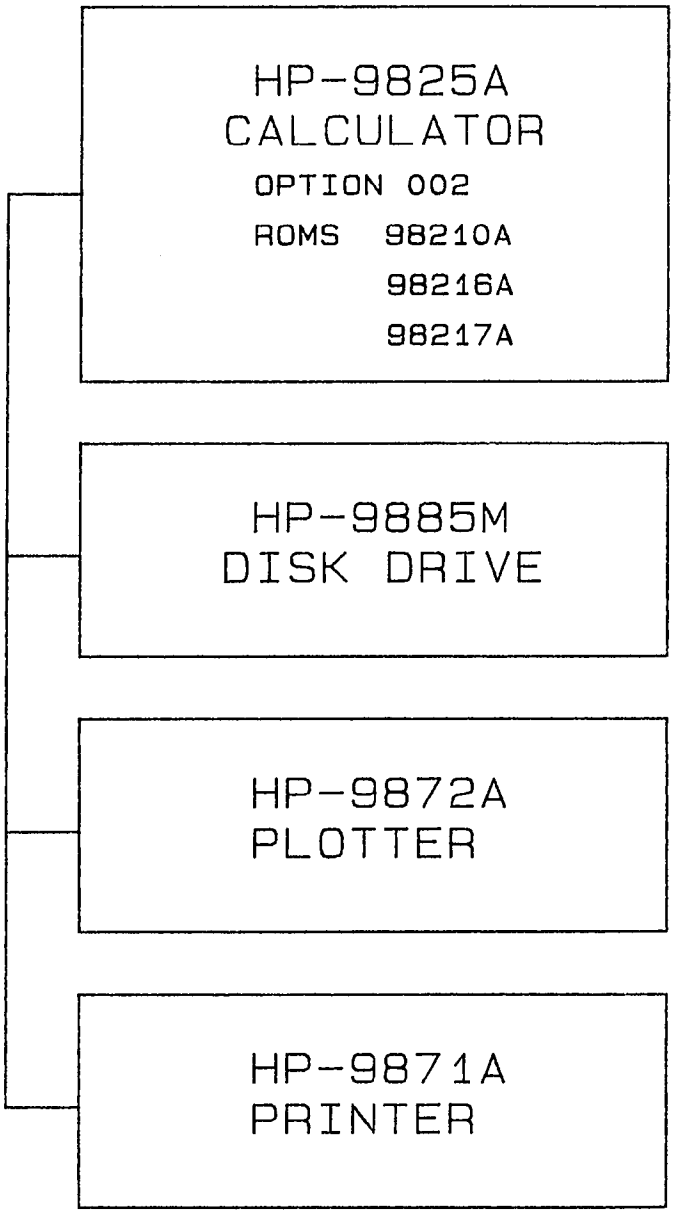

FIGURE A.1 COMPUTER SYSTEM CONFIGURATION

Lines 20 thru 31 load the solution matrices A and C to form equation (36). Line 20 includes the load function at H(P,1) only since the coefficient of H in equation (36) is zero for K=2 and 3. Lines 21 through 25 load matrices A and C at locations 3,1 through 6,3. Lines 26 through 28 load matrices A and C at locations 3,4 through 6,6. Lines 29 and 30 load matrices A and C at locations 1,1 through 2,7. Line 31 loads the driving function in matrices A and C at locations 4,7 through 6,7.

The solution matrices are now passed to the complex matrix solution subroutine. Line 35 loads the solution $I_{1,1}$, thru $I_{2,3}$ into matrix D. This matrix is stored on disc. Line 38 establishes a file number depending on the feedpoint location and antenna length.

Line 41 is the end of the main program. The following lines are various subroutines to perform repetitive operations. Within these subroutines p numbers are used as simple variables. They are particular to each subroutine and do not have global values. The numbers used in the subroutine have a one to one positional relationship to the numbers in parenthesis of the corresponding call statements.

Lines 43 through 47 calculate the load function and driving function of equations (30) and (31). Lines 49 through 80 solve the complex matrix equations of equation (35). The method of solution is the Gauss-Jordan method with row pivoting. Row pivoting is used to improve accuracy. In this solution method, the matrices A and C are reduced to identity matrices of size 6 X 6. The remaining column (column 7) is then the solution.

The solution process must be carried out simultaneously for the real and imaginary parts of equation (35). Lines 81 through 87 provide

the complex arithmetic for these operations. Lines 51 through 55 find the largest leading coefficient. Line 56 checks for a non-zero matrix. Lines 57 through 61 interchange this pivot row with the current working row if necessary. Lines 62 and 63 normalize the pivot row; that is, these lines create a 1 on the diagonal. Lines 66 through 70 reduce all other rows in the matrix; that is, these lines create zeros in the matrix below the diagonal. Lines 71 and 72 check for a zero determinate. Lines 73 through 80 do the backsolve process; that is, these lines create zeros above the diagonal. The remaining column (column 7) is the solution and is placed in matrices X and Y. Lines 81 through 87 are the complex arithmatic operations necessary to solve the complex matrix equations.

Lines 88 through 94 are used to calculate the numerical integration of equation (37). The inputs needed by this integral and equation (29) are the following:

a. Z position on antenna.

b. L lower limit of integration.

c. U upper limit of integration.

d. B beta.

e. A antenna radius in meters.

f. K degree of polynomional approximation presently being evaluated

Lines 92 and 93 are the call statements to generate the real part of the Q matrix (Q) and the imaginary part of the Q matrix (R). Lines 95 through 99 establish the continuity relationships of equations (38) and (39). Lines 100 through 114 are the relationships necessary to accomplish the numerical integrations of equations (37) and (29).

Equation (29) can be expanded in the following manner

$$F(z,s) = \frac{\cos(\beta R)}{R} - \frac{j\sin(\beta R)}{R} - \frac{\cos\beta z\cos(\beta r)}{r} + \frac{j\cos\beta z\sin(\beta r)}{r} . \quad (A1)$$

Separating equation (A1) into real and imaginary parts and accounting for F(z,s) and F(z,-s) from equation (29) results in the following expressions

$$\mathrm{Re}[F(z,s)+F(z,-s)] = \frac{\cos\beta R_1}{R_1} - \frac{2\cos\beta z\cos\beta r}{r} + \frac{\cos(\beta R)}{R} \quad (A2)$$

$$\mathrm{Im}[F(z,s)+F(z,-s)] = -\frac{\sin\beta R_1}{R_1} + \frac{2\cos\beta z\sin\beta r}{r} - \frac{\sin(\beta R)}{R} \quad (A3)$$

where $r = (s^2 + a^2)^{1/2}$, $R_1 = [(z-s)^2+a^2]^{1/2}$, $R = [(z+s)^2+a^2]^{1/2}$. (A4)

Substituting equations (A2) and (A3) into equation (37) and changing the integral to a summation results in the following

$$\mathrm{Re}[Q(z,i,k)] = \frac{1}{(z_{i+1})^{k-1}}\left(\frac{z_{i+1}-z_i}{N}\right)\sum_{j=1}^{N} \mathrm{Re}[F(z,s_j)+F(z,-s_j)]s_j^{k-1} \quad (A5)$$

$$\mathrm{Im}[Q(z,i,k)] = \frac{1}{(z_{i+1})^{k-1}}\left(\frac{z_{i+1}-z_i}{N}\right)\sum_{j=1}^{N} \mathrm{Im}[F(z,s_j)+F(z,-s_j)]s_j^{k-1} \quad (A6)$$

where $s_j = z_i + \left(\frac{z_{i+1}-z_i}{N}\right)j - \frac{z_{i+1}-z_i}{2N}$. (A7)

Relationships (A5), (A6), and (A7) are used in lines 100 through 114 to calculate the Q terms given by equation (37).

A.3 Current Distribution - PLTCUR

The program PLTCUR is used to plot the current distribution of the

antenna on paper. The current distribution is plotted for each antenna at several selected frequencies. Figure A.2 shows a typical current distribution plot.

Line 2 is a plotter initialization statement. Lines 3 and 4 are statements dimensioning arrays. Line 5 selects the frequencies to be plotted from data file D. Lines 7 through 9 load the data file from disk to array D. Lines 10 and 11 establish the feedpoint height and antenna length from the file number N. Lines 12 through 22 are plotter scaling and labeling statements. Lines 23 through 28 calculate the real part R and the imaginary part I of the current on the antenna at position $0<Z<D$ from equation (32). Lines 30 through 33 calculate the same currents for $D<Z<L$. Lines 34 through 38 calculate the magnitude and phase of these currents. Lines 40 through 45 plot the real part, imaginary part, magnitude, and phase of the current relative to the maximum amplitude.

A.4 Field Pattern - PLTFLD

The program PLTFLD is used to plot the elevation field pattern of the antenna on paper. The field pattern is plotted for each antenna at several selected frequencies. Figure A.3 shows a typical field pattern plot.

Line 2 is an initialization statement. Lines 3 and 4 are statements dimensioning arrays. Line 5 selects the frequencies to be plotted from data file D. Lines 7 through 8 load the data file from disc to array D. Lines 9 and 10 establish the feedpoint height and antenna length from the file number N. Lines 11 through 21 are plotter scaling and labeling statements. Lines 22 through 27 calculate the real part R and the imaginary part I of the current on the antenna at

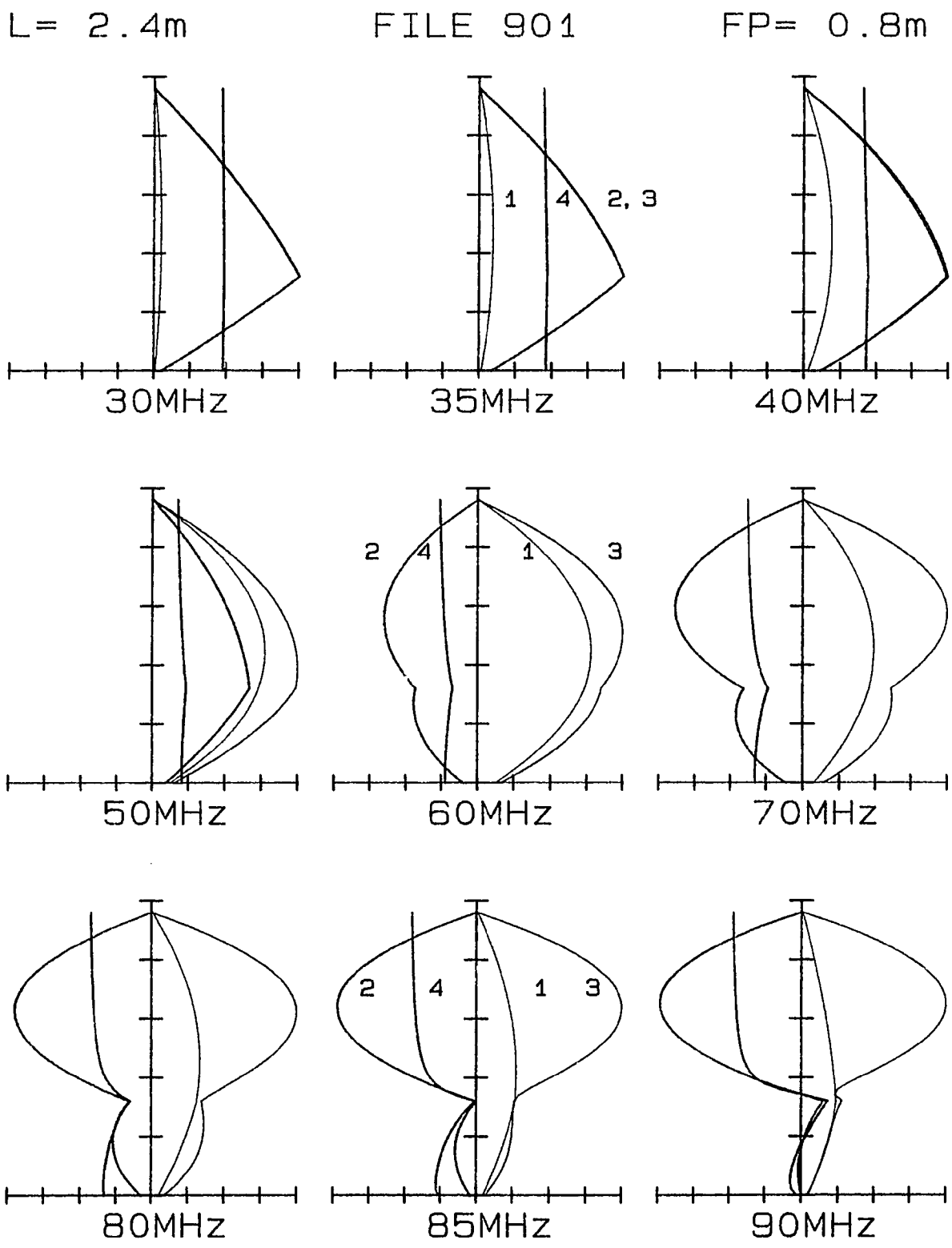

FIGURE A.2 TYPICAL NORMALIZED CURRENT DISTRIBUTIONS

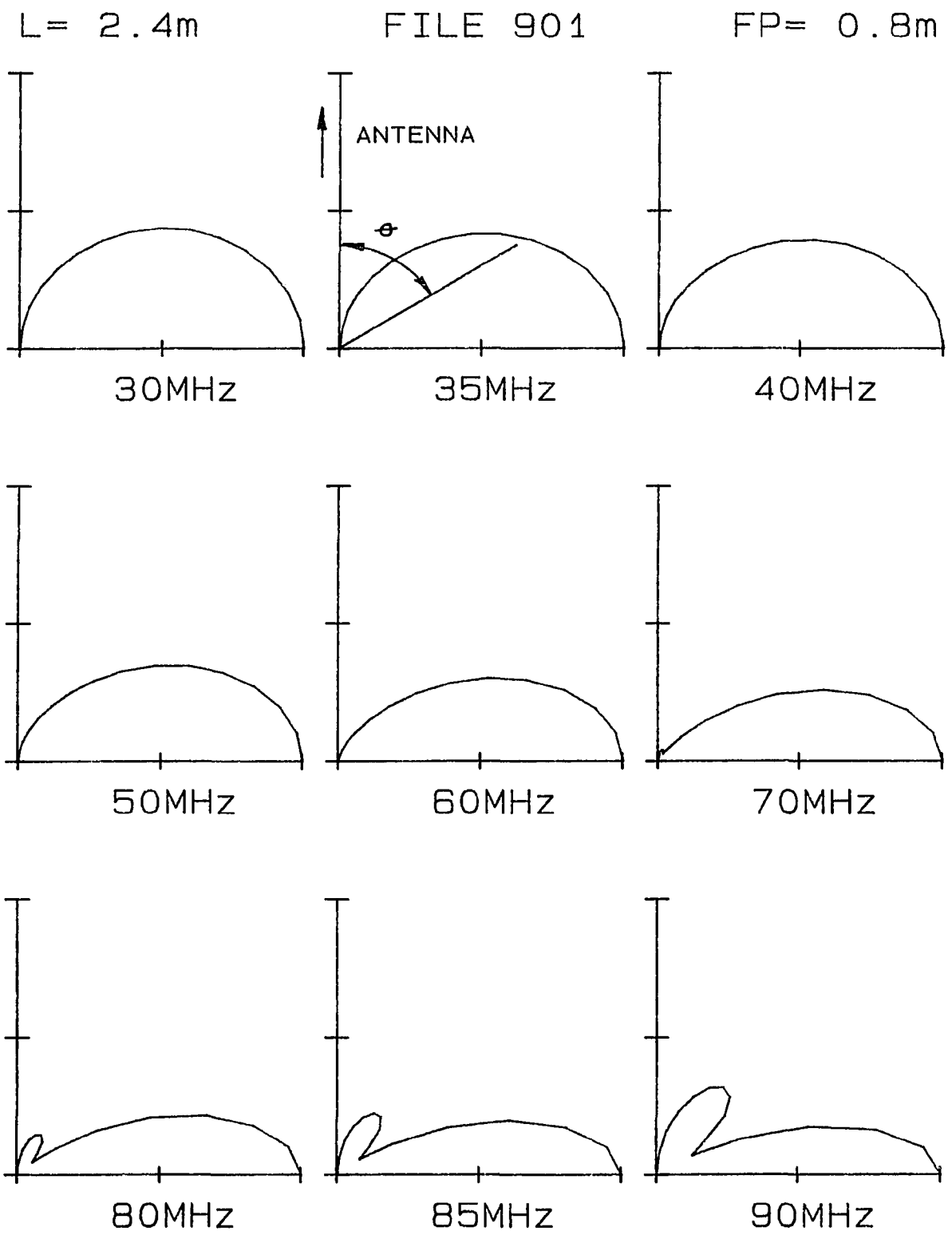

FIGURE A.3 TYPICAL NORMLIZED FIELD PATTERNS

position 0<Z<D from equation (32). Lines 29 through 32 calculate the same currents for D<Z<L. Lines 33 through 37 calculate the magnitude and phase of these currents. Line 40 varies angle A from 0 to 90 degrees in radians. Lines 41 through 45 calculate βcos(A) from equation (49). Line 51 plots the magnitude of the field pattern as a function of the angle A.

A.5 Impedance - PLTIMP

The program PLTIMP is used to plot the antenna input impedance versus frequency on paper. A typical antenna input impedance plot is shown in Figure A.4.

Line 3 is an initialization statement. Line 4 is a statement dimensioning arrays. Lines 5 through 7 load the data file from disk. Line 9 is a plotter scaling statement. Lines 11 through 19 plot a simplified smith chart on the paper. Lines 21 through 23 calculate the antenna input admittance from equation (42). That is, since the driving function V_g was set equal to 1 volt, the antenna input admittance is simply the input current. Line 24 converts the input admittance to impedance. Line 25 changes the input impedance to the X and Y coordinates of a smith chart. Line 27 plots the X and Y coordinates of this input impedance. Line 28 is the end of this program. Lines 29 through 31 are a subroutine to convert admittance to impedance. Lines 32 through 35 are a subroutine to convert impedance to X and Y coordinates on a smith chart normalized to 50 ohms.

A.6 Field Strength - CALV/M

The program CALV/M is used to calculate the field strength in volts/ meter on the horizon. This calculation is made for each antenna and each frequency. The output is stored on disk for use later.

FILE 901

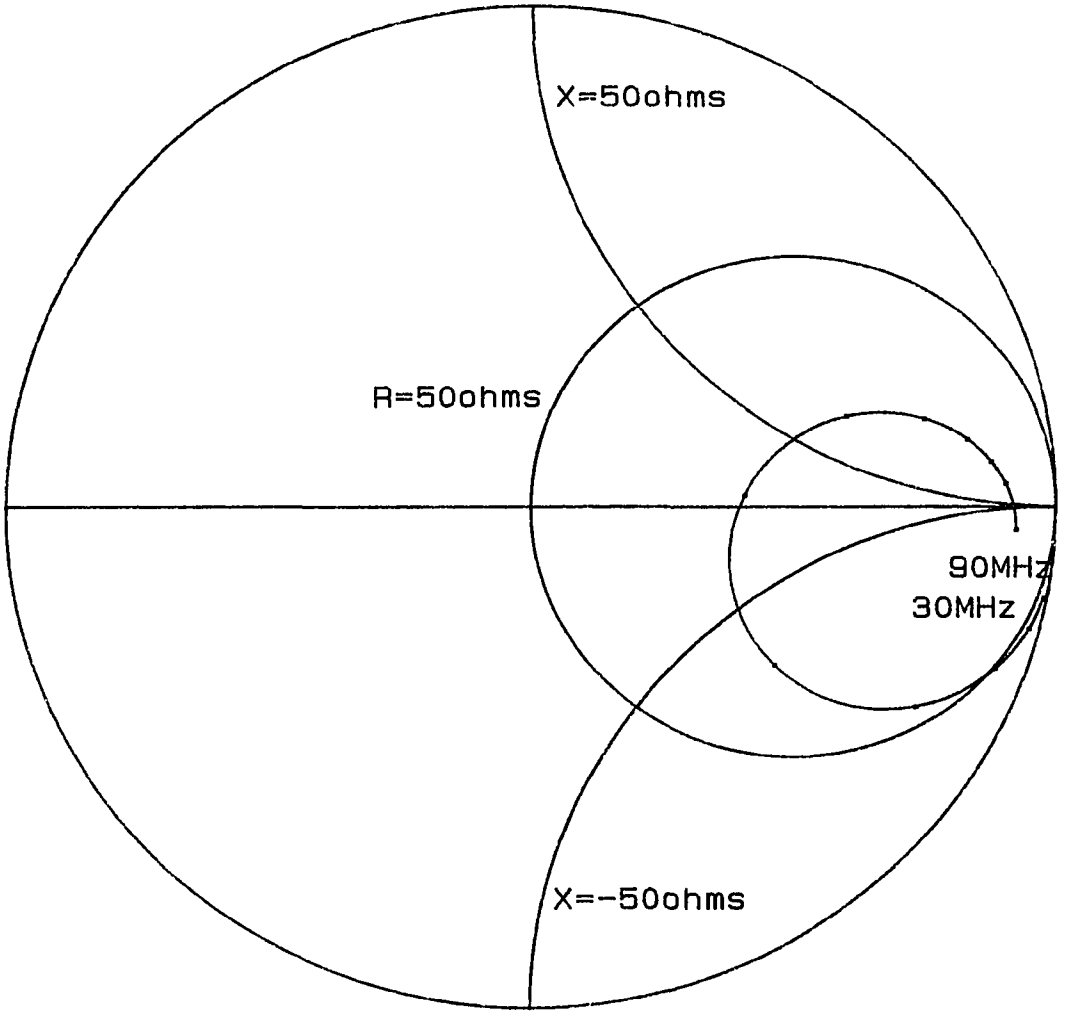

FREQUENCY STEPS OF 5MHz
FROM 30MHz TO 90MHz

FIGURE A.4 TYPICAL IMPEDANCE NORMALIZED TO 50 OHMS

Lines 2 and 3 are statements dimensioning arrays. Lines 4 through 6 select the file from disk and load array D. Lines 7 and 8 calculate the feedpoint height and antenna length corresponding to the file number N. Lines 11 through 15 calculate the real part R and the imaginary part I of the current on the antenna at position 0<Z<D from equation (32). Lines 17 through 20 calculate the same currents for D<Z<L. Line 21 through 25 determine the magnitude and phase of the current. Lines 27 through 29 calculate the field strength on the horizon from equation (50). Line 33 calculates the normalization factor of equation (52). Line 34 calculates the field strength for equal input power as in equation (53) and loads the result into matrix V. This matrix is stored on disk in lines 36 and 37 for use later.

A.7 Gain - PLV/M1

The program PLV/M1 is used to plot antenna gain on the horizon relative to a quarter wave monopole versus frequency. In this program the antenna length is fixed and a family of curves is plotted for various values of feedpoint height. A typical gain plot is showm in Figure A.5.

Line 2 is an initialization statement. Line 3 is a statement dimensioning arrays. Line 4 loads the data file from disk into matrix V. The antenna length is entered in line 5. Line 9 is a call statement to establish the field strength of the reference antenna (a quarter wave monopole at each frequency). Lines 10 through 12 calculate the gain of the antenna in dB relative to the quarter wave monopole. Lines 13 through 21 are plotter scaling and labeling statements. Lines 22 through 28 calculate the proper data point within matrix V and plot this gain versus frequency. Lines 30 through 41 calculate the field strength

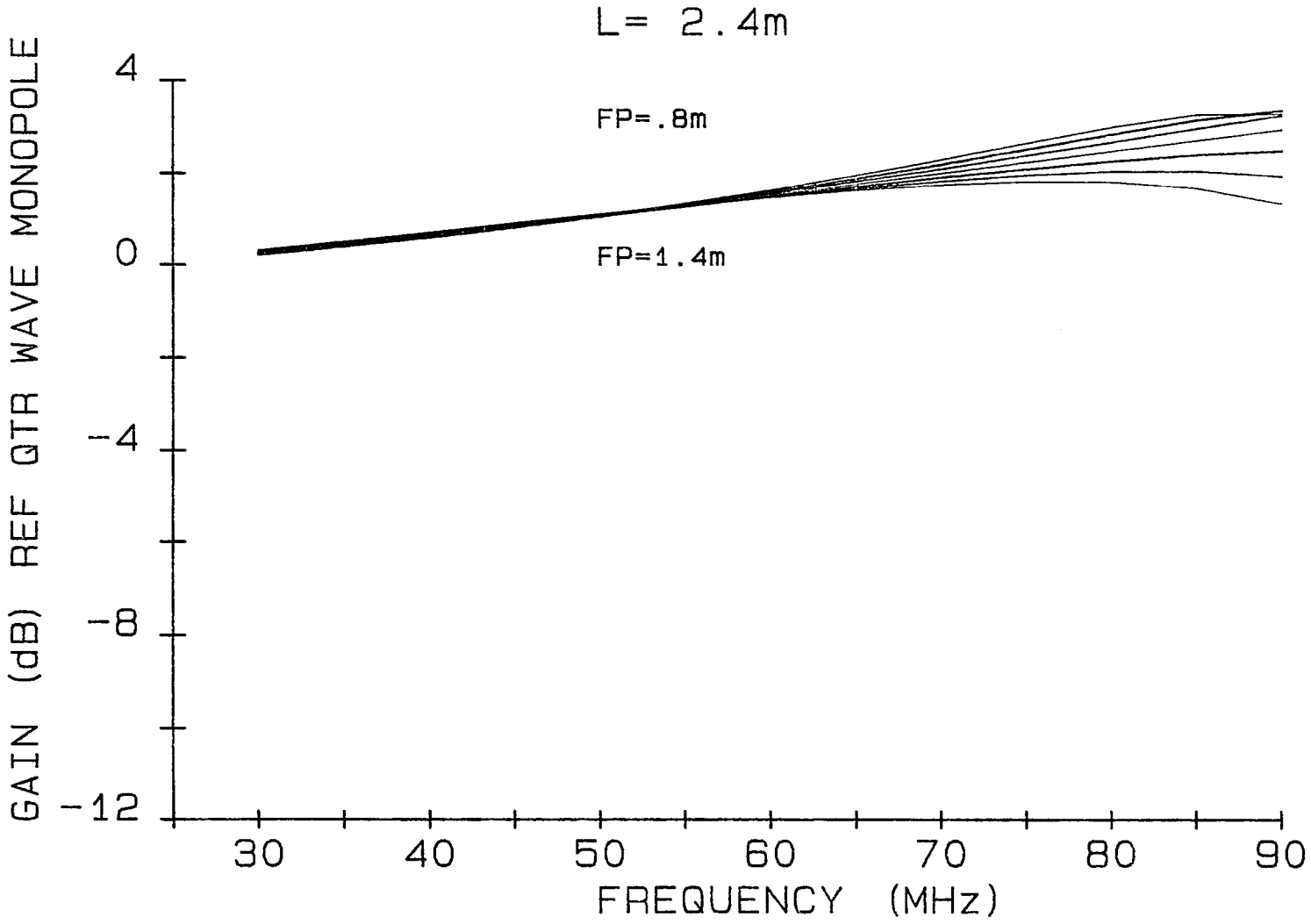

FIGURE A.5 GAIN ON HORIZON

on the horizon of a quarter wave monopole. This reference antenna is assumed to have a sine wave distribution of current.

A.8 Gain - PLV/M2

The program PLV/M2 is used to plot antenna gain on the horizon relative to a quarter wave monopole versus frequency. In this program the feedpoint height is fixed and a family of curves is plotted for various values of antenna length. A typical gain plot is shown in Figure A.6.

The program PLV/M2 has line by line similarity to program PLV/M1.

A.9 Equalizer Network - MATCH1

The program MATCH1 is used to find the best VSWR using the pi network of Figure 4.2(d) and the input impedance associated with an antenna of length 2.5 meters and a feedpoint height of 1.0 meter.

Line 2 is a dimension statement. Lines 3 through 5 select particular values of inductance and capacitance. Lines 6 and 7 are the input or antenna impedance. The frequencies selected for matching are shown in line 8. Lines 10 through 14 vary the values of inductance and capacitance. Lines 15 through 21 calculate the effect of various transformation ratios. Lines 34 through 42 are subroutines for the complex division operation and the calculation of VSWR.

A.10 Equalizer Network - MATCH2

The program MATCH2 is used to find the best VSWR using the T network of Figure 4.2(c) and the input impedance associated with an network of Figure 4.2(c) and the input impedance associated with an antenna of length 2.5 meters and a feedpoint height of 1.0 meter.

The program is very similar to program MATCH1. Changes are evident in lines 16 through 22 to reflect the different network configuration.

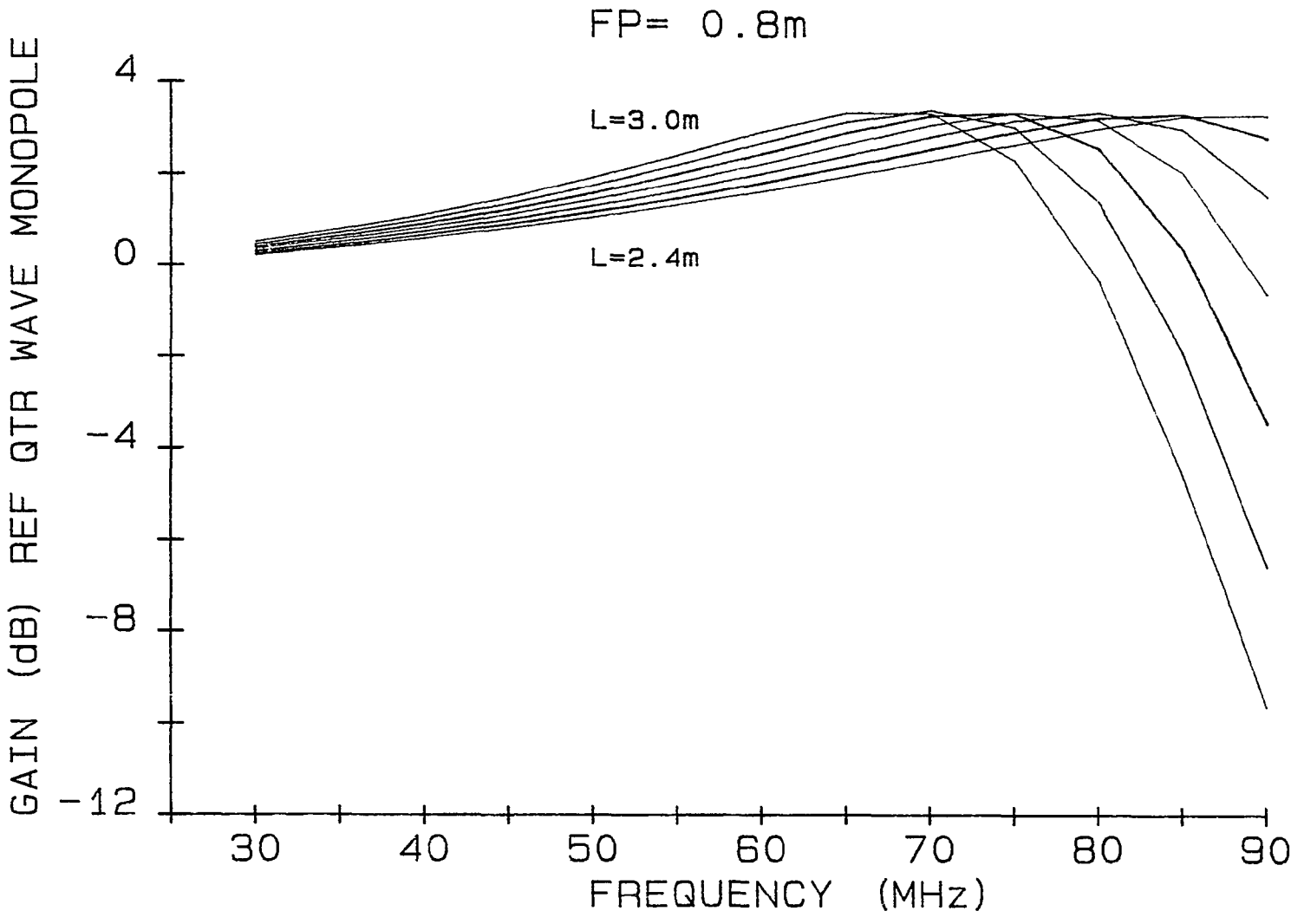

FIGURE A.6 GAIN ON HORIZON

A.11 Equalizer Network - MATCH3

The program MATCH3 is used to find the best VSWR using the network of Figure 4.3 and the input impedance associated with an antenna of length 2.5 meters and a feedpoint height of 1.0 meter.

The program MATCH3 is very similar to the two programs above. The only change is in the calculation of the network to include an autotransformer in lines 15 through 18.

```
0: "PROGRAM TO CALCULATE CURRENT DISTRIBUTION ON ANTENNA":
1: "PROGRAM NAME CALCUR":
2: dim X[6],Y[6],Z[4],L[3],M[1],G[4],M$[4],N$[3]
3: dim A[6,7],C[6,7],Q[6,7],R[6,7],H[4,1],D[13,12]
4: rad;.0041275→A;0→L[1]
5: "FEEDPOINT HEIGHT":for D=.8 to 1.4 by .1;D→L[2]
6: "ANTENNA LENGTH":for C=2.4 to 3 by .1;C→L[3]
7: L[2]/2→Z[1];L[2]→Z[2];L[2]+(L[3]-L[2])/2→Z[3];L[3]→Z[4]
8: for F=30 to 90 by 5
9: "BETA":2*π*F/300→B
10: "CALCULATE Q&R MATRIX":cll 'Q&R'
11: "BASE ISOLATION CHOKE":
12: 1/4ππ(2)25^2→r8;2πFr8tn^6→r9
13: -1/2πF2tn^(-6)→r10;r9*r10/(r9+r10)→M[1]
14: "P= 4 POINTS ON ANTENNA Z[P]":
15: "CALCULATE LOAD FUNCTION AND DRIVING FUNCTION":
16: for P=1 to 4;Z[P]→Z
17: cll 'H(z,zi)'(Z,L[1],B,M[1],H[P,1])
18: cll 'G(z)'(Z,L[2],B,1,G[P]);next P
19: "LOAD SOLUTION MATRICES A[]=REAL, C[]=IMAGINARY":
20: for P=1 to 4;Q[P+2,1]-H[P,1]→A[P+2,1];next P
21: 1→I;for K=1 to 3;for P=1 to 4
22: R[P+2,K+3*I-3]→C[P+2,K+3*I-3]
23: if K=1 and I=1;gto +2
24: Q[P+2,K+3*I-3]→A[P+2,K+3*I-3]
25: next P;next K
26: 2→I;for K=1 to 3;for P=1 to 4
27: Q[P+2,K+3*I-3]→A[P+2,K+3*I-3]
28: R[P+2,K+3*I-3]→C[P+2,K+3*I-3]
29: next P;next K
30: for K=1 to 7;for P=1 to 2
31: Q[P,K]→A[P,K];R[P,K]→C[P,K];next P;next K
32: for P=1 to 4;0→A[P+2,7];G[P]→C[P+2,7];next P
33: "SOLVE FOR CURRENTS X[] & Y[]":
34: cll 'SOLVE'
35: if flg4;stp
36: for I=1 to 6;X[I]→D[(F-25)/5,I]
37: Y[I]→D[(F-25)/5,I+6];next I
38: next F
```

FIGURE A.7 PROGRAM CALCUR

```
39: "STORE ON DISK":
40: fxd 0;str(900+7(10*D-8)+10*C-23)→M$;M$[2,4]→N$
41: asgn N$,1,0
42: sprt 1,D[*],"end"
43: next C;next D;end
44: "ROUTINE TO CALCULATE LOAD FUNCTION":
45: "G(z)":
46: "H(z,zi)":0→p5
47: 2*cos(p3*p1)*sin(p3*p2)→p5
48: -sin(p3*abs(p1-p2))-sin(p3*abs(p1+p2))+p5→p5
49: p4*p5/60→p5;ret
50: "ROUTINE TO SOLVE COMPLEX MATRIX EQUATIONS":
51: "SOLVE":cfg 4;0→I;6→N
52: "BRANCH TO BACKSOLVE":if (I+1→I)=N;gto +21
53: "FIND MAX PIVOT ROW":I-1→K;0→p1
54: if (K+1→K)>N;gto +4
55: cll 'CMOD'(A[K,I],C[K,I],p2)
56: if (p2→p3)>p1;p3→p1;K→p4
57: gto -3
58: "IF MAX PIVOT=0, DET=0":if p1=0;sfg 4;dsp "DET=0";ret
59: "NO SWITCH ROWS IF":I→J;if I=p4;gto +5
60: "INTERCHANGE ROW I WITH PIVOT ROW p4":
61: A[I,J]→p3;A[p4,J]→A[I,J];p3→A[p4,J];jmp (J+1→J)>N+1
62: I→J
63: C[I,J]→p3;C[p4,J]→C[I,J];p3→C[p4,J];jmp (J+1→J)>N+1
64: "NORMALIZE PIVOT ROW":I+1→J;A[I,I]→p1;C[I,I]→p5
65: cll 'CDIV'(A[I,J],C[I,J],p1,p5,p6,C[I,J]);p6→A[I,J]
66: if(J+1→J)>N+1;gto-1
67: I→K
68: if (K+1→K)>N;gto -16
69: "REDUCTION OF OTHER ROWS":I+1→J
70: cll 'CMULT'(A[K,I],C[K,I],A[I,J],C[I,J],p7,p8)
71: cll 'CSUBT'(A[K,J],C[K,J],p7,p8,A[K,J],C[K,J])
72: if (J+1→J)<N+2;gto -2
73: gto -5
74: "CHECK DET=0":cll 'CMOD'(A[N,N],C[N,N],p9)
75: if p9=0;0→p1;gto -17
76: "BACKSOLVE":
77: cll 'CDIV'(A[N,N+1],C[N,N+1],A[N,N],C[N,N],X[N],Y[N])
78: N→I
79: "SUBROUTINE FINISHED":if (I-1→I)<1;ret
80: N→K;0→p12→p13
81: cll 'CMULT'(A[I,K],C[I,K],X[K],Y[K],p10,p11)
82: cll 'CADD'(p10,p11,p12,p13,p12,p13)
83: if (K-1→K)>=I+1;gto -2
84: cll 'CSUBT'(A[I,N+1],C[I,N+1],p12,p13,X[I],Y[I]);gto -5
```

FIGURE A.7 PROGRAM CALCUR CONTINUED

```
85: "COMPLEX ARITHMETIC":
86: "CADD":p1+p3→p5;p2+p4→p6;ret
87: "CSUBT":p1-p3→p5;p2-p4→p6;ret
88: "CMULT":p1*p3-p2*p4→p5;p2*p3+p1*p4→p6;ret
89: "CDIV":(p1*p3+p2*p4)/(p3^2+p4^2)→p5
90: (p2*p3-p1*p4)/(p3^2+p4^2)→p6;ret
91: "CMOD":√(p1^2+p2^2)→p3;ret
92: "Q & R MATRIX CALCULATION":
93: "Q&R":
94: for I=1 to 2;L[I]→L;L[I+1]→U
95: for P=1 to 4;Z[P]→Z;for K=1 to 3
96: cll "RQ(z,i,k)"(Z,L,U,B,A,K,Q[P+2,K+3*I-3])
97: cll "IQ(z,i,k)"(Z,L,U,B,A,K,R[P+2,K+3*I-3])
98: next K;next P;next I
99: "CONTINUITY EQUATIONS":
100: for K=1 to 3;0→Q[2,K]→R[2,K]
101: 1→Q[1,K]→R[1,K]→Q[2,K+3]→R[2,K+3];next K
102: 0→Q[1,7]→Q[2,7]→R[1,7]→R[2,7];-1→Q[1,4]→R[1,4]
103: -L[2]/L[3]→Q[1,5]→R[1,5];-(L[2]/L[3])^2→Q[1,6]→R[1,6]
104: ret
105: "NUMERICAL INTEGRATION":
106: "RQ(z,i,k)":0→p7
107: for T=1 to 100;T*.01*(p3-p2)-.005*(p3-p2)+p2→S
108: √(S^2+p5^2)→p8;√((p1-S)^2+p5^2)→p9
109: √((p1+S)^2+p5^2)→p10
110: S^(p6-1)*cos(p4*p9)/p9+p7→p7
111: -(S^(p6-1)*2*cos(p4*p1)*cos(p4*p8)/p8)+p7→p7
112: S^(p6-1)*cos(p4*p10)/p10+p7→p7
113: next T;.01*(p3-p2)*p7/p3^(p6-1)→p7;ret
114: "IQ(z,i,k)":0→p7
115: for T=1 to 100;T*.01*(p3-p2)-.005*(p3-p2)+p2→S
116: √(S^2+p5^2)→p8;√((p1-S)^2+p5^2)→p9
117: √((p1+S)^2+p5)→p10
118: -(S^(p6-1)*sin(p4*p9)/p9)+p7→p7
119: S^(p6-1)*2*cos(p4*p1)*sin(p4*p8)/p8+p7→p7
120: -(S^(p6-1)*sin(p4*p10)/p10)+p7→p7
121: next T;.01*(p3-p2)*p7/p3^(p6-1)→p7;ret
```

FIGURE A.7 PROGRAM CALCUR CONTINUED

```
0: "PROGRAM TO PLOT CURRENT DISTRIBUTION":
1: "PROGRAM NAME PLTCUR":
2: pclr;lbl " ";deg;wrt 705,"VS10"
3: dim D[13,12],M$[4],N$[3],G[9]
4: dim R[0:60],I[0:60],M[0:60],P[0:60]
5: "G[]=SELECTED FREQUENCIES FROM D[]":1→G[1];2→G[2]
6: 3→G[3];5→G[4];7→G[5];9→G[6];11→G[7];12→G[8];13→G[9]
7: ent "ENTER FILE NUMBER",N
8: fxd 0;str(N)→M$;M$[2,4]→N$
9: asgn N$,1;sread 1,D[*]
10: "L=ANTENNA LENGTH":2.4+.1*int((N-901)mod7)→L
11: "D=FEEDPOINT HEIGHT":.8+.1*int((N-901)/7)→D
12: fxd 1;pen# 1;wrt 705,"PA1000,9700";lbl "L=",L,"m"
13: fxd 0;pen# 1;wrt 705,"PA3400,9700";lbl "FILE",N
14: fxd 1;pen# 1;wrt 705,"PA5700,9700";lbl "FP=",D,"m"
15: for F=1 to 9;scl -6,58,-2,11.4
16: ofs (F-1)mod3*9,(3-int((F+2)/3))*3.5
17: pen# 1;xax 0,1,-4,4;yax 0,.5,0,3
18: if F<4;fxd 0;plt -2,-.3,1;lbl 25+F*5,"MHz"
19: if F=4;fxd 0;plt -2,-.3,1;lbl " 50MHz"
20: if F=5;fxd 0;plt -2,-.3,1;lbl " 60MHz"
21: if F=6;fxd 0;plt -2,-.3,1;lbl " 70MHz"
22: if F>6;fxd 0;plt -2,-.3,1;lbl 45+F*5,"MHz"
23: "Z=POSITION ON ANTENNA":
24: for Z=0 to D by .05;0→V→W;for K=1 to 3
25: if Z=0;D[G[F],1]→V;D[G[F],7]→W;gto +3
26: D[G[F],K]*abs(Z/D)^(K-1)+V→V
27: D[G[F],K+6]*abs(Z/D)^(K-1)+W→W;next K
28: V→R[Z*20];W→I[Z*20];next Z
29: "R[]=REAL CURRENT, I[]=IMAGINARY CURRENT":
30: for Z=D to L by .05;0→V→W;for K=1 to 3
31: D[G[F],K+3]*abs(Z/L)^(K-1)+V→V
32: D[G[F],K+9]*abs(Z/L)^(K-1)+W→W;next K
33: V→R[Z*20];W→I[Z*20];next Z
34: for T=0 to 20L-1
35: √(R[T]^2+I[T]^2)→M[T];atn(I[T]/R[T])→P[T]
36: if R[T]<0 and I[T]>0;180+P[T]→P[T]
37: if R[T]<0 and I[T]<0;P[T]-180→P[T]
38: next T;0→M[20L];P[20L-1]→P[20L]
39: "M[]=MAGNITUDE, P[]=PHASE":max(M[*])→M
40: for S=1 to 4;for Z=0 to L by .05
41: if S=1;pen# 2;plt R[20*Z]*4/M,Z
42: if S=2;pen# 3;plt I[20*Z]*4/M,Z
43: if S=3;pen# 4;plt M[20*Z]*4/M,Z
44: if S=4;pen# 1;plt P[20*Z]/45,Z
45: next Z;pen;next S;pen;next F
46: pen# 1;csiz 1;plt -22,-.7,1;lbl "REAL green  IMAGINARY"
47: pen# 1;csiz 1;lbl " red  MAGNITUDE blue  PHASE black"
48: pen# 2;plt -19.5,-.8;plt -17.3,-.8;pen
49: pen# 3;plt -11.5,-.8;plt -10,-.8;pen
50: pen# 4;plt -4.5,-.8;plt -2.5,-.8;pen
51: pen# 1;plt 1.5,-.8;plt 4,-.8;pen
```

FIGURE A.8 PROGRAM PLTCUR

```
0: "PROGRAM TO PLOT FIELD DISTRIBUTION":
1: "PROGRAM NAME PLTFLD":
2: pclr;lbl " ";rad;wrt 705,"VS10"
3: dim R[0:30],I[0:30],M[0:30],P[0:30],F[0:30]
4: dim D[13,12],M$[4],N$[3],G[9]
5: "G[]=SELECTED FREQUENCIES FROM D[]":1→G[1];2→G[2]
6: 3→G[3];5→G[4];7→G[5];9→G[6];11→G[7];12→G[8];13→G[9]
7: ent "ENTER FILE NUMBER",N
8: fxd 0;str(N)→M$;M$[2,4]→N$;asgn N$,1;sread 1,D[*]
9: "FEEDPOINT HEIGHT":.1*int((N-901)/7)+.8→D
10: "ANTENNA LENGTH":.1*int((N-901)mod7)+2.4→L
11: fxd 1;pen# 1;wrt 705,"PA1000,9700";lbl "L=",L,"m"
12: fxd 0;pen# 1;wrt 705,"PA3400,9700";lbl "FILE",N
13: fxd 1;pen# 1;wrt 705,"PA5700,9700";lbl "FP=",D,"m"
14: for F=1 to 9;scl -2,63,-5,38
15: ofs (F-1)mod3*9,(3-int((F+2)/3))*12
16: pen# 1;xax 0,4,0,8;yax 0,4,0,8
17: if F<4;fxd 0;pen# 1;plt 2,-1.5,1;lbl 25+5*F,"MHz"
18: if F=4;fxd 0;pen# 1;plt 2,-1.5,1;lbl " 50MHz"
19: if F=5;fxd 0;pen# 1;plt 2,-1.5,1;lbl " 60MHz"
20: if F=6;fxd 0;pen# 1;plt 2,-1.5,1;lbl " 70MHz"
21: if F>6;fxd 0;pen# 1;plt 2,-1.5,1;lbl 5*F+45,"MHz"
22: "Z=POSITION ON ANTENNA":
23: for Z=0 to D by .1;0→V→W;for K=1 to 3
24: if Z=0;D[G[F],1]→V;D[G[F],7]→W;gto +3
25: D[G[F],K]*abs(Z/D)^(K-1)+V→V
26: D[G[F],K+6]*abs(Z/D)^(K-1)+W→W;next K
27: V→R[Z*10];W→I[Z*10];next Z
28: "R[]=REAL CURRENT, I[]=IMAGINARY CURRENT":
29: for Z=D to L by .1;0→V→W;for K=1 to 3
30: D[G[F],K+3]*abs(Z/L)^(K-1)+V→V
31: D[G[F],K+9]*abs(Z/L)^(K-1)+W→W;next K
32: V→R[Z*10];W→I[Z*10];next Z
33: for T=0 to 10*L-1
34: √(R[T]^2+I[T]^2)→M[T];atn(I[T]/R[T])→P[T]
35: if R[T]<0 and I[T]>0;π+P[T]→P[T]
36: if R[T]<0 and I[T]<0;P[T]-π→P[T]
37: next T;0→M[10L];P[10L-1]→P[10L]
38: "M[]=MAGNITUDE, P[]=PHASE":
```

FIGURE A.9 PROGRAM PLTFLD

```
39: "I=ANGLE IN DEGREES, F[]=FIELD STRENGTH":
40: for I=0 to 90 by 6;2*π*I/360→A;0→r1→r2
41: if F<4;2*π*(25+5*F)*cos(A)/300→B
42: if F=4;2*π*50*cos(A)/300→B
43: if F=5;2*π*60*cos(A)/300→B
44: if F=6;2*π*70*cos(A)/300→B
45: if F>6;2*π*(5*F+45)*cos(A)/300→B
46: for T=0 to 10*L by 1;.1*T→Z
47: M[T]*(cos(P[T]+Z*B)+cos(P[T]-Z*B))+r1→r1
48: M[T]*(sin(P[T]+Z*B)+sin(P[T]-Z*B))+r2→r2;next T
49: sin(A)*√(r1^2+r2^2)→F[I/6];next I;max(F[*])→M
50: for I=0 to 90 by 6;2*π*I/360→A
51: pen# 3;plt F[I/6]*sin(A)*8/M,F[I/6]*cos(A)*8/M
52: next I;pen;next F;pen
53: pen# 1;plt -9,24;plt -4,27;pen
54: pen# 1;plt -9.5,29;plt -9.5,31;pen
55: csiz 1;pen# 1;plt -8.5,30,1;lbl "ANTENNA"
```

FIGURE A.9 PROGRAM PLTFLD CONTINUED

```
0: "PROGRAM TO PLOT":
1: "ANTENNA INPUT IMPEDANCE ON SMITH CHART":
2: "PROGRAM NAME PLTIMP":
3: pclr;lbl "";deg;wrt 705,"VS5"
4: dim D[13,12],M$[4],N$[3]
5: ent "ENTER FILE NUMBER",N
6: fxd 0;str(N)→M$;M$[2,4]→N$
7: asgn N$,1;sread 1,D[*]
8: fxd 0;pen# 1;wrt 705,"PA3400,9700";lbl "FILE",N
9: scl -1.4,4.1,-2,1.7
10: pen# 1;wrt 705,"SM"
11: "DRAW SMITH CHART":
12: for I=0 to 360 by 2;plt cos(I),sin(I)
13: next I;plt -1,0;pen
14: for I=0 to 360 by 2;plt .5cos(I)+.5,.5sin(I)
15: next I
16: for I=90 to 180 by 2;plt cos(I)+1,sin(I)-1
17: next I;pen
18: for I=180 to 270 by 2;plt cos(I)+1,sin(I)+1
19: next I;pen
20: for F=1 to 13
21: "CALCULATE ANTENNA INPUT ADMITTANCE":
22: 0→G→B;for K=1 to 3
23: D[F,K]+G→G;D[F,K+6]+B→B;next K
24: cll 'GBtoRX'(G,B,R,I)
25: cll 'RXtoXY'(R,I,X,Y)
26: "PLOT ANTENNA INPUT IMPEDANCE":
27: wrt 705,"SM.";pen# 3;plt X,Y,1
28: next F;end
29: "ROUTINE TO CONVERT G&B TO R&X":
30: "GBtoRX":
31: p1/(p1^2+p2^2)→p3;-p2/(p1^2+p2^2)→p4;ret
32: "ROUTINE TO CONVERT R&X TO X&Y ON SMITH CHART":
33: "RXtoXY":
34: p1/50→p1;p2/50→p2;(p1+1)^2+p2^2→p5
35: (p1^2-1+p2^2)/p5→p3;2p2/p5→p4;ret
```

FIGURE A.10 PROGRAM PLTIMP

```
0: "PROGRAM TO CALCULATE VOLTS/METER ON HORIZON":
1: "PROGRAM NAME CALV/M":
2: dim R[0:30],I[0:30],M[0:30],P[0:30]
3: dim D[13,12],M$[4],N$[3],V[49,13];deg
4: for N=901 to 949
5: fxd 0;str(N)→M$;M$[2,4]→N$
6: asgn N$,1;sread 1,D[*]
7: "FEEDPOINT HEIGHT":.1*int((N-901)/7)+.8→D
8: "ANTENNA LENGTH":.1*int((N-901)mod7)+2.4→L
9: "Z=POSITION ON ANTENNA":
10: for F=1 to 13
11: for Z=0 to D by .1;0→V→W;for K=1 to 3
12: if Z=0;D[F,1]→V;D[F,7]→W;gto +3
13: D[F,K]*abs(Z/D)^(K-1)+V→V
14: D[F,K+6]*abs(Z/D)^(K-1)+W→W;next K
15: V→R[Z*10];W→I[Z*10];next Z
16: "R[]=REAL PART, I[]=IMAGINARY PART":
17: for Z=D to L by .1;0→V→W;for K=1 to 3
18: D[F,K+3]*abs(Z/L)^(K-1)+V→V
19: D[F,K+9]*abs(Z/L)^(K-1)+W→W;next K
20: V→R[Z*10];W→I[Z*10];next Z
21: for T=0 to 10*L-1 by 1
22: √(R[T]^2+I[T]^2)→M[T];atn(I[T]/R[T])→P[T]
23: if R[T]<0 and I[T]>0;180+P[T]→P[T]
24: if R[T]<0 and I[T]<0;P[T]-180→P[T]
25: next T;0→M[10L];P[10L-1]→P[10L]
26: "M[]=MAGNITUDE, P[]=PHASE":
27: 0→r1→r2;for T=0 to 10*L
28: 2M[T]cos(P[T])+r1→r1;2M[T]sin(P[T])+r2→r2
29: next T;√(r1^2+r2^2)→E
30: "E=FIELD STRENGTH":
31: "V[]=NORMALIZED FIELD STRENGTH":
32: "C=NORMALIZATION FACTOR":
33: √(1/(D[F,1]+D[F,2]+D[F,3]))→C
34: E*C→V[N-900,F]
35: next F;next N
36: asgn "V/M",1,0
37: sprt 1,V[*],"end"
38: end
```

FIGURE A.11 PROGRAM CALV/M

```
0: "PROGRAM TO PLOT GAIN ON HORIZON VERSUS FREQUENCY":
1: "PROGRAM NAME PLV/M1":
2: pclr;lbl "";rad;wrt 705,"VS5"
3: dim M[0:30],V[49,13],Q[13]
4: asgn "V/M",1;sread 1,V[*]
5: ent "ENTER ANTENNA LENGTH 2.4<L<3.0",L
6: if Nmod.1#0;beep;gto -1
7: if L>3;beep;gto -2
8: if L<2.4;beep;gto -3
9: cll 'QTR'
10: for J=1 to 49;for I=1 to 13
11: "GAIN IN dB":20log(V[J,I]/Q[I])→V[J,I]
12: next I;next J
13: scl 10,155,-19,17
14: fxd 0;pen# 1;xax -14,5,25,90
15: fxd 0;csiz ;for I=30 to 90 by 10
16: plt I-3,-15,1;lbl I;next I
17: plt 50,-16,1;lbl "FREQUENCY (MHz)"
18: fxd 0;yax 25,2,-14,2,2
19: deg;pen# 1;plt 17,-14,1;csiz 1.5,2.2,1,90
20: lbl "GAIN (dB) REF QTR WAVE MONOPOLE"
21: fxd 1;csiz ;plt 50,3,1;lbl "L=",L,"m"
22: 10L-23→A;2→C
23: for B=A to 49 by 7
24: if C=5;2→C
25: pen# C
26: for F=1 to 13
27: plt 25+5F,V[B,F]
28: next F;C+1→C;pen;next B;pen
29: pen# 1;csiz 1;plt 55,1,1;lbl "FP=.8m"
30: pen# 1;csiz 1;plt 55,-2,1;lbl "FP=1.4m"
31: end
32: "ROUTINE TO CALCULATE VOLTS/METER ON HORIZON":
33: "FOR QUARTER WAVE MONOPOLE AT EACH FREQUENCY":
34: "QTR":
35: "M[]=MAGNITUDE":
36: "E=FIELD STRENGTH, Q[]=NORMALIZED FIELD STRENGTH":
37: rad;for F=1 to 13
38: for T=0 to 300/(4*(25+5F)) by .1;T→Z
39: sin((π/2)Z/(300/4(25+5F)))/37.5→M[T];next T
40: 0→E;for T=0 to 300/4(25+5F) by .1;T→Z
41: E+2M[T]→E;next T
42: E*√37.5→Q[F]
43: next F;ret
```

FIGURE A.12 PROGRAM PLV/M1

```
0: "PROGRAM TO PLOT GAIN ON HORIZON VERSUS FREQUENCY":
1: "PROGRAM NAME PLV/M2":
2: pclr;lbl "";rad;wrt 705,"VS5"
3: dim M[0:30],V[49,13],Q[13]
4: asgn "V/M",1;sread 1,V[*]
5: ent "ENTER FEEDPOINT  .8<FP<1.4",D
6: if Dmod.1#0;beep;gto -1
7: if D>1.4;beep;gto -2
8: if D<.8;beep;gto -3
9: cll 'QTR'
10: for J=1 to 49;for I=1 to 13
11: "GAIN IN dB":20log(V[J,I]/Q[I])→V[J,I]
12: next I;next J
13: scl 10,155,-19,17
14: fxd 0;pen# 1;xax -14,5,25,90
15: fxd 0;csiz ;for I=30 to 90 by 10
16: plt I-3,-15,1;lbl I;next I
17: plt 50,-16,1;lbl "FREQUENCY (MHz)"
18: fxd 0;yax 25,2,-14,2,2
19: deg;pen# 1;plt 17,-14,1;csiz 1.5,2.2,1,90
20: lbl "GAIN (dB) REF QTR WAVE MONOPOLE"
21: fxd 1;csiz ;plt 50,3,1;lbl "FP=",D,"m"
22: 10D-8→A;2→C
23: for B=7A+1 to 7A+7 by 1
24: if C=5;2→C
25: pen# C
26: for F=1 to 13
27: plt 25+5F,V[B,F]
28: next F;C+1→C;pen;next B;pen
29: pen# 1;csiz 1;plt 55,1,1;lbl "L=3.0m"
30: pen# 1;csiz 1;plt 55,-2,1;lbl "L=2.4m"
31: end
32: "ROUTINE TO CALCULATE VOLTS/METER ON HORIZON":
33: "FOR QUARTER WAVE MONOPOLE AT EACH FREQUENCY":
34: "QTR":
35: "M[]=MAGNITUDE":
36: "E=FIELD STRENGTH, Q[]=NORMALIZED FIELD STRENGTH":
37: rad;for F=1 to 13
38: for T=0 to 300/(4*(25+5F)) by .1;T→Z
39: sin((π/2)Z/(300/4(25+5F)))/37.5→M[T];next T
40: 0→E;for T=0 to 300/4(25+5F) by .1;T→Z
41: E+2M[T]→E;next T
42: E*√37.5→Q[F]
43: next F;ret
```

FIGURE A.13 PROGRAM PLV/M2

```
0: "PROGRAM TO CALCULATE BEST VSWR USING PI NETWORK":
1: "PROGRAM NAME MATCH1":
2: dim C[7],L[7],R[10],X[10],F[5],V[5],A[8];2000→Z
3: 1e-30→L[1];.05→L[2];.1→L[3];.2→L[4];.5→L[5]
4: 1→L[6];1e30→L[7];100→C[6];1e30→C[7]
5: 1e-30→C[1];5→C[2];10→C[3];20→C[4];50→C[5]
6: 25→R[1];51→R[2];90→R[3];286→R[4];1312→R[5]
7: -481→X[1];-229→X[2];-44→X[3];307→X[4];62→X[5]
8: 30→F[1];40→F[2];50→F[3];70→F[4];90→F[5]
9: for I=2 to 7
10: for J=1 to 6
11: for K=1 to 6
12: for L=2 to 7
13: for M=2 to 7
14: for N=1 to 6
15: for F=1 to 5;2*π*F[F]→W
16: cll 'CDIV'(1,0,R[F],X[F],G,B)
17: B+W*C[J]*tn^(-6)-1/(W*L[I])→B
18: cll 'CDIV'(1,0,G,B,R,X)
19: X+W*L[K]-1/(W*C[L]*tn^(-6))→X
20: cll 'CDIV'(1,0,R,X,G,B)
21: B+W*C[N]*tn^(-6)-1/(W*L[M])→B
22: cll 'CDIV'(1,0,G,B,R[F+5],X[F+5])
23: next F
24: for T=1 to 4 by .5;for F=1 to 5
25: cll 'VSWR'(R[F+5]/T,X[F+5]/T,50,V[F])
26: next F
27: if max(V[*])>Z;gto +3
28: max(V[*])→Z→A[1];I→A[2];J→A[3];K→A[4]
29: L→A[5];M→A[6];N→A[7];T→A[8]
30: next T
31: fxd 2;dsp Z,I,J,K
32: next N;next M;next L
33: next K;next J;next I
34: for P=1 to 8;flt 3;prt A[P];next P
35: end
36: "CDIV":
37: (p1*p3+p2*p4)/(p3^2+p4^2)→p5
38: (p2*p3-p1*p4)/(p3^2+p4^2)→p6;ret
39: "VSWR":
40: p1/p3→p9;p2/p3→p10;(p9+1)^2+p10^2→p5
41: (p9^2-1+p10^2)/p5→p6
42: 2*p10/p5→p7;√(p6^2+p7^2)→p8
43: if p8>.999;1000→p4;ret
44: (1+p8)/(1-p8)→p4;ret
```

FIGURE A.14 PROGRAM MATCH1

```
0: "PROGRAM TO CALCULATE BEST VSWR USING T NETWORK":
1: "PROGRAM NAME MATCH2":
2: dim C[7],L[7],R[10],X[10],F[5],V[5],A[8];2000→Z
3: 1e-30→L[1];.05→L[2];.1→L[3];.2→L[4];.5→L[5]
4: 1→L[6];1e30→L[7];100→C[6];1e30→C[7]
5: 1e-30→C[1];5→C[2];10→C[3];20→C[4];50→C[5]
6: 25→R[1];51→R[2];90→R[3];286→R[4];1312→R[5]
7: -481→X[1];-229→X[2];-44→X[3];307→X[4];62→X[5]
8: 30→F[1];40→F[2];50→F[3];70→F[4];90→F[5]
9: for I=1 to 6
10: for J=2 to 7
11: for K=2 to 7
12: for L=1 to 6
13: for M=1 to 6
14: for N=2 to 7
15: for F=1 to 5;2*π*F[F]→W
16: X[F]+L[I]*W-1/(W*C[J]*tn^(-6))→X
17: cll 'CDIV'(1,0,R[F],X,G,B)
18: B+W*C[L]*tn^(-6)-1/(W*L[K])→B
19: cll 'CDIV'(1,0,G,B,R[F+5],X)
20: X+W*L[M]-1/(W*C[N]*tn^(-6))→X[F+5]
21: next F
22: for T=3 to 8 by .5;for F=1 to 5
23: cll 'VSWR'(R[F+5]/T,X[F+5]/T,50,V[F])
24: next F
25: if max(V[*])>Z;gto +3
26: max(V[*])→Z→A[1];I→A[2];J→A[3];K→A[4]
27: L→A[5];M→A[6];N→A[7];T→A[8]
28: next T
29: fxd 2;dsp Z,I,J,K
30: next N;next M;next L
31: next K;next J;next I
32: for P=1 to 8;fxd 2;prt A[P];next P
33: end
34: "CDIV":
35: (p1*p3+p2*p4)/(p3^2+p4^2)→p5
36: (p2*p3-p1*p4)/(p3^2+p4^2)→p6;ret
37: "VSWR":
38: p1/p3→p9;p2/p3→p10;(p9+1)^2+p10^2→p5
39: (p9^2-1+p10^2)/p5→p6
40: 2*p10/p5→p7;√(p6^2+p7^2)→p8
41: if p8>.999;1000→p4;ret
42: (1+p8)/(1-p8)→p4;ret
```

FIGURE A.15 PROGRAM MATCH2

```
0: "PROGRAM TO CALCULATE BEST VSWR USING AUTOTRANSFORMER":
1: "PROGRAM NAME MATCH3":
2: dim C[7],L[7],R[10],X[10],F[5],V[5],A[8];2000→Z
3: 1e-30→L[1];.05→L[2];.1→L[3];.2→L[4];.5→L[5];1→L[6]
4: 1e-30→C[1];5→C[2];10→C[3];20→C[4];50→C[5];100→C[6]
5: 1e30→L[7]→C[7]
6: 25→R[1];51→R[2];90→R[3];286→R[4];1312→R[5]
7: -481→X[1];-229→X[2];-44→X[3];307→X[4];62→X[5]
8: 30→F[1];40→F[2];50→F[3];70→F[4];90→F[5]
9: for I=2 to 6
10: for J=2 to 6
11: for K=.3 to .5 by .02
12: for L=2 to 6
13: for M=2 to 6
14: for N=2 to 6
15: for F=1 to 5;2*π*F[F]→W
16: WW(L[J]+K√(L[I]L[J]))^2→Q
17: cll "CDIV"(Q,0,R[F],X[F]+W(L[I]+L[J]),R,X)
18: cll "CDIV"(1,0,R,X+WL[J],G,B)
19: cll "CDIV"(1,0,G,B+WC[L]tn^(-6),R[F+5],X)
20: X+WL[M]-1/WC[N]tn^(-6)→X[F+5]
21: cll "VSWR"(R[F+5],X[F+5],50,V[F])
22: next F
23: if max(V[*])>Z;gto +3
24: max(V[*])→Z→A[1];I→A[2];J→A[3];K→A[4];L→A[5]
25: M→A[6];N→A[7];T→A[8]
26: fxd 2;dsp Z,N,M
27: next N;next M;next L
28: next K;next J;next I
29: for I=1 to 8;flt 3;prt A[I];next I
30: end
31: "CDIV":
32: (p1*p3+p2*p4)/(p3^2+p4^2)→p5
33: (p2*p3-p1*p4)/(p3^2+p4^2)→p6;ret
34: "VSWR":
35: p1/p3→p9;p2/p3→p10;(p9+1)^2+p10^2→p5
36: (p9^2-1+p10^2)/p5→p6
37: 2*p10/p5→p7;√(p6^2+p7^2)→p8
38: if p8>.999;1000→p4;ret
39: (1+p8)/(1-p8)→p4;ret
```

FIGURE A.16 PROGRAM MATCH3

APPENDIX B

BASE ISOLATED CHOKE

B.1 Introduction

The base isolation choke is the mechanism that mechanically and electrically connects the whip antenna to the supporting structure. This appendix will describe the purpose for the base isolation choke and the electrical parameters will be determined. Results of an investigation conducted to find the most optimum method to obtain the desired electrical performance will be presented.

B.2 Purpose

The base isolation choke is a very important part of the overall antenna structure. Its purpose is to isolate the antenna from the support structure. This is desirable for two reasons. Previous experience has shown that an antenna isolated from its platform will have fewer and less severe pattern variations and nulls. In addition, the input impedance of the antenna will be independant of its platform if properly isolated. The method of isolating antenna currents from the platform is to provide a high impedance between the antenna and the platform. Since the whip antenna of this thesis is fed above the mounting surface, a method of providing both the feed and the isolation must be found. A coaxial cable choke of the form shown in Figure B.1 will solve both problems. The interior of the coaxial cable constitutes a transmission line that extends from the base to the feedpoint of the antenna. The exterior of the coaxial cable from the feedpoint to the cable choke is the lower antenna element. At the area of the cable choke the coaxial cable is configured to present a high impedance from the lower antenna element to the mounting surface. The interior

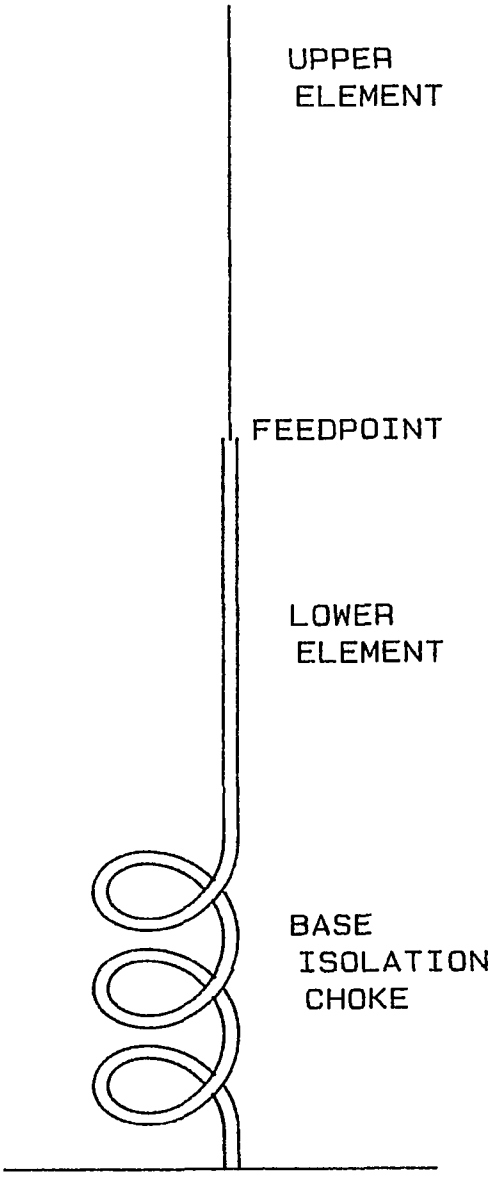

FIGURE B.1 BASE ISOLATION CHOKE

transmission line of the coaxial cable and the exterior cable choke do not interfere with each other. They perform the functions described above seperately and distinctly.

B.3 Electrical Parameters

It is desirable that the base isolation choke be high impedance. It is not obvious whether this high impedance should be inductive or capacitive. It is clear that the resistive losses should be as low as possible.

The base choke can be characterized by a resonant frequency (f_c) and an equivalent reactance (X_{ch}) which is capacitive ($X_{ch} = -1/\omega C_d$). Other characterizations are possible but for this investigation resonant frequency and distributed capacity are the most appropriate. Two additional computer programs were written to examine the effects of varying these electrical parameters. They are described briefly in the paragraphs below.

B.3.1 Computer Programs

Two computer programs were written to investigate the effects of varying the resonant frequency and distributed capacity of the base choke. The first program calculates the Q matrix of equation (37) for fixed antenna length and feedpoint height. The second program solves for the current on the antenna for various values of base choke resonant frequency and distributed capacity.

B.3.1.1 Q-Matrix - CALQβR

The computer program CALQβR calculates the Q matrix of equation (37). This program is presented at the end of this appendix. The calculation is made for a fixed antenna length and feedpoint height.

Line 2 is a statement dimensioning arrays. Line 3 establishes the

angular units as radians and specifies the antenna length. Line 4 selects the points where a solution of equation (41) will be required. Line 5 selects the frequency of study. Line 7 is a call to calculate the real and imaginary parts of the Q matrix. Lines 9 through 14 store the results of these calculations on disk in a file number selected by the frequency. Line 15 is the end of the main program. Lines 16 through 42 are a subroutine to calculate the Q matrix. Lines 20 and 21 are the call statements. Lines 23 through 27 establish the continuity relationships of equations (38) and (39). Lines 28 through 42 perform the numerical integration of equation (37). This integration is described in more detail in Appendix A.4.

B.3.1.2 Current Distribution - CALBIC

The computer program CALBIC calculates the current distribution of the antenna while varying the electrical parameters of the base isolation choke. This program is presented at the end of this appendix.

This program has functional similarity to program CALCUR. The essential differences are in lines 9 thru 18. Line 9 varys the resonant frequency (R) of the base choke from 25 MHz to 85MHz. The distributed capacity (matrix T) is selected to be 2pf, 5pf, or 10pf. Lines 13 and 14 determine the impedance of the load (matrix M). Lines 15 through 18 read the value of the Q matrix calculated by program CALQ8R into matrices Q and R. The program then continues similarly to program CALCUR described in appendix A.2.

B.3.2 Conclusions

The current distribution on the antenna can be plotted using program PLTCUR from Appendix A.3. An analysis of these plots will show the optimum resonant frequency and distributed capacity for the base

isolation choke. Interesting current distribution plots are included at the end of this appendix. Discussions in the following paragraphs will reference these plots by file number.

Files 961, 963, 965 are plots of current distribution with increasing values of resonant frequency (f= 25, 45, 65 MHz). It is most apparent in file 965 that increasing the resonant frequency of the base choke results in increasing amounts of base current especially at 30 MHz, 35 MHz, and 40 MHz. These distributions are undesirable because the antenna is not isolated from its support structure. This will result in field pattern, gain, and antenna impedance variations due to the antenna's dependence on the supporting structure. This analysis shows that the base isolation choke must have a resonant frequency lower than the lowest operating frequency. That is, the base isolation choke must be capacitive in order to prevent out of phase currents from developing on the antenna.

Files 961, 968 and 975 are plots of current distribution with increasing values of distributed capacity (C= 2, 5, 10pf). It is apparent in file 968 and more so in file 975 that increasing values of distributed capacity result in increasing amounts of base current especially at higher frequencies. The reason for this is that increasing the distributed capacity will decrease the impedance of the base isolation choke at frequencies above resonance. Increased base current is undesireable as discussed above. Therefore, the distributed capacity of the base isolation choke should be as small as possible.

B.4 Physical Construction

It was determined in section B.3 above that the base isolation choke should have a resonant frequency lower than the lowest operating

frequency and a distributed capacity as low as possible. The lowest operating frequency is 30 MHz. A coaxial cable choke self-resonant at 25 MHz would meet this requirement. A lower self-resonant frequency could be chosen but more inductance would be required. That is, for a fixed distributed capacity, inductance is inversely proportional to frequency squared [37]. It is physically more difficult to build a larger value of inductance. Therefore, the self-resonant frequency was fixed at 25 MHz. The following investigation was conducted to determine a physical realization of the base choke with minimum distributed capacity.

A coaxial cable choke can be made by winding the coaxial cable on a ferrite rod or toroid. If a ferrite rod is used, some of the flux produced will be lost since there is a gap in the magnetic path. This will result in less inductance per turn as compared to a toroid. More turns and consequently longer wire will be required to make a particular value of inductance on a rod than a toroid. Both more turns and longer wire create more distributed capacity. Therefore, a toroid is a better choice than a rod on which to wind the base isolation choke.

Several physical configurations of toroids were constructed to determine which produced the least distributed capacity. The toroids were wound with sufficient turns to be self-resonant as close as possible to 25 MHz. The impedance of the base isolation chokes were measured at several frequencies on an RX meter. Figure B.2 shows the capacity plotted as a function of $1/f^2$. A straight line is drawn through the data points. The line strikes the frequency axis at the resonant frequency. The line strikes the capacity axis at a value equal to the distributed capacity. Therefore, the base isolation choke with

the least distributed capacity can easily be determined from this plot.

The physical construction of the base isolation choke with the least distributed capacity is rather unique. A patent application is currently being processed. Figure B.3 shows the winding pattern. Instead of winding the toroid continuously in one direction as shown in Figure B.3(a), the toroid is cross-wound (see Figure B.3(b)). In this configuration the toroid is first wound half way in one direction. The cable then crosses the center of the toroid toward the beginning end. The other half of the winding is then completed in the opposite direction. The purpose of this winding technique is to reduce the distributed capacity. This is accomplished in the following manner. The toroid can be thought of as two series inductors with their associated distributed capacities. These capacities are now also in series thus reducing the overall distributed capacity.

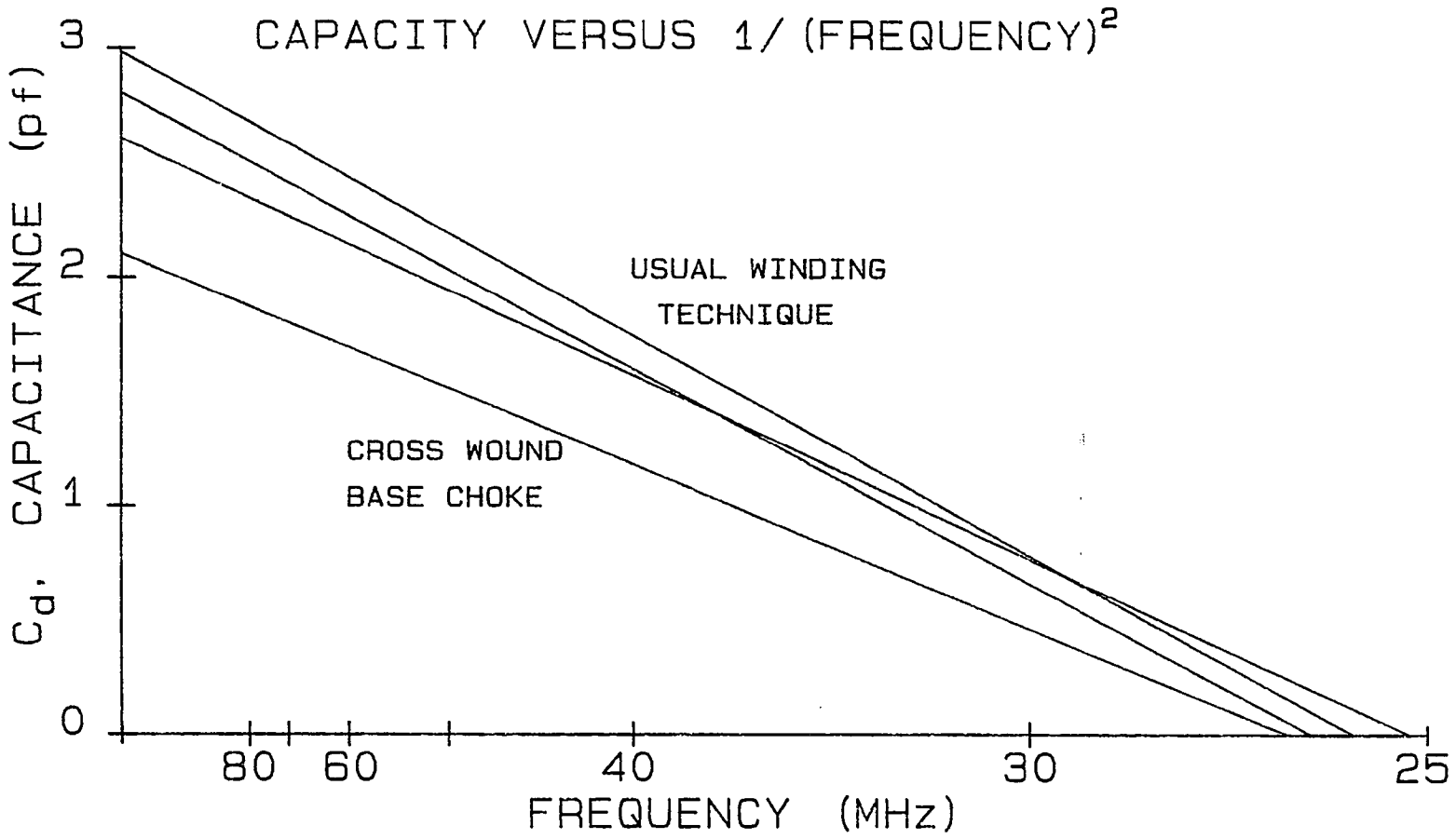

FIGURE B.2 DISTRIBUTED CAPACITY VERSUS 1/FREQUENCY

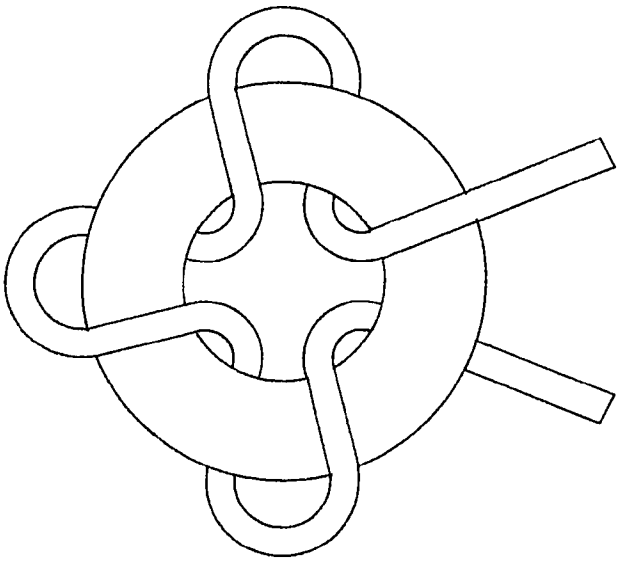

(a) USUAL WINDING

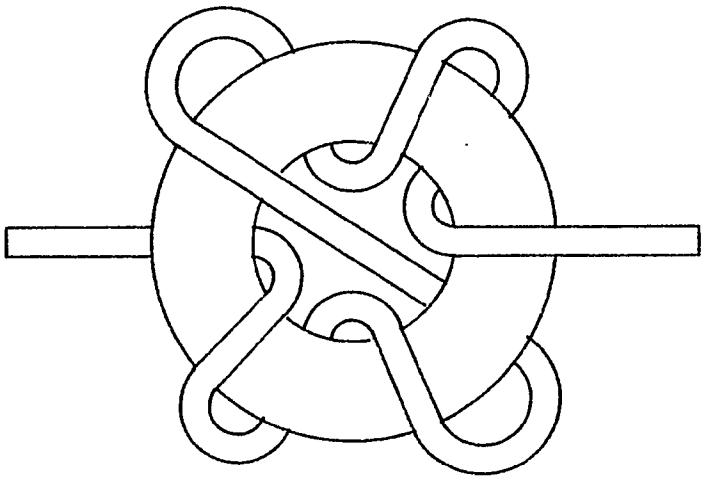

(b) CROSS-WOUND

FIGURE B.3 WINDING PATTERN

```
0: "PROGRAM TO CALCULATE Q & R MATRICES":
1: "PROGRAM NAME CALQ&R":
2: dim Q[6,7],R[6,7],Z[4],L[3],M$[4],N$[3]
3: rad;.0041275→A;0→L[1];1→L[2];2.5→L[3]
4: L[2]/2→Z[1];L[2]→Z[2];L[2]+(L[3]-L[2])/2→Z[3];L[3]→Z[4]
5: for F=30 to 90 by 5
6: "BETA":2*π*F/300→B
7: "CALCULATE Q&R MATRIX":cll 'Q&R'
8: "STORE ON DISK":
9: fxd 0;str(F+100)→M$;M$[2,4]→N$
10: asgn N$,1,0
11: sprt 1,Q[*],"end"
12: fxd 0;str(F+101)→M$;M$[2,4]→N$
13: asgn N$,1,0
14: sprt 1,R[*],"end"
15: next F;end
16: "Q & R MATRIX CALCULATION":
17: "Q&R":
18: for I=1 to 2;L[I]→L;L[I+1]→U
19: for P=1 to 4;Z[P]→Z;for K=1 to 3
20: cll 'RQ(z,i,k)'(Z,L,U,B,A,K,Q[P+2,K+3*I-3])
21: cll 'IQ(z,i,k)'(Z,L,U,B,A,K,R[P+2,K+3*I-3])
22: next K;next P;next I
23: "CONTINUITY EQUATIONS":
24: for K=1 to 3;0→Q[2,K]→R[2,K]
25: 1→Q[1,K]→R[1,K]→Q[2,K+3]→R[2,K+3];next K
26: 0→Q[1,7]→Q[2,7]→R[1,7]→R[2,7];-1→Q[1,4]→R[1,4]
27: -L[2]/L[3]→Q[1,5]→R[1,5];-(L[2]/L[3])^2→Q[1,6]→R[1,6]
28: ret
29: "NUMERICAL INTEGRATION":
30: "RQ(z,i,k)":0→p7
31: for T=1 to 100;T*.01*(p3-p2)-.005*(p3-p2)+p2→S
32: √(S^2+p5^2)→p8;√((p1-S)^2+p5^2)→p9
33: √((p1+S)^2+p5^2)→p10
34: S^(p6-1)*cos(p4*p9)/p9+p7→p7
35: -(S^(p6-1)*2*cos(p4*p1)*cos(p4*p8)/p8)+p7→p7
36: S^(p6-1)*cos(p4*p10)/p10+p7→p7
37: next T;.01*(p3-p2)*p7/p3^(p6-1)→p7;ret
38: "IQ(z,i,k)":0→p7
39: for T=1 to 100;T*.01*(p3-p2)-.005*(p3-p2)+p2→S
40: √(S^2+p5^2)→p8;√((p1-S)^2+p5^2)→p9
41: √((p1+S)^2+p5^2)→p10
42: -(S^(p6-1)*sin(p4*p9)/p9)+p7→p7
43: S^(p6-1)*2*cos(p4*p1)*sin(p4*p8)/p8+p7→p7
44: -(S^(p6-1)*sin(p4*p10)/p10)+p7→p7
45: next T;.01*(p3-p2)*p7/p3^(p6-1)→p7;ret
```

FIGURE B.4 PROGRAM CALQ&R

```
0: "PROGRAM TO CALCULATE CURRENT DISTRIBUTION ON ANTENNA":
1: "WHILE VARYING THE BASE ISOLATION CHOKE":
2: "PROGRAM NAME CALBIC":
3: dim X[6],Y[6],Z[4],L[3],M[1],G[4],T[3],M$[4],N$[3]
4: dim A[6,7],C[6,7],Q[6,7],R[6,7],H[4,1],D[13,12]
5: rad;.0041275→A;0→L[1];1→L[2];2.5→L[3]
6: 2→T[1];5→T[2];10→T[3]
7: L[2]/2→Z[1];L[2]→Z[2];L[2]+(L[3]-L[2])/2→Z[3];L[3]→Z[4]
8: "BASE ISOLATION CHOKE":
9: for T=1 to 3;for R=25 to 85 by 10
10: for F=30 to 90 by 5
11: "BETA":2*π*F/300→B
12: if R=F;1e6→M[1];gto +3
13: 1/4ππ2R^2→r8;2πFr8tn^6→r9
14: -1/2πFT[T]tn^(-6)→r10;r9*r10/(r9+r10)→M[1]
15: fxd 0;str(F+100)→M$;M$[2,4]→N$
16: asgn N$,1;sread 1,Q[*]
17: fxd 0;str(F+101)→M$;M$[2,4]→N$
18: asgn N$,1;sread 1,R[*]
19: "P= 4 POINTS ON ANTENNA Z[P]":
20: "CALCULATE LOAD FUNCTION AND DRIVING FUNCTION":
21: for P=1 to 4;Z[P]→Z
22: cll 'H(z,zi)'(Z,L[1],B,M[1],H[P,1])
23: cll 'G(z)'(Z,L[2],B,1,G[P]);next P
24: "LOAD SOLUTION MATRICES A[]=REAL, C[]=IMAGINARY":
25: for P=1 to 4;Q[P+2,1]-H[P,1]→A[P+2,1];next P
26: 1→I;for K=1 to 3;for P=1 to 4
27: R[P+2,K+3*I-3]→C[P+2,K+3*I-3]
28: if K=1 and I=1;gto +2
29: Q[P+2,K+3*I-3]→A[P+2,K+3*I-3]
30: next P;next K
31: 2→I;for K=1 to 3;for P=1 to 4
32: R[P+2,K+3*I-3]→C[P+2,K+3*I-3]
33: Q[P+2,K+3*I-3]→A[P+2,K+3*I-3]
34: next P;next K
35: for K=1 to 7;for P=1 to 2
36: Q[P,K]→A[P,K];R[P,K]→C[P,K];next P;next K
37: for P=1 to 4;0→A[P+2,7];G[P]→C[P+2,7];next P
38: "SOLVE FOR CURRENTS X[] & Y[]":
39: cll 'SOLVE'
40: if flg4;stp
41: for I=1 to 6;X[I]→D[(F-25)/5,I];Y[I]→D[(F-25)/5,I+6]
42: next I;next F
43: "STORE ON DISK":
44: fxd 0;str(960+(T-1)7+(R-15)/10)→M$;M$[2,4]→N$
45: asgn N$,1,0
46: sprt 1,D[*],"end"
47: next R;next T;end
```

FIGURE B.5 PROGRAM CALBIC

```
48: "ROUTINE TO CALCULATE LOAD FUNCTION":
49: "G(z)":
50: "H(z,zi)":0→p5
51: 2*cos(p3*p1)*sin(p3*p2)→p5
52: -sin(p3*abs(p1-p2))-sin(p3*abs(p1+p2))+p5→p5
53: p4*p5/60→p5;ret
54: "ROUTINE TO SOLVE COMPLEX MATRIX EQUATIONS":
55: "SOLVE":cfg 4;0→I;6→N
56: "BRANCH TO BACKSOLVE":if (I+1→I)=N;gto +21
57: "FIND MAX PIVOT ROW":I-1→K;0→p1
58: if (K+1→K)>N;gto +4
59: cll 'CMOD'(A[K,I],C[K,I],p2)
60: if (p2→p3)>p1;p3→p1;K→p4
61: gto -3
62: "IF MAX PIVOT=0, DET=0":if p1=0;sfg 4;dsp "DET=0";ret
63: "NO SWITCH ROWS IF":I→J;if I=p4;gto +5
64: "INTERCHANGE ROW I WITH PIVOT ROW p4":
65: A[I,J]→p3;A[p4,J]→A[I,J];p3→A[p4,J];jmp (J+1→J)>N+1
66: I→J
67: C[I,J]→p3;C[p4,J]→C[I,J];p3→C[p4,J];jmp (J+1→J)>N+1
68: "NORMALIZE PIVOT ROW":I+1→J;A[I,I]→p1;C[I,I]→p5
69: cll 'CDIV'(A[I,J],C[I,J],p1,p5,p6,C[I,J]);p6→A[I,J]
70: if(J+1→J)>N+1;gto-1
71: I→K
72: if (K+1→K)>N;gto -16
73: "REDUCTION OF OTHER ROWS":I+1→J
74: cll 'CMULT'(A[K,I],C[K,I],A[I,J],C[I,J],p7,p8)
75: cll 'CSUBT'(A[K,J],C[K,J],p7,p8,A[K,J],C[K,J])
76: if (J+1→J)<N+2;gto -2
77: gto -5
78: "CHECK DET=0":cll 'CMOD'(A[N,N],C[N,N],p9)
79: if p9=0;0→p1;gto -17
80: "BACKSOLVE":
81: cll 'CDIV'(A[N,N+1],C[N,N+1],A[N,N],C[N,N],X[N],Y[N])
82: N→I
83: "SUBROUTINE FINISHED":if (I-1→I)<1;ret
84: N→K;0→p12→p13
85: cll 'CMULT'(A[I,K],C[I,K],X[K],Y[K],p10,p11)
86: cll 'CADD'(p10,p11,p12,p13,p12,p13)
87: if (K-1→K)>=I+1;gto -2
88: cll 'CSUBT'(A[I,N+1],C[I,N+1],p12,p13,X[I],Y[I]);gto -5
89: "COMPLEX ARITHMETIC":
90: "CADD":p1+p3→p5;p2+p4→p6;ret
91: "CSUBT":p1-p3→p5;p2-p4→p6;ret
92: "CMULT":p1*p3-p2*p4→p5;p2*p3+p1*p4→p6;ret
93: "CDIV":(p1*p3+p2*p4)/(p3^2+p4^2)→p5
94: (p2*p3-p1*p4)/(p3^2+p4^2)→p6;ret
95: "CMOD":√(p1^2+p2^2)→p3;ret
```

FIGURE B.5 PROGRAM CALBIC CONTINUED

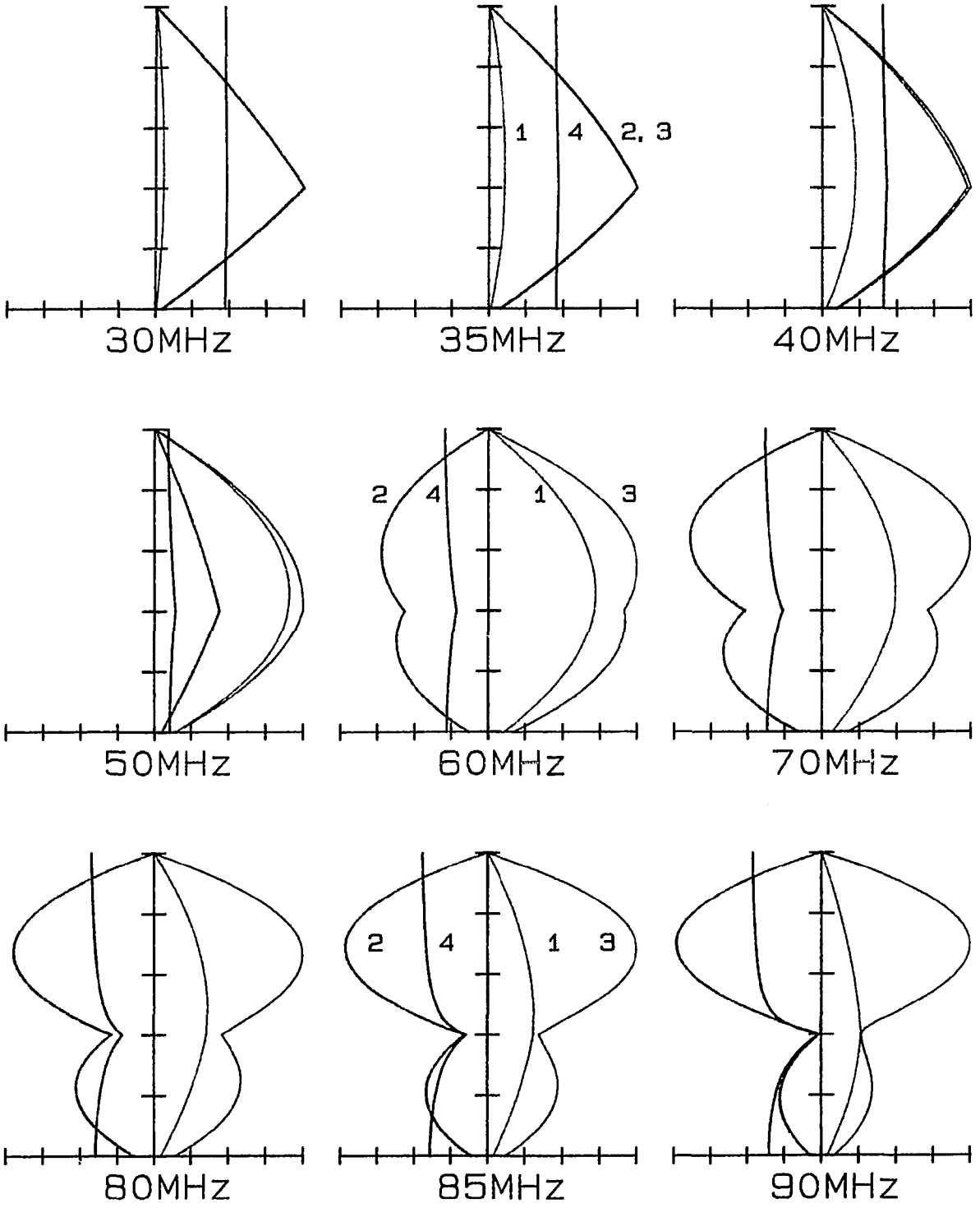

REAL (1) IMAGINARY (2) MAGNITUDE (3) PHASE (4)

FIGURE B.6 FILE 961 NORMALIZED CURRENT DITRIBUTIONS FOR BASE ISOLATION CHOKE RESONANT FREQUENCY = 25 MHZ AND DISTRIBUTED CAPACITY = 2 PICOFARADS

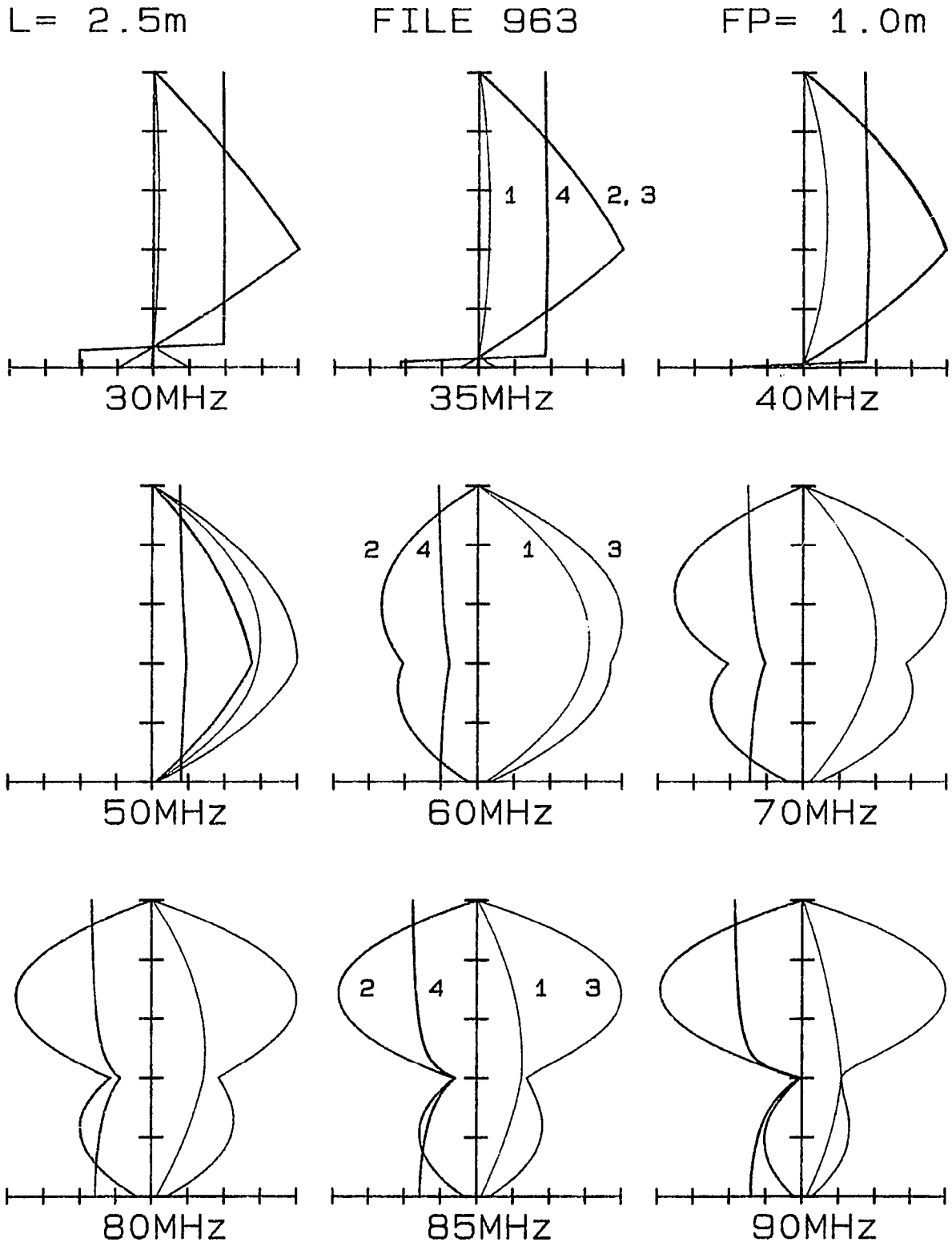

FIGURE B.7 FILE 963 NORMALIZED CURRENT DITRIBUTIONS FOR BASE ISOLATION CHOKE RESONANT FREQUENCY = 45 MHZ AND DISTRIBUTED CAPACITY = 2 PICOFARADS

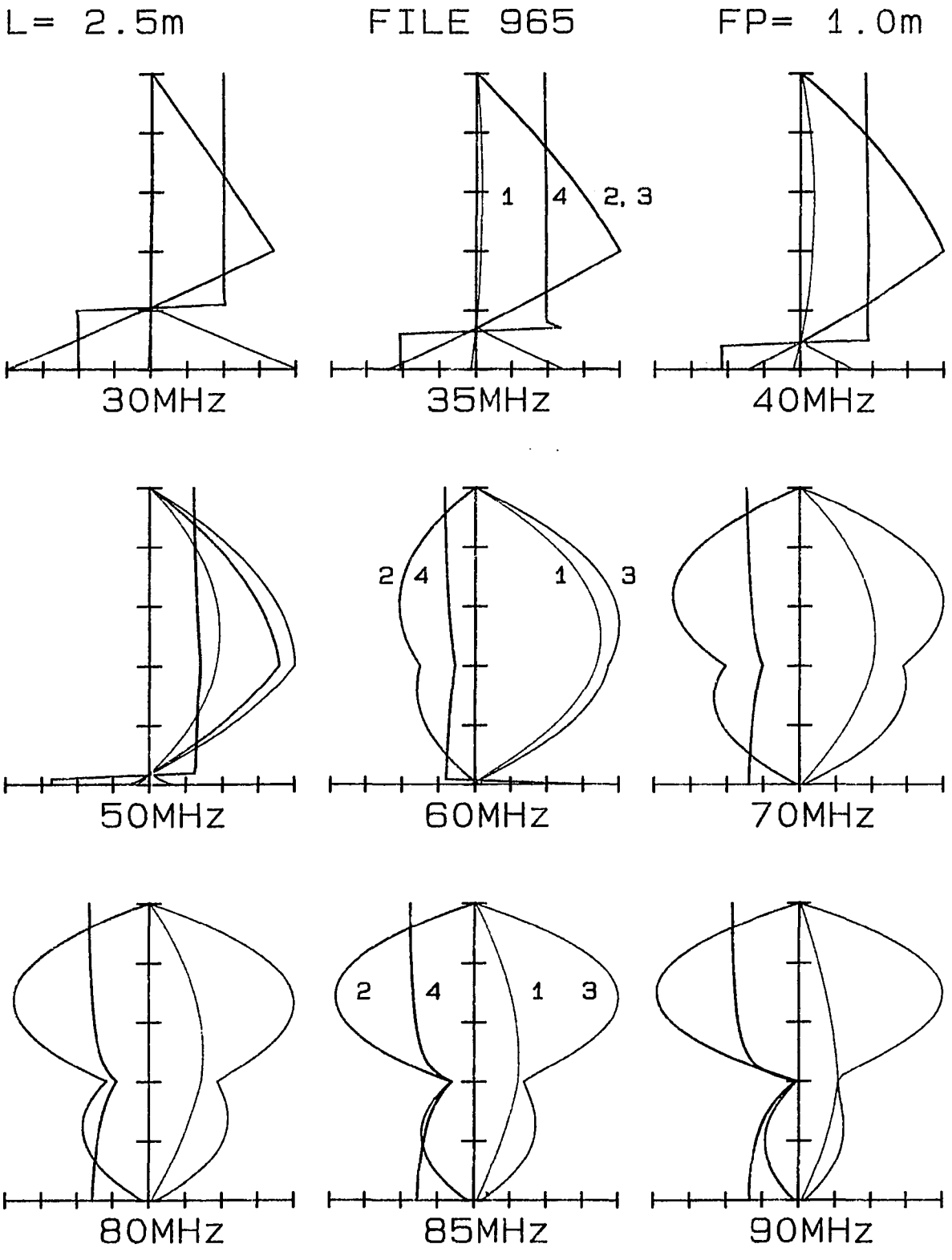

FIGURE B.8 **FILE 965 NORMALIZED CURRENT DITRIBUTIONS FOR BASE ISOLATION CHOKE RESONANT FREQUENCY = 65 MHZ AND DISTRIBUTED CAPACITY = 2 PICOFARADS**

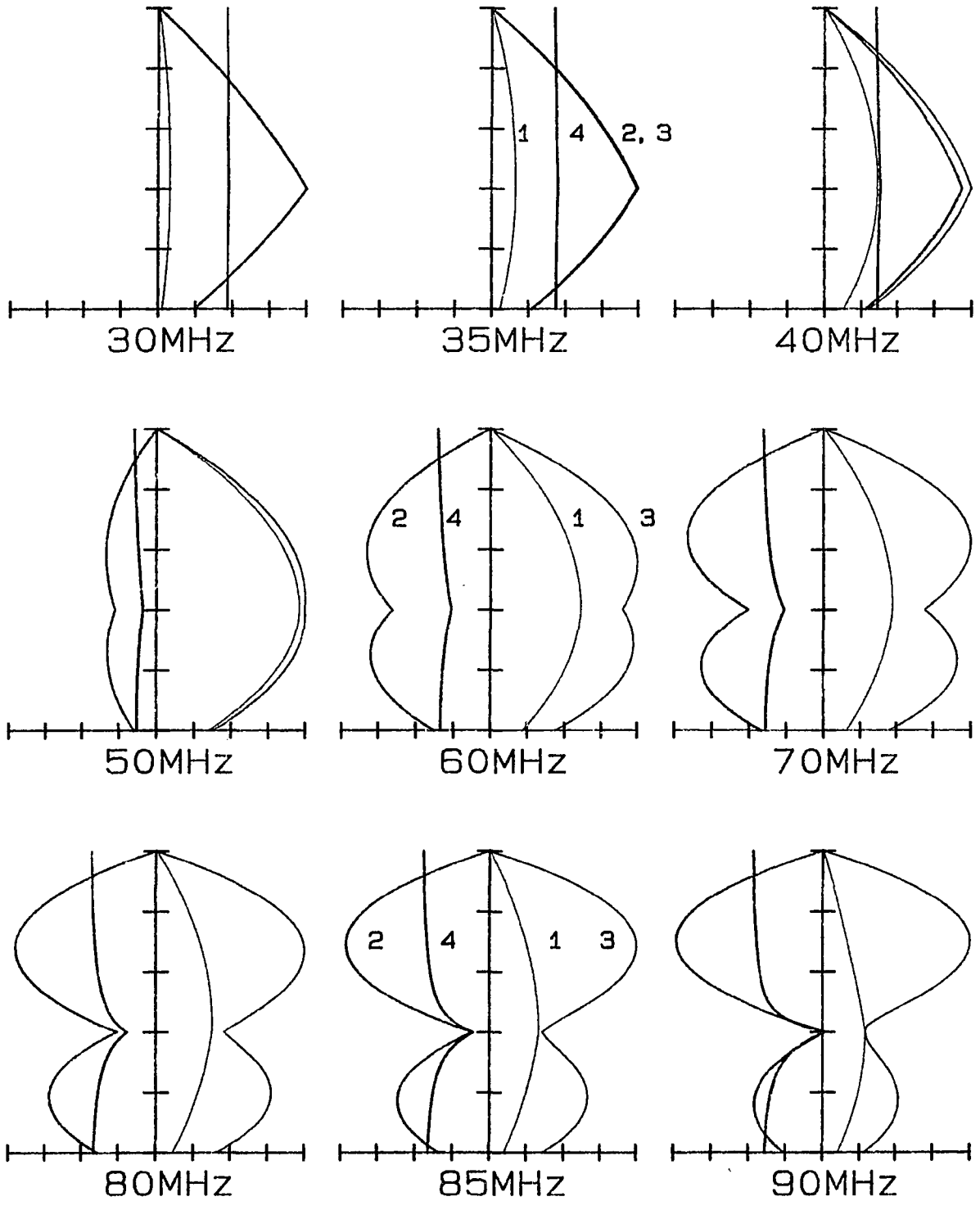

REAL (1) IMAGINARY (2) MAGNITUDE (3) PHASE (4)

FIGURE B.9 **FILE 968 NORMALIZED CURRENT DITRIBUTIONS FOR BASE ISOLATION CHOKE RESONANT FREQUENCY = 25 MHZ AND DISTRIBUTED CAPACITY = 5 PICOFARADS**

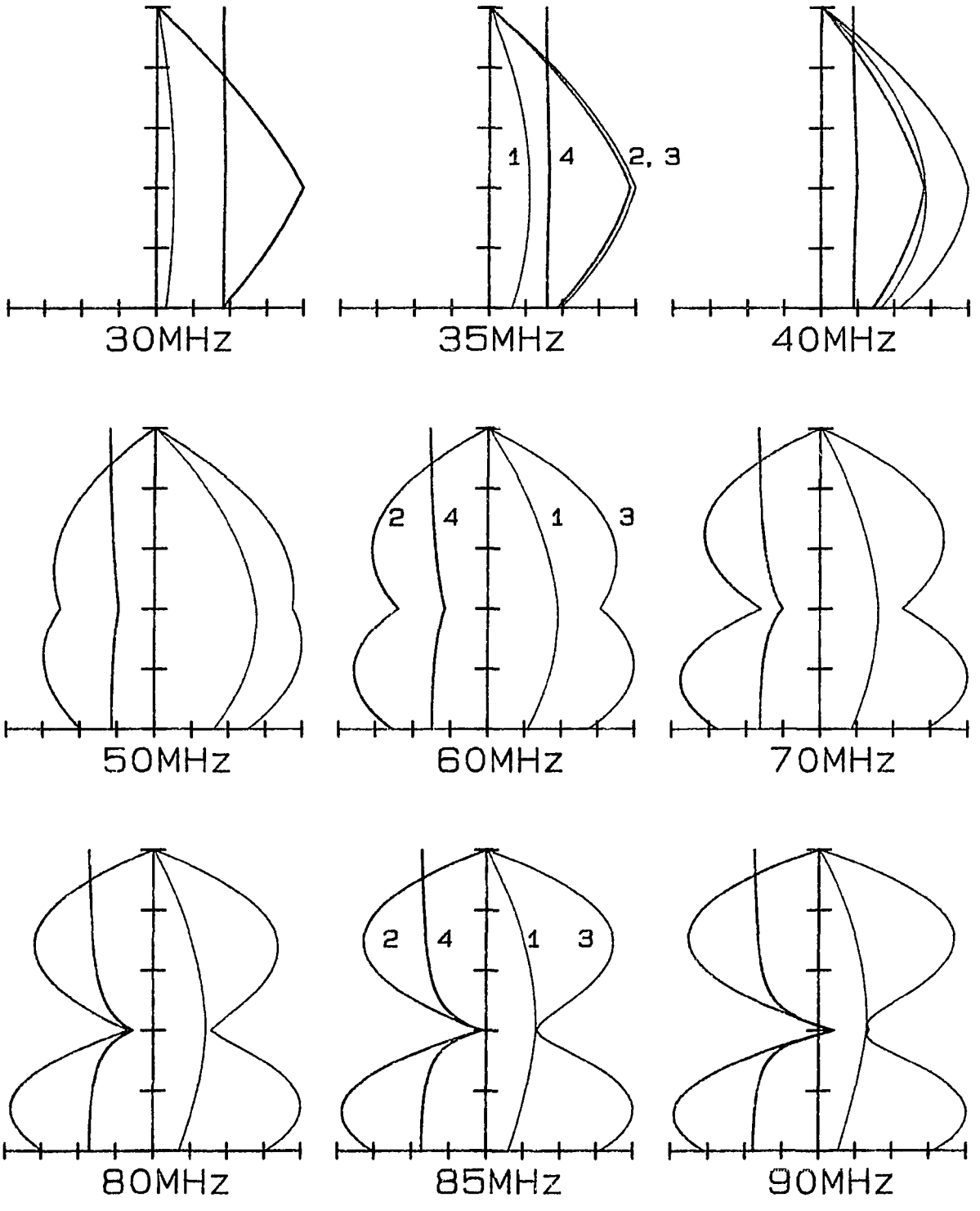

FIGURE B.10 FILE 975 NORMALIZED CURRENT DITRIBUTIONS FOR BASE ISOLATION CHOKE RESONANT FREQUENCY = 25 MHZ AND DISTRIBUTED CAPACITY = 10 PICOFARADS

APPENDIX C

GAIN ON THE HORIZON

Complete plots of gain on the horizon relative to a quarter wave monopole are discussed in this appendix. The computer programs of Appendix A.6, A.7, and A.8 are used to generate these gain plots. The plots are included at the end of this appendix.

Figures C.1 through C.7 hold the feedpoint height constant and vary the antenna length. Examination of these plots at 30 MHz shows that an antenna length of 3.0 meters has the highest gain.

Figures C.8 through C.14 hold the antenna length constant and vary the feedpoint height. At an antenna length of 3.0 meters, the most optimum antenna has a feedpoint height of 1.4 meters.

It is interesting to determine what causes such a large variation in gain at 90 MHz. For an antenna length of 3.0 meters, compare the field patterns and current distribution for feedpoint heights of .8 meters and 1.4 meters in Figures C.15, C.16, C.17, and C.18. The field patterns and current distribution plots are included at the end of this chapter. The field pattern of Figure C.15 shows most of the radiation going into the sky and little on the horizon. The field pattern of Figure C.16 shows most of the radiation energy directed along the horizon.

Examination of the current distributions shows why the gain and field patterns are so different. The current distribution plot shows the real, imaginary, magnitude and phase of current on the antenna. Figure C.18 at 90 MHz shows the current magnitude to have two major lobes. The phase of this current is roughly the same. Therefore the

radiation due to both lobes will add on the horizon. Figure C.17 at 90 MHz also shows the current magnitude to have two major lobes. However, the relative phase difference of these two lobes is 180 degrees. Therefore, the radiation will tend to cancel on the horizon and produce less gain.

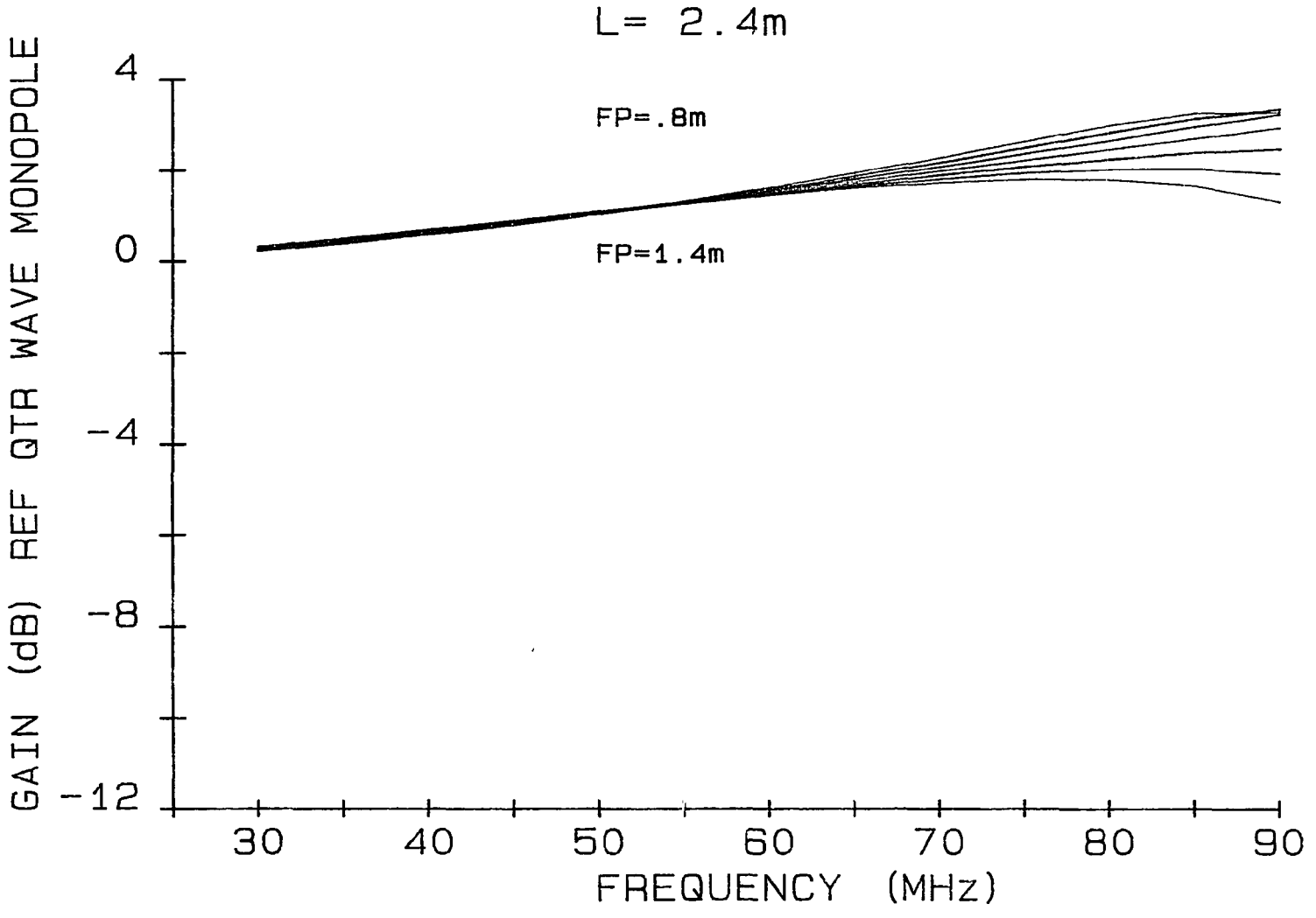

FIGURE C.1 GAIN (LENGTH = 2.4 METERS)

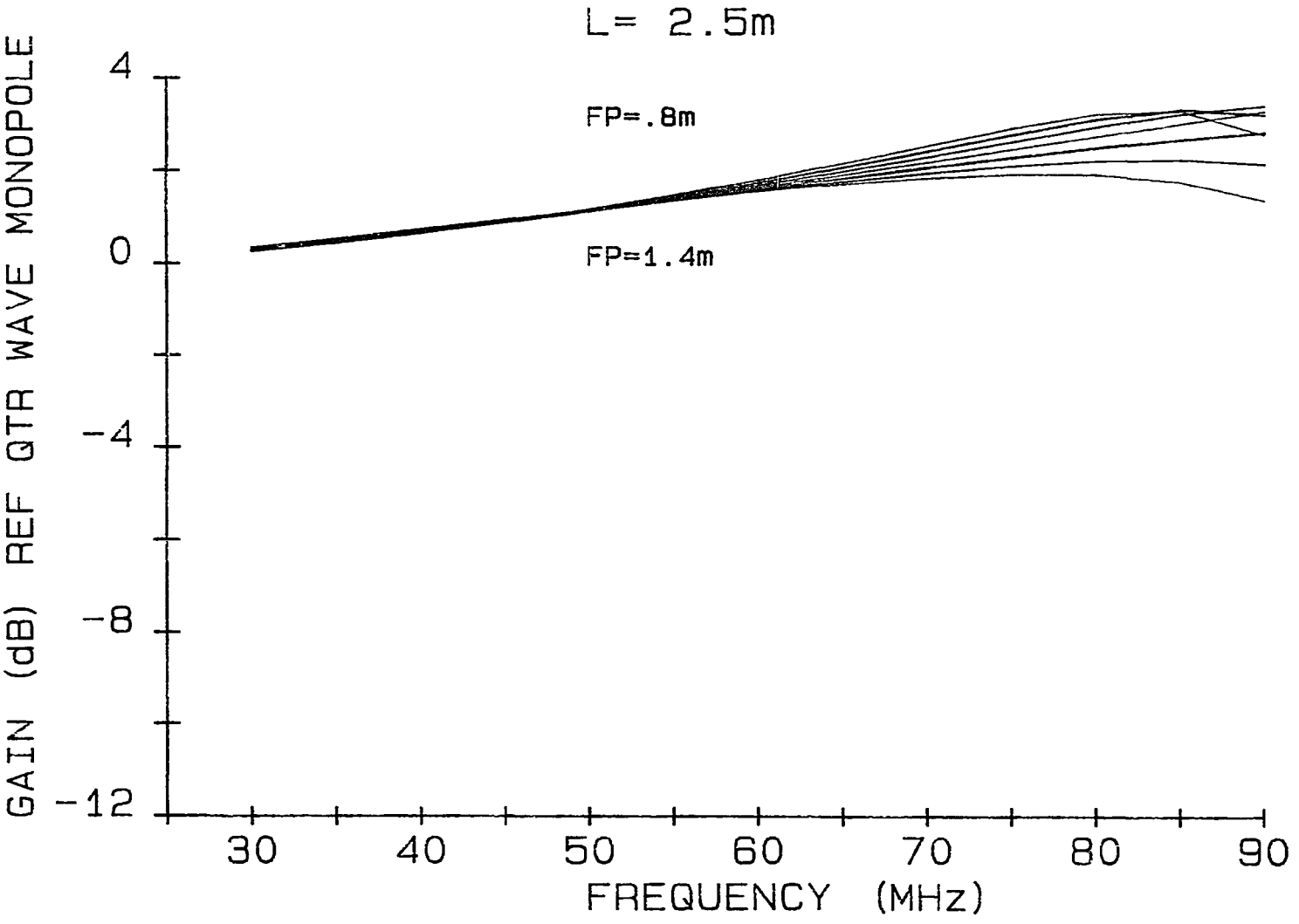

FIGURE C.2 GAIN (LENGTH = 2.5 METERS)

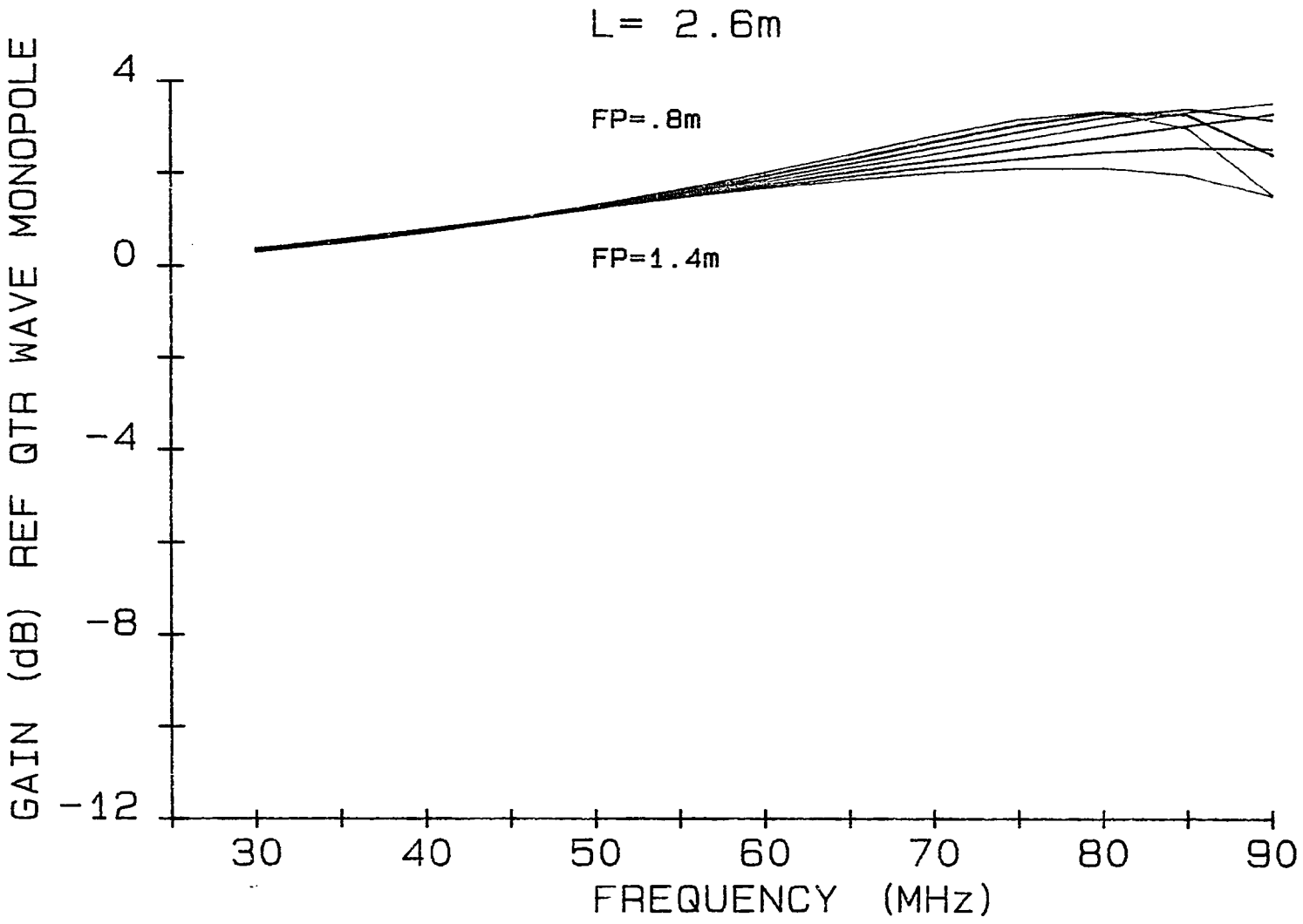

FIGURE C.3 GAIN (LENGTH = 2.6 METERS)

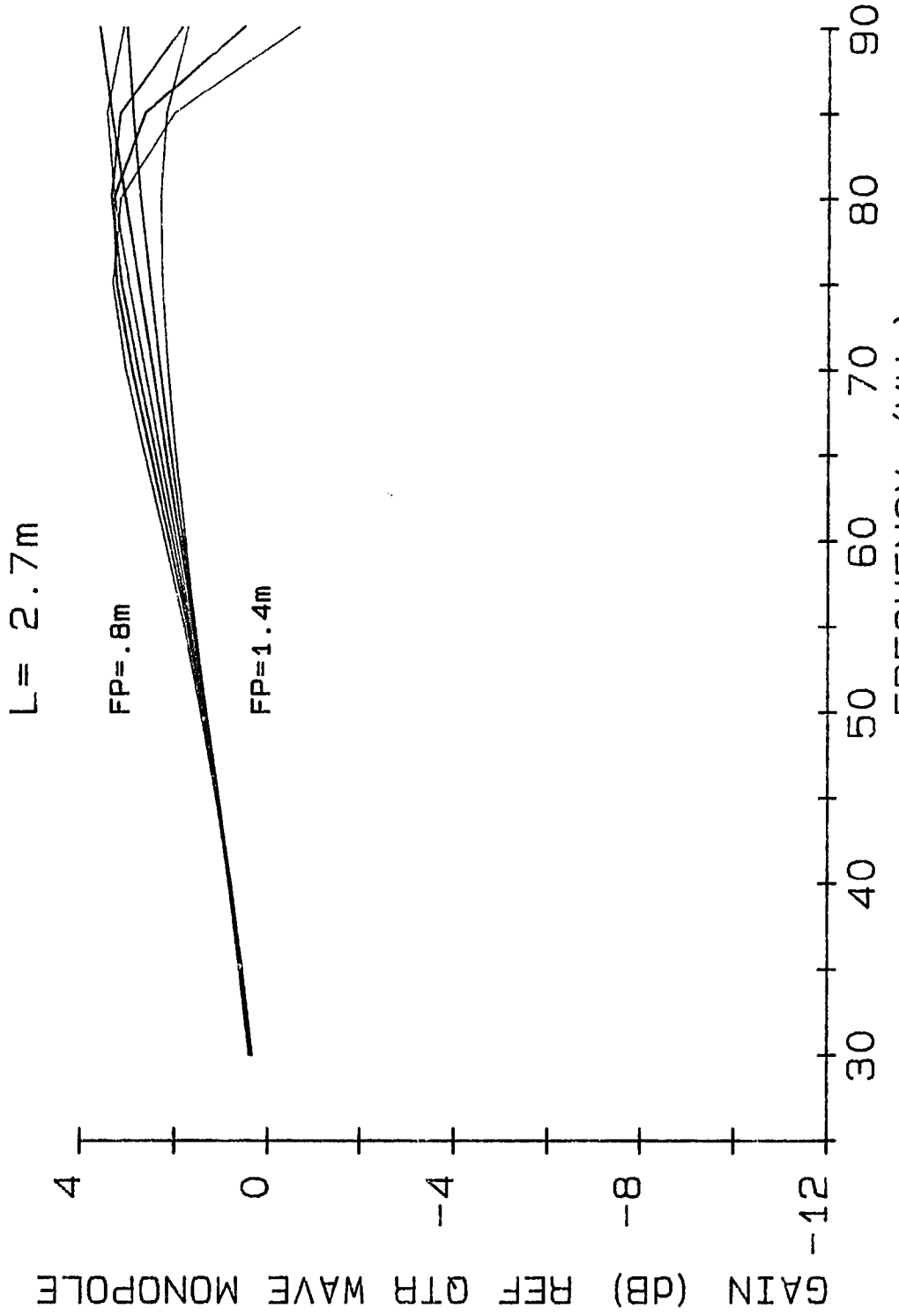

FIGURE C.4 GAIN (LENGTH = 2.7 METERS)

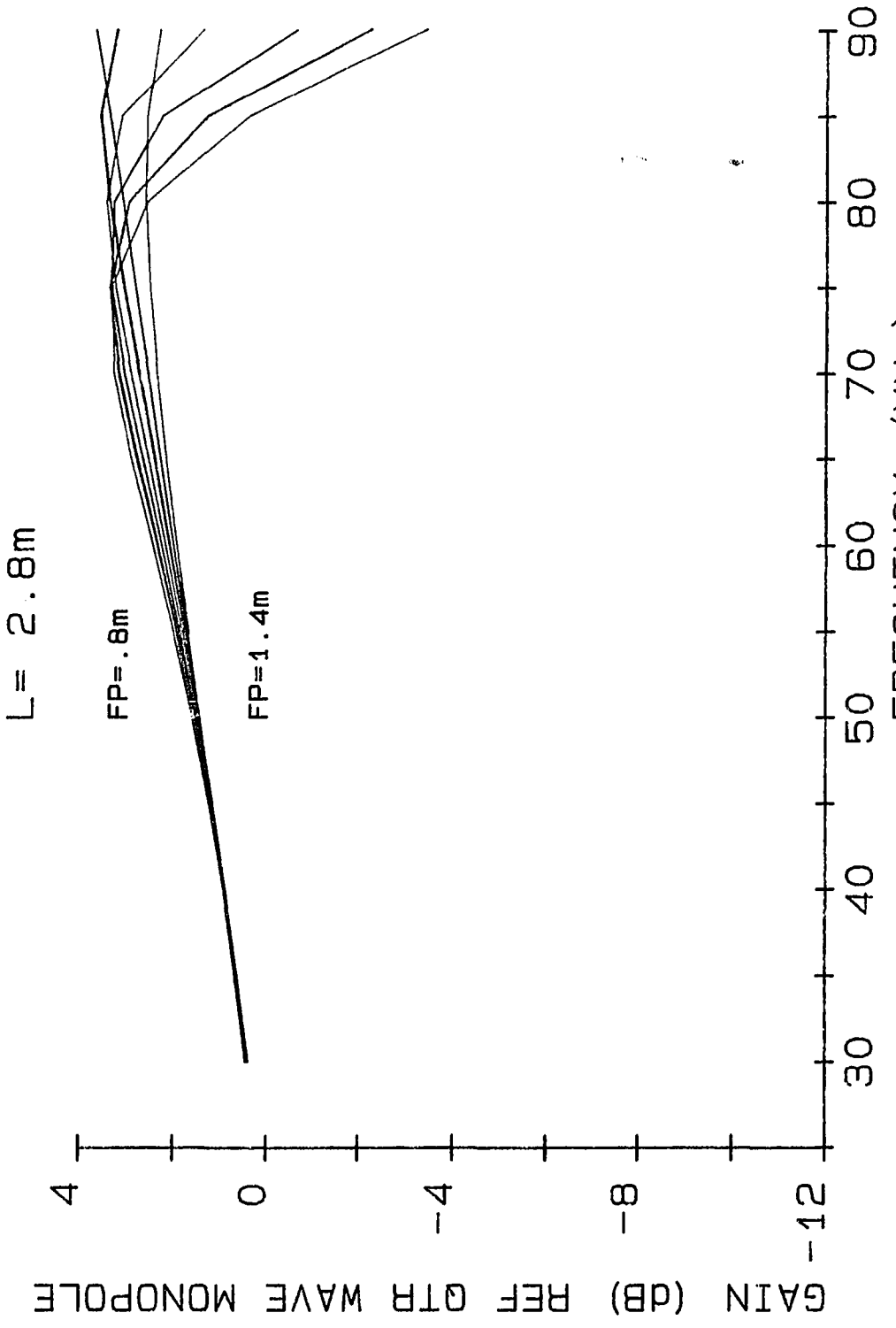

FIGURE C.5 GAIN (LENGTH = 2.8 METERS)

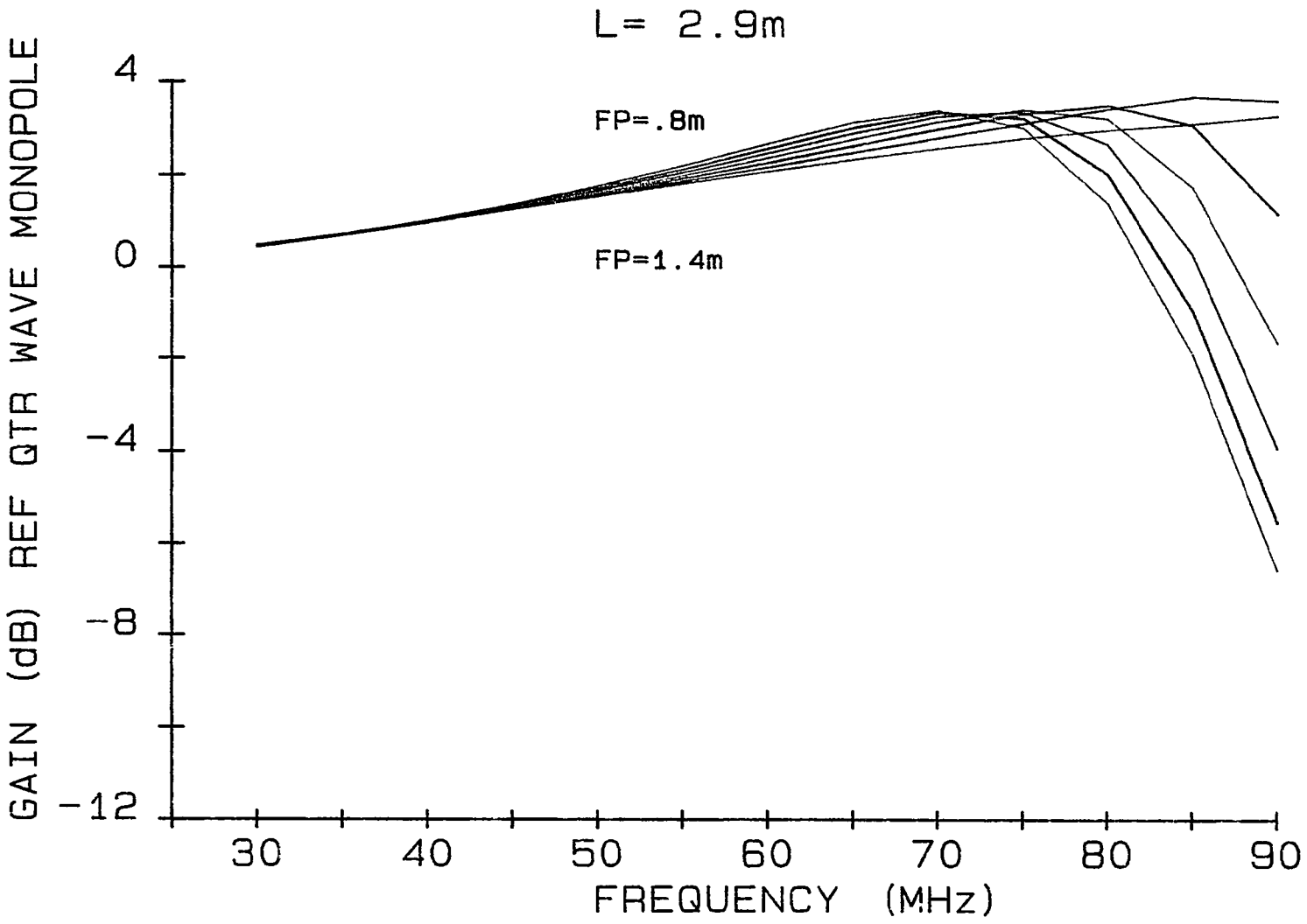

FIGURE C.6 GAIN (LENGTH = 2.9 METERS)

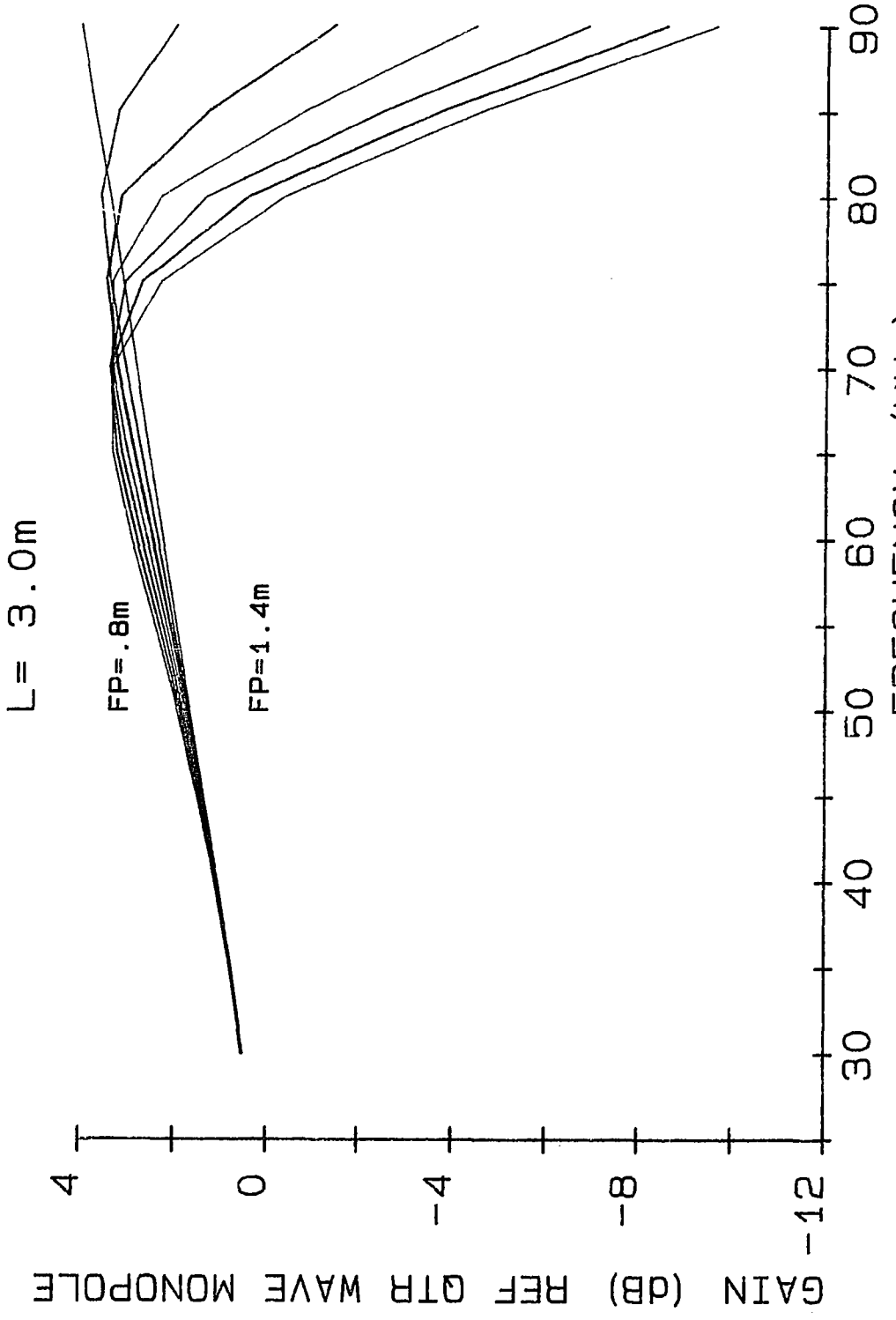

FIGURE C.7 GAIN (LENGTH = 3.0 METERS)

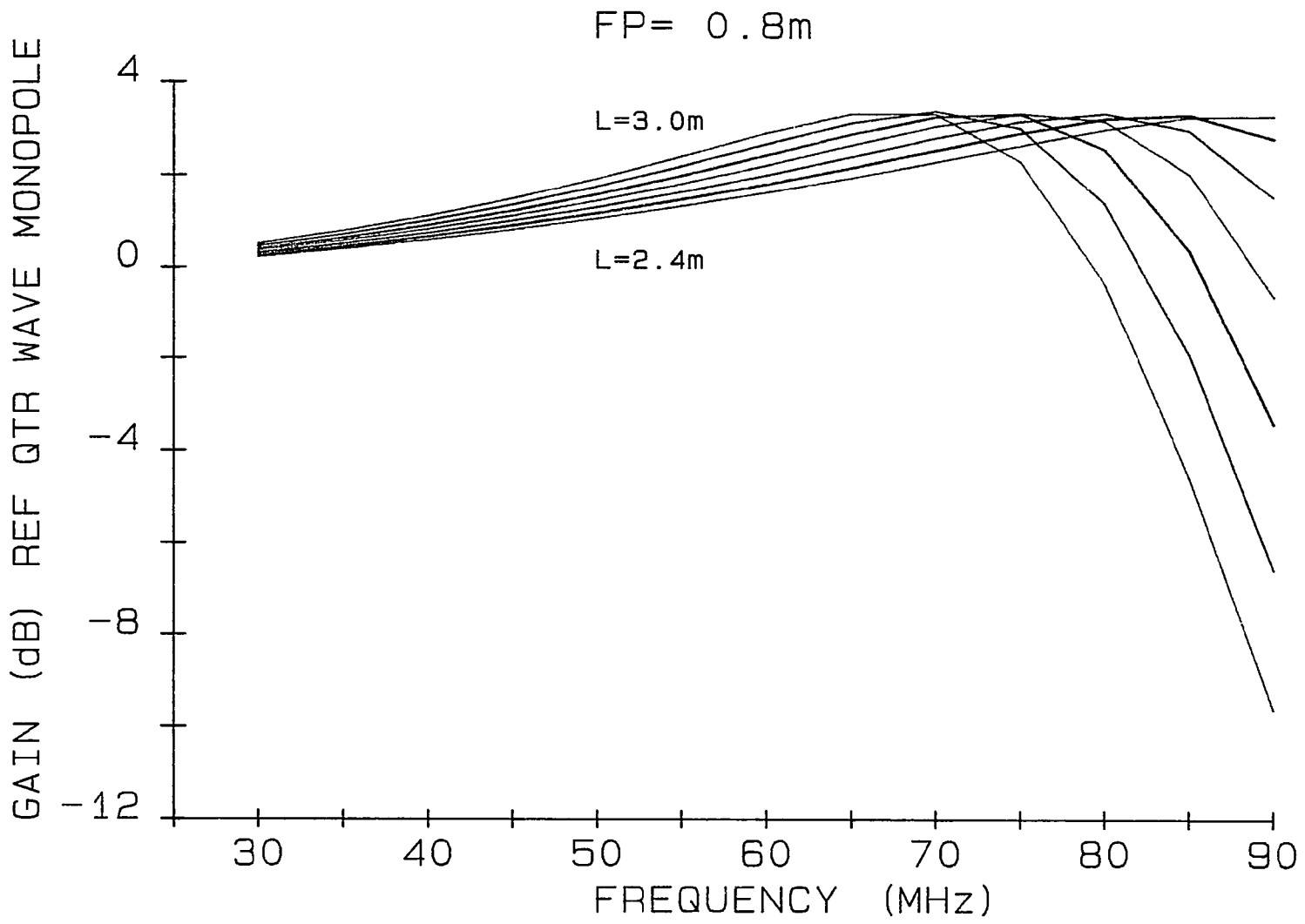

FIGURE C.8 GAIN (FEEDPOINT = 0.8 METERS)

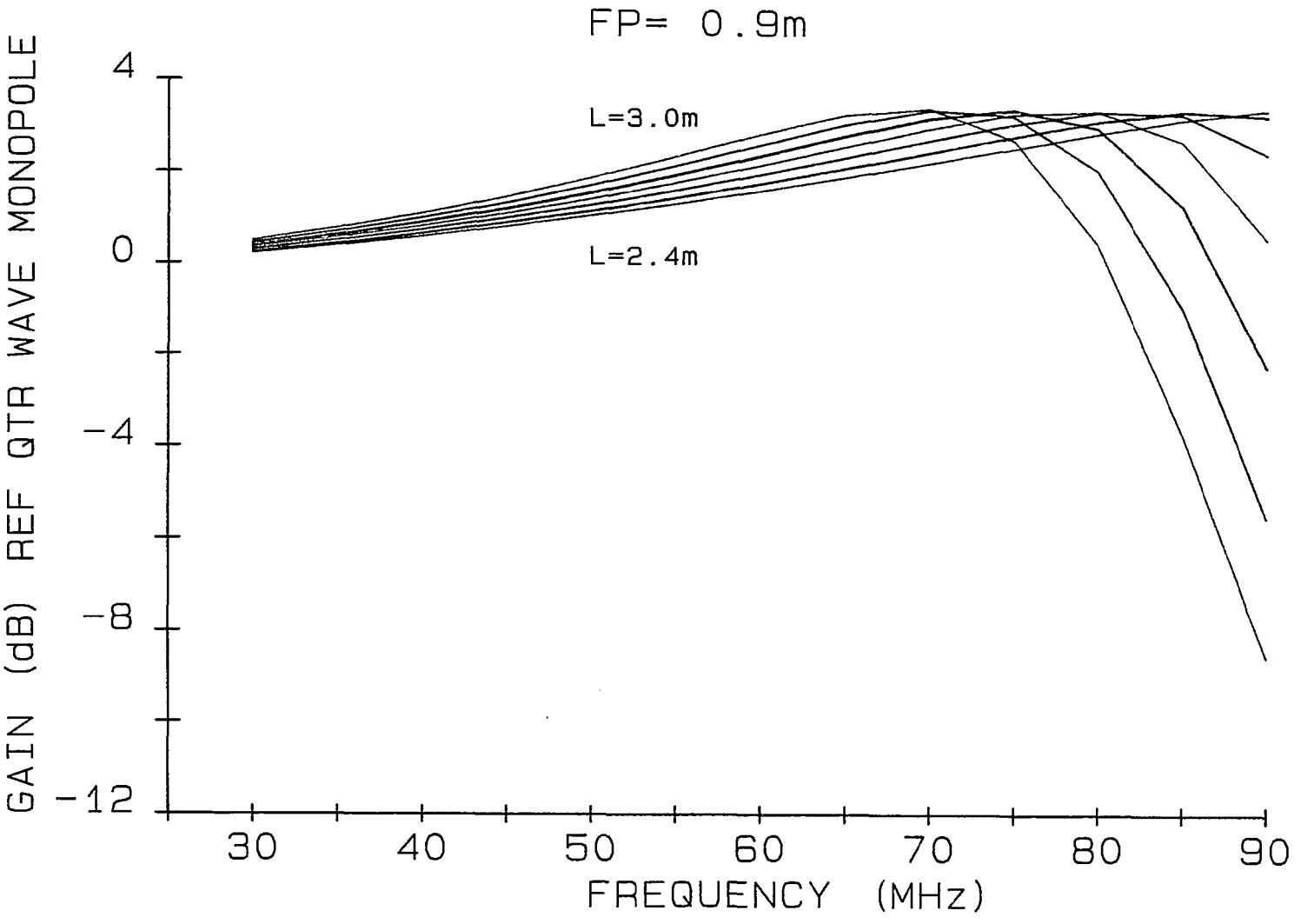

FIGURE C.9 GAIN (FEEDPOINT = 0.9 METERS)

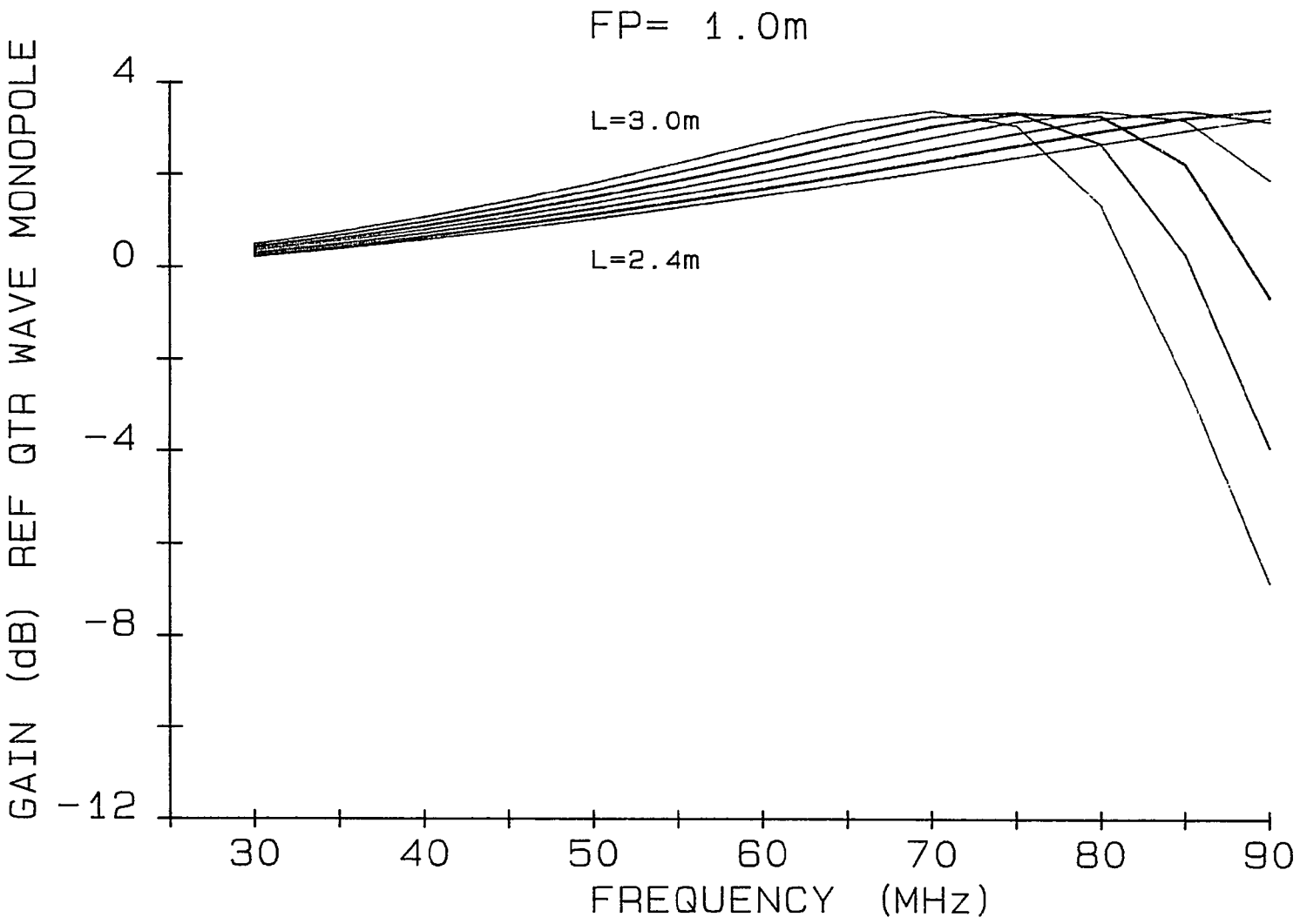

FIGURE C.10 GAIN (FEEDPOINT = 1.0 METERS)

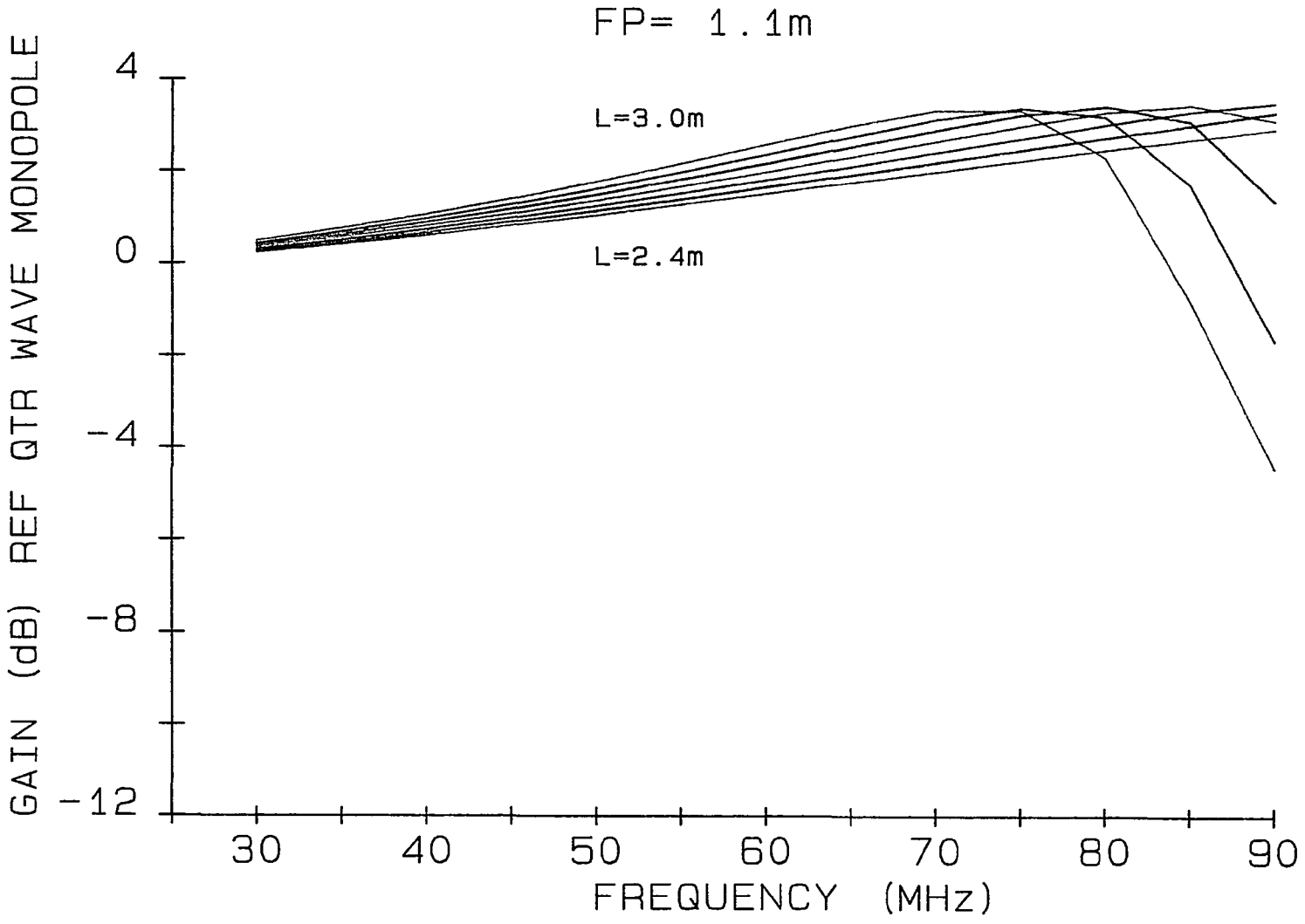

FIGURE C.11 GAIN (FEEDPOINT = 1.1 METERS)

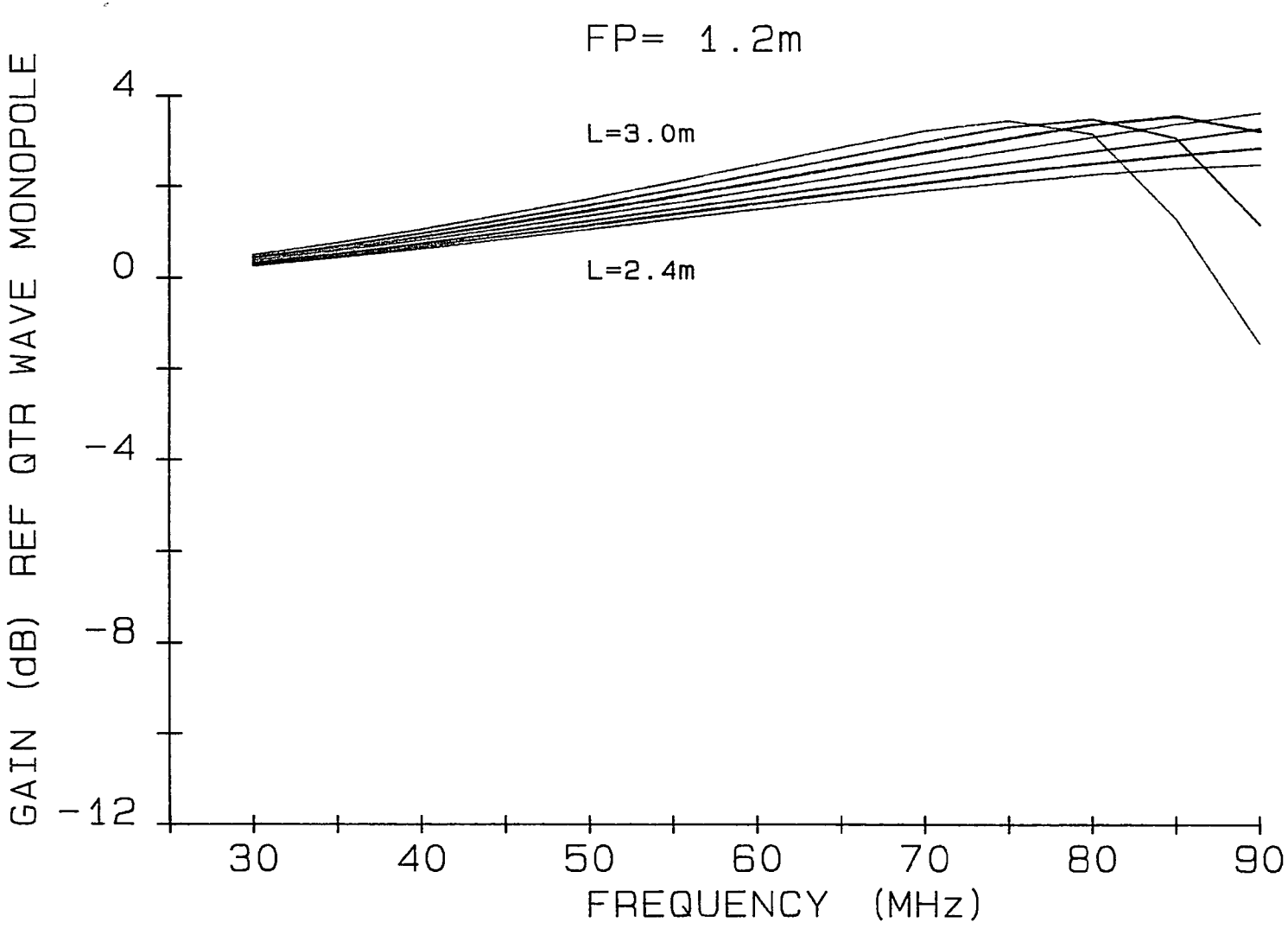

FIGURE C.12 GAIN (FEEDPOINT = 1.2 METERS)

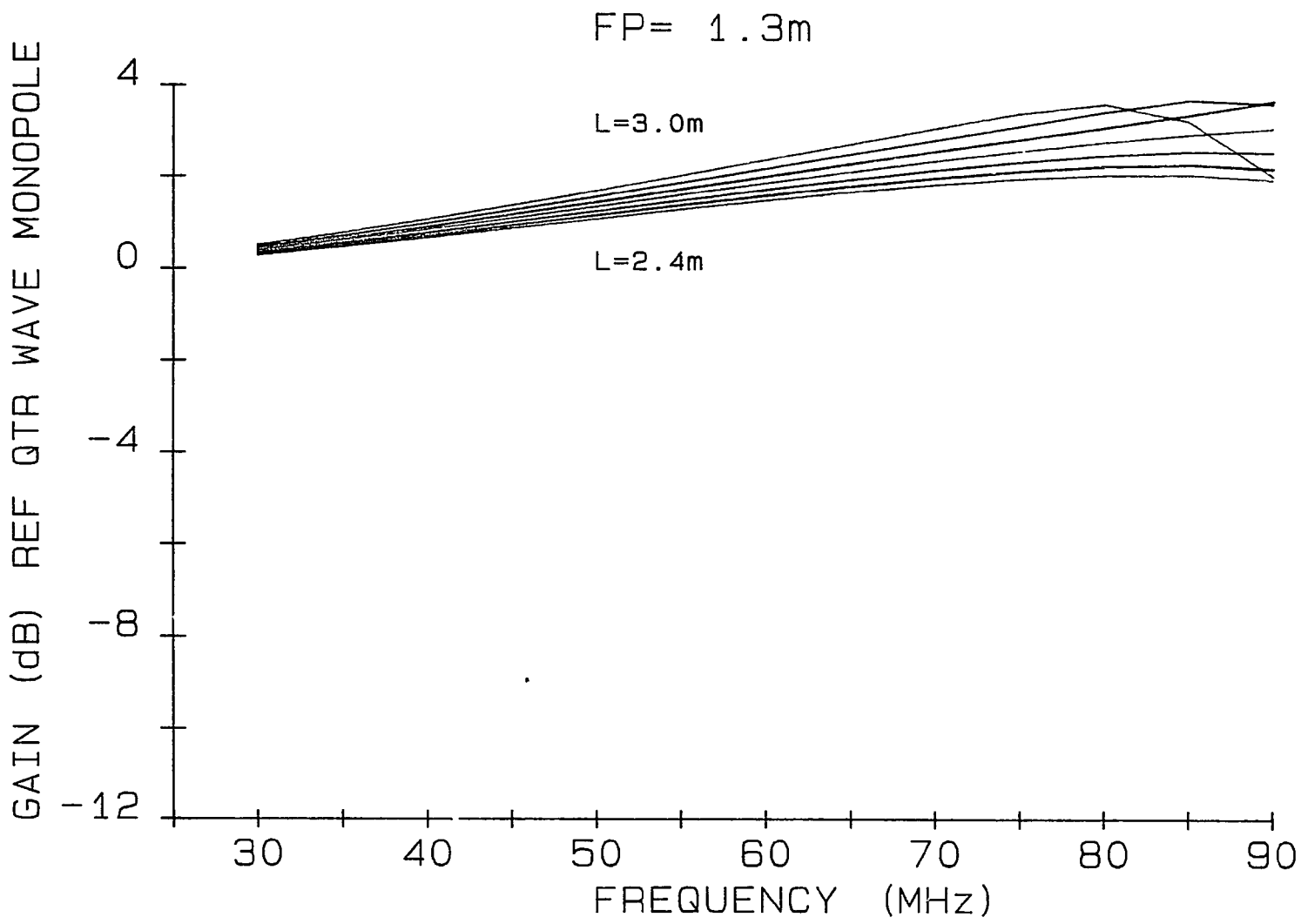

FIGURE C.13 GAIN (FEEDPOINT = 1.3 METERS)

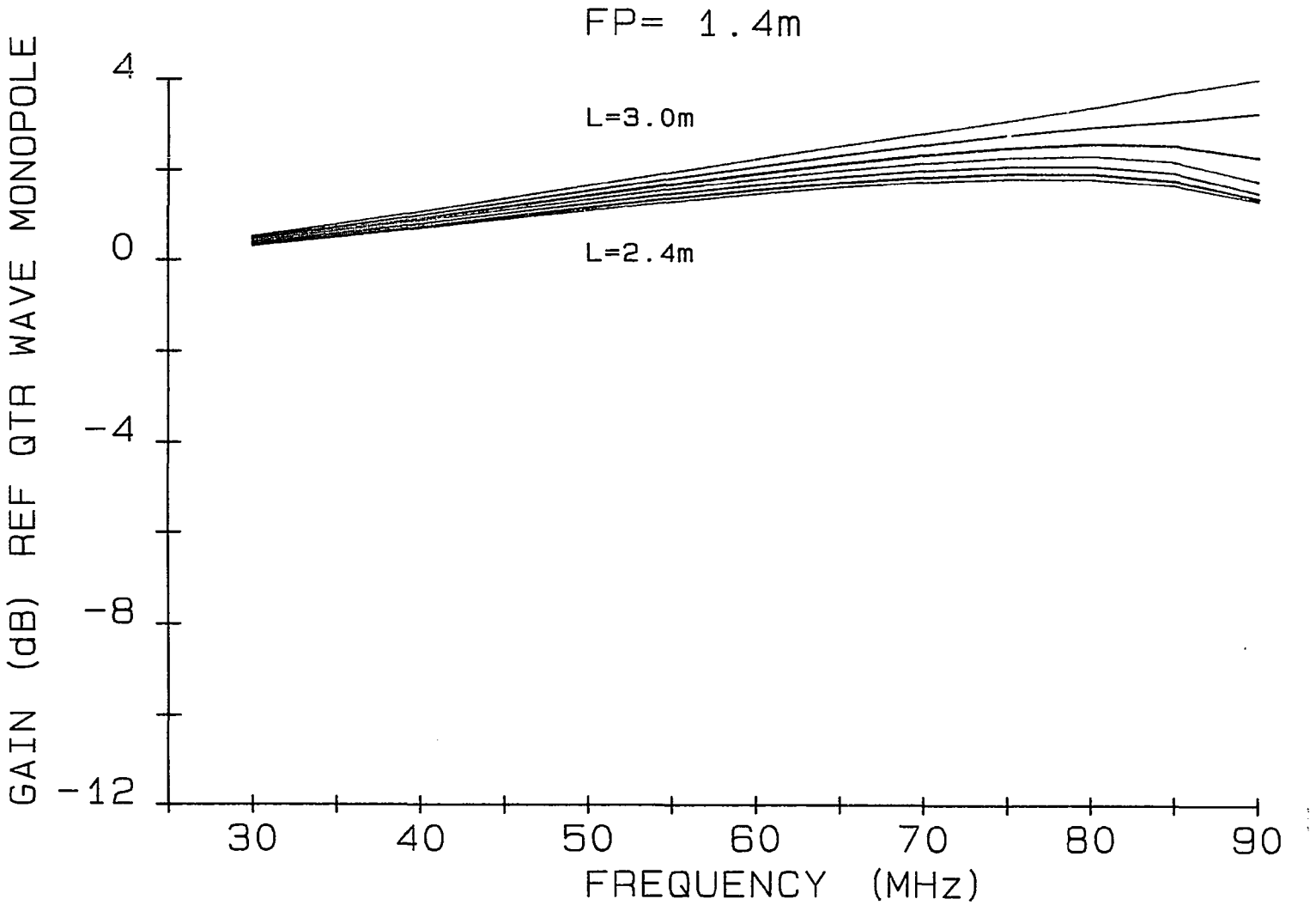

FIGURE C.14 GAIN (FEEDPOINT = 1.4 METERS)

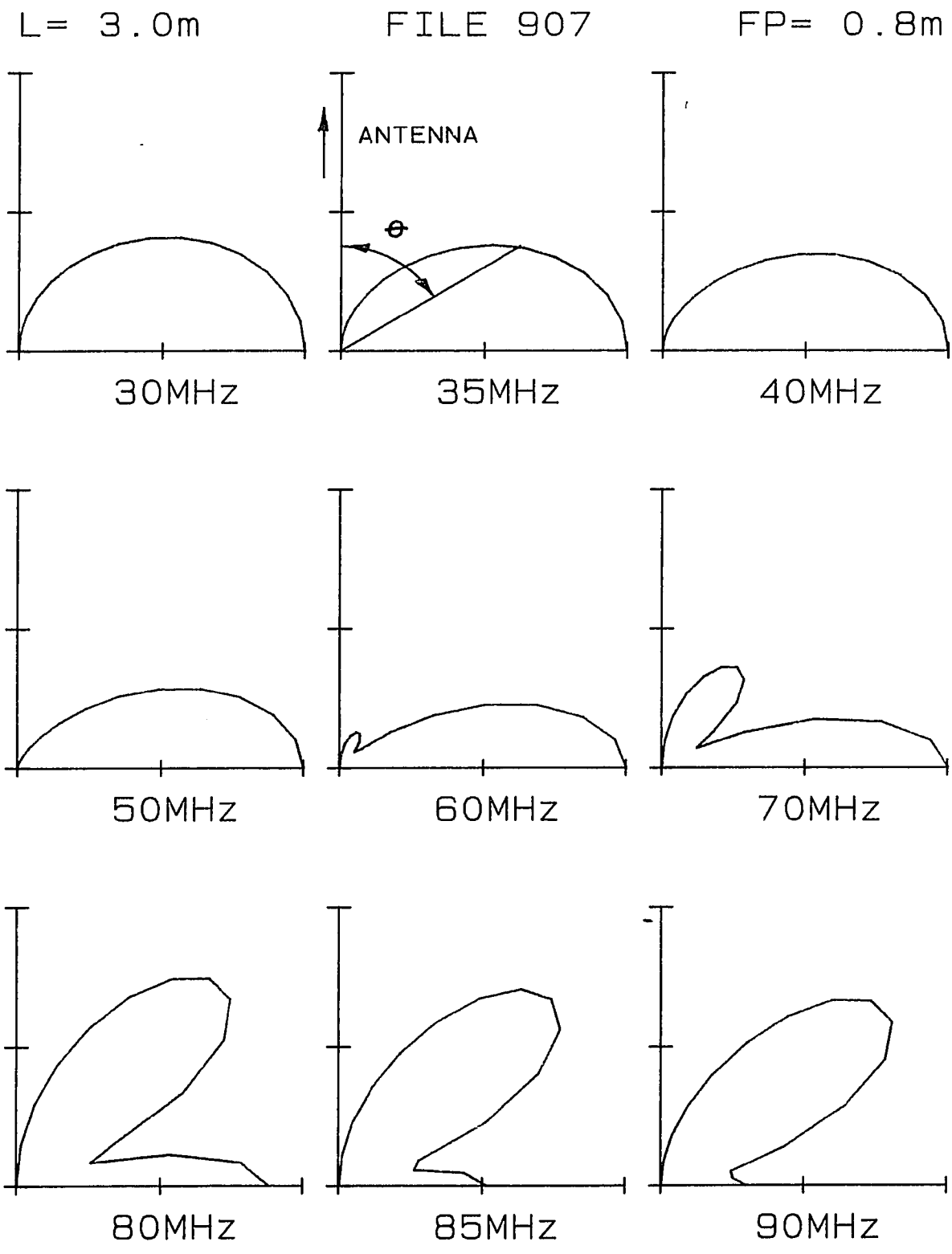

FIGURE C.15 FILE 907 NORMALIZED FIELD PATTERNS

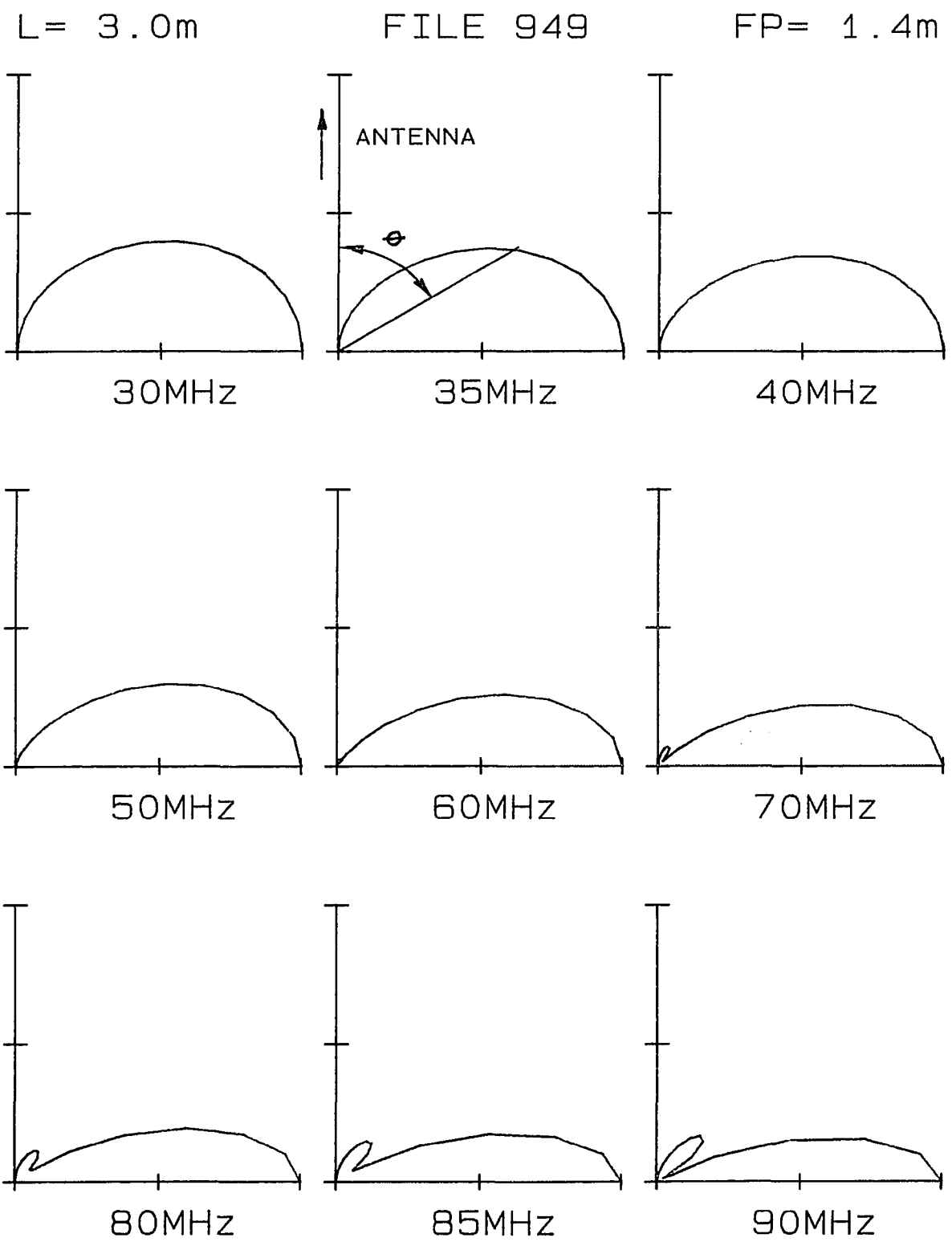

FIGURE C.16 FILE 949 NORMALIZED FIELD PATTERNS

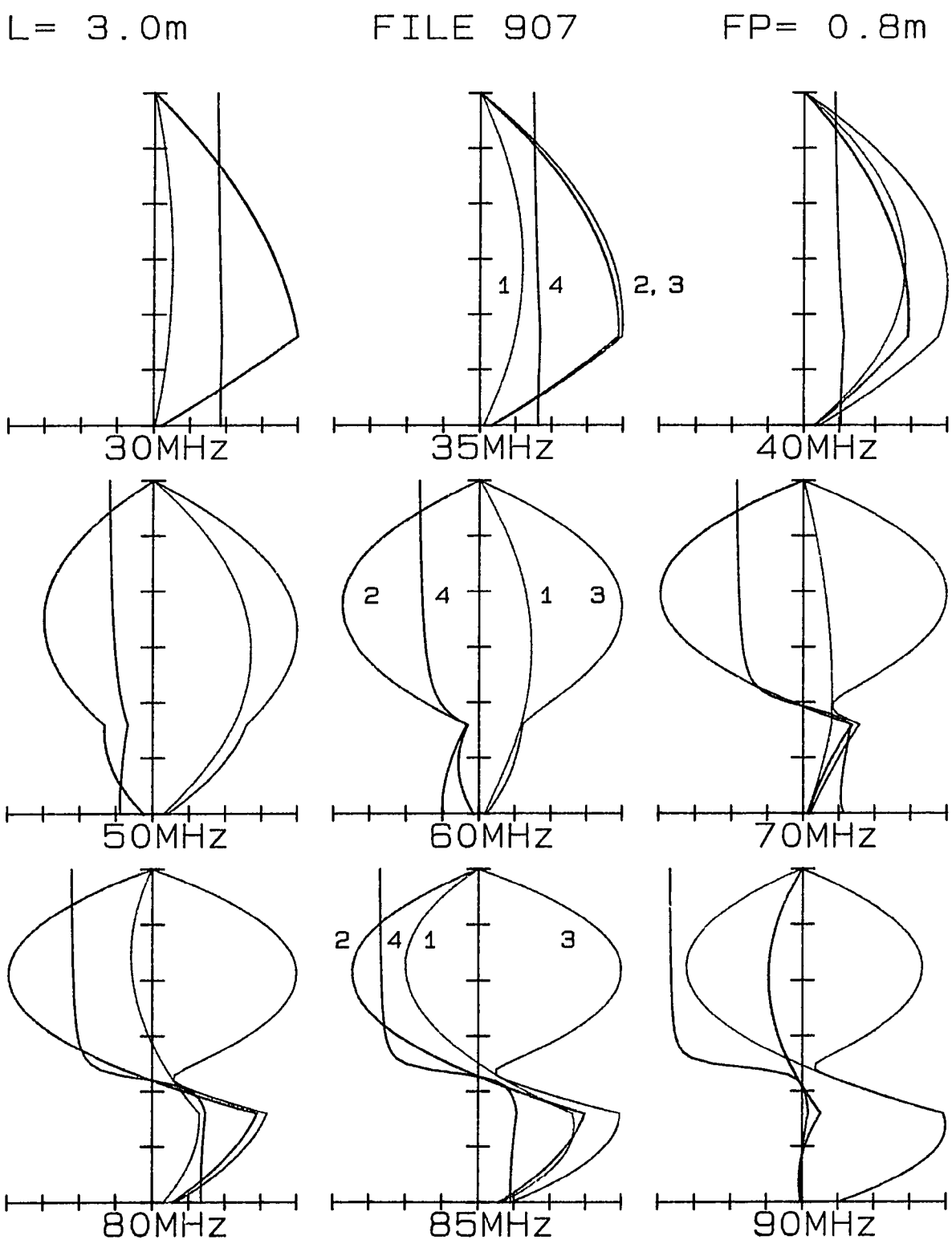

FIGURE C.17 FILE 907 NORMALIZED CURRENT DISTRIBUTIONS

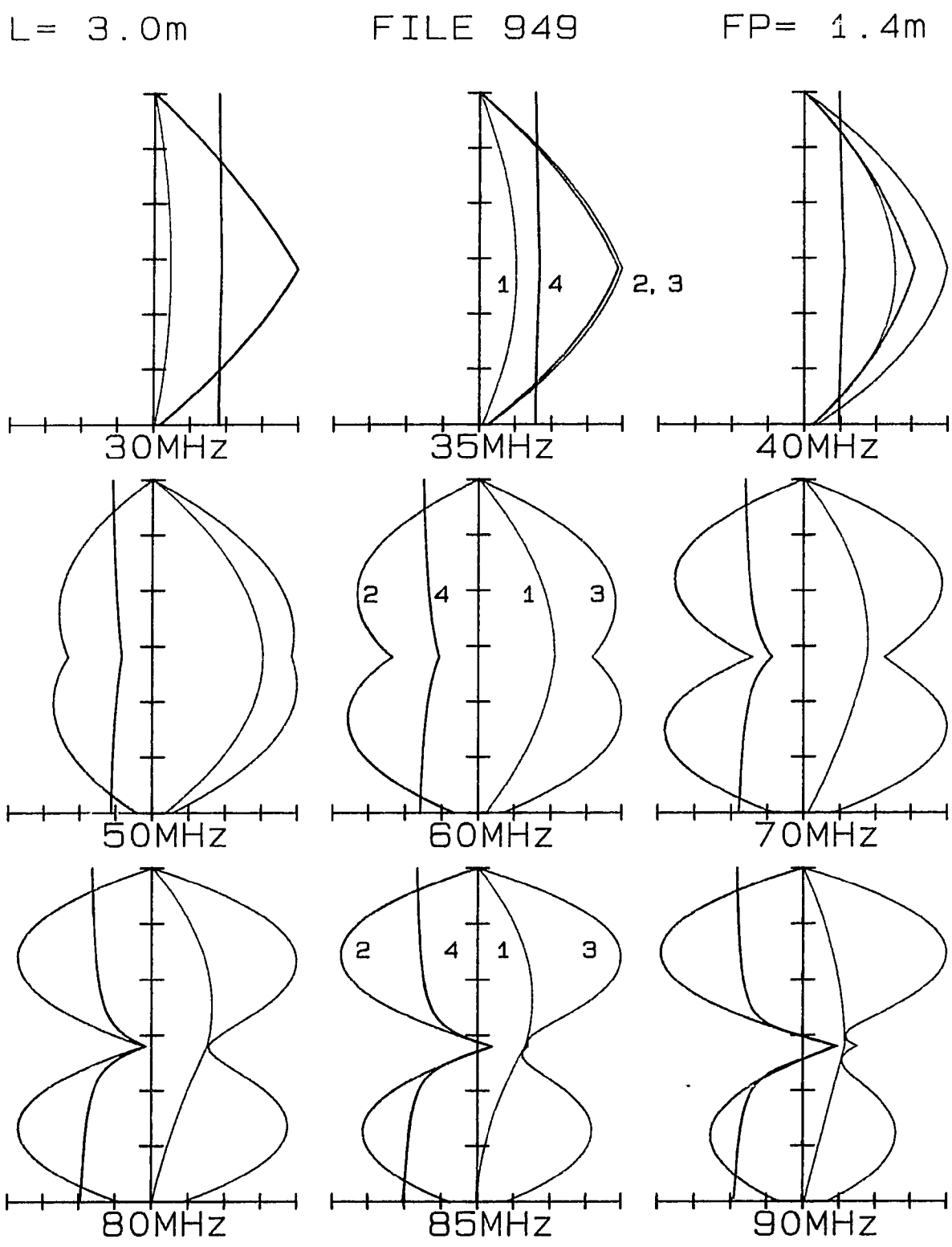

FIGURE C.18 FILE 949 NORMALIZED CURRENT DISTRIBUTIONS

APPENDIX D

MATCHING

D.1 Introduction

This appendix will develop a rationale and a method to determine the best possible tolerance of match for a given band pass load. The matching problem is a very difficult multi-variable non-linear problem not solvable by ordinary analytic methods. The procedure presented here makes use of an optimal design computer program [38]. The program is used to determine the best possible tolerance of match for a given number of variables.

D.2 Network Function

The equalizer network to be determined can be represented as shown in Figure D.1. The resistance of the generator is arbitrary since it can be changed with an ideal transformer or a Darlington transformation. It is sufficient to determine the tolerance of match at the load equalizer interface with the load as the reference. The complex reflection coefficient can be expressed as

$$\rho = (Z_e - Z_1^*)/(Z_e - Z_1) \quad . \tag{D.1}$$

The power gain at this interface can be expressed as

$$G(\omega^2) = 1 - |\rho|^2 \quad . \tag{D.2}$$

Substituting equation (D.1) into (D.2) results in the following relationship

$$G(\omega^2) = \frac{4R_1(\omega)R_e(\omega)}{|Z_1(\omega)+Z_e(\omega)|^2} \quad . \tag{D.3}$$

It is desired to maximize equation (D.1) for each frequency in the passband. $R_1(\omega)$ and $X_1(\omega)$ are the known frequency load data. $R_e(\omega)$ and $Z_e(\omega)$ are the equalizer real and imaginary impedances to be determined.

The network function of the equalizer as viewed from the load can be expressed as a ratio of two polynomials

$$Z_e(s) = \frac{p(s)}{q(s)} \quad . \tag{D.4}$$

In this expression, the order of the polynomial p(s) is equal to, one more, or one less than the order of polynomial q(s) because $Z_e(s)$ must be a driving point impedance. An s-plane plot of equation (D.4) with $p(s)= Ks(s^2 + 2As + A^2+ B^2)$ and $q(s)= s^2 + 2Cs + C^2 + D^2$ is shown in Figure D.1. In this figure, all poles (s_{pi}) and zeros (s_{oi}) must be either on or to the left of the frequency axis in order to have a physically realizable network. The magnitude and phase of the network can be expressed in the following manner.

$$|Z_e(s)| = \prod_{i=1}^{N} \frac{|s-s_{oi}|}{|s-s_{pi}|} \tag{D.5}$$

$$Arg(Z_e(s)) = \sum_{i=1}^{N} arg(s-s_{oi}) - arg(s-s_{pi}) \quad . \tag{D.6}$$

Looking at Figure D.1 and equations (D.5) and (D.6), it is reasonable to expect the network function to have the greatest variations when the frequencies of the poles and zeros are closest to the observation

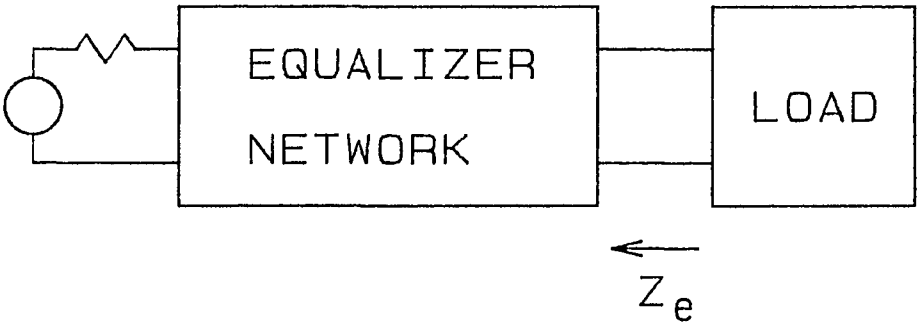

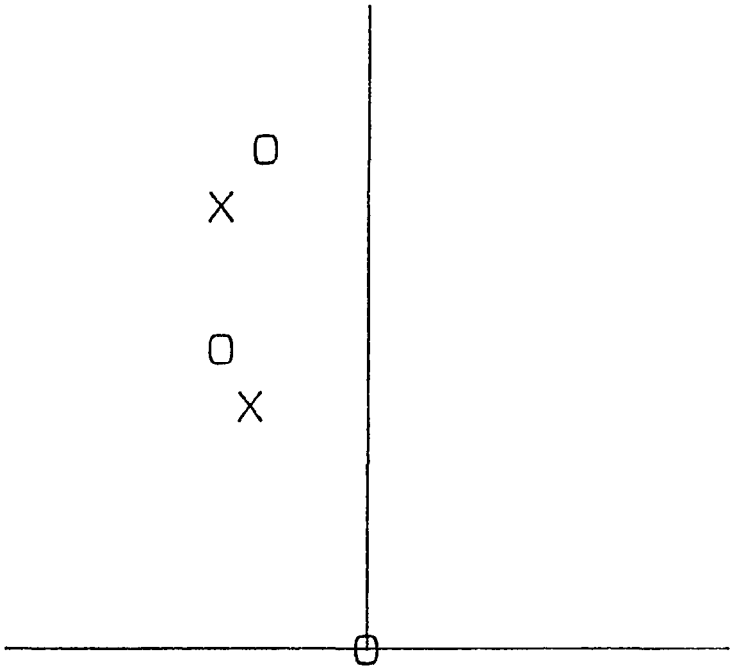

$$p(s) = Ks(s^2 + 2As + A^2 + B^2)$$
$$q(s) = s^2 + 2Cs + C^2 + D^2$$

FIGURE D.1 EQUALIZER NETWORK AND S-PLANE PLOT

frequency. Therefore, for the band pass equalizer, the poles and zeros should be in or near the pass band frequencies. This, then will limit the range of interesting frequencies for the poles and zeros.

The real part of the network function for a passive network is non-negative [6]. This requirement would be time consuming to check even for a computer. However, for a limited number of poles and zeros this can be done easily. Determine the real part of the network function. Find the derivative with respect to frequency and set this equation equal to zero. The roots of this equation are the extrema values. If the real part of the network function is non-negative at theses frequencies, it is non-negative everywhere.

D.3 Procedure

A method for determining the best possible tolerance of match for a given load function and network complexity can now be described. Assume a network function is given by

$$Z_e(s) = \frac{Ks(s^2 + 2As + A^2 + B^2)}{s^2 + 2Cs + C^2 + D^2} \quad . \tag{D.7}$$

In equation (D.7), $-A$ and $\pm B$ are the real and imaginary coordinates of the complex zeroes; $-C$ and $\pm D$ are the real and imaginary coordinates of the complex poles. Equation (D.7) can be rewritten as follows.

$$Z_e(j\omega) = \frac{K(-j\omega^3 - 2A\omega^2 + jA^2\omega + jB^2\omega)}{-\omega^2 + 2Cj\omega + C^2 + D^2} = \frac{N}{D} \tag{D.8}$$

N is the numerator and D is the denominator of equation (D.8). The real part of this function must be non-negative for all frequencies. It is sufficient to show that the numerator of the real part of equation

equation (D.8) is non-negative for all frequencies. The numerator of the real part of equation (D.8) can be expressed in the following manner

$$\text{Num}[\text{Re}(Z_e(j\omega))] = \text{Re}[ND^*] = (-2A\omega^2)(-\omega^2 + C^2 + D^2) \tag{D.9}$$

$$- (-j\omega^3 + jA^2\omega + jB^2\omega)(2Cj\omega)$$

$$\text{Re}[ND^*] = 2A\omega^4 - 2AC^2\omega^2 - 2AD^2\omega^2 - 2C\omega^4 + 2A^2\omega^2 + 2CB^2\omega^2 \tag{D.10}$$

Equation (D.10) is now required to be non-negative at all frequencies. It is sufficient to check this only at the extrema values. The derivative of equation (D.10) is set equal to zero,i.e.,

$$8A\omega^3 - 4AC^2\omega - 4AD^2\omega - 8C\omega^3 + 4CA^2\omega + 4CB^2\omega = 0 \tag{D.11}$$

Equation (D.11) is solved for frequency squared,

$$\omega^2 = \frac{AC^2 + AD^2 - CA^2 - CB^2}{2(A - C)} \tag{D.12}$$

Equation (D.10) is then required to be non-negative at only the frequencies of equation (D.12).

A computer optimization process is then conducted using COD [38] to maximize equation (D.3) using the independent variables of equation (D.5) (A,B,C,D,K) subject to the restrictions of equations (D.10) and (D.12). The result is then the best possible tolerance of match for the network function assumed. For a given network complexity there are a limited number of network functions possible to characterize a passive linear network.

Network synthesis of this characteristic function will in the most general case result in two transformers per pole. For even a two pole network, this becomes impractical to build. Nevertheless, a design

guideline has been established.

Using the impedance versus frequency characteristics of a base isolated antenna 2.5 meters in length with a feedpoint height of 1.0 meter as a load, several optimization processes were conducted. The network function of equation (D.7) was modified so as to contain no transformers. The best power gain of equation (D.3) was determined for increasing numbers of poles. A similar analysis was conducted conducted using only one transformer. This data is plotted in Figure D.2. This plot shows that the power gain increases for increasing numbers of poles. The restriction on the network to contain no transformers reduces the power gain considerably. With one transformer and two poles, the power gain of the network is very close to the best possible obtainable with no restrictions (that is, 2 poles, 4 transformers). The final matching network discussed in Chapter 4 is exactly of this type.

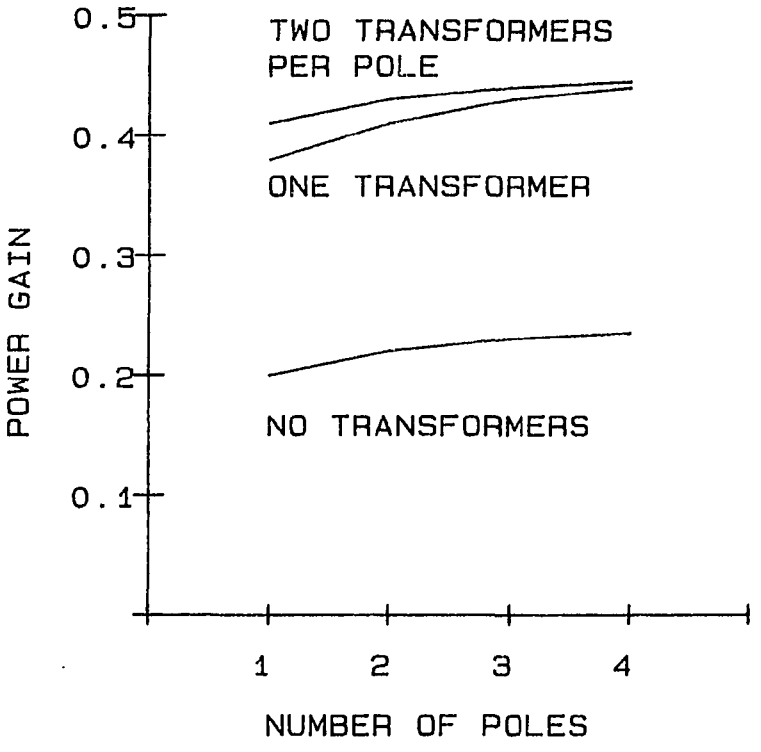

FIGURE D.2 POWER GAIN VERSUS NUMBER OF POLES

REFERENCES

1. TM 11-5985-230-12P, "Antenna Base AB-15", Headquarters Department of the Army.

2. Richard Weissenberger, "Production Validation Test-Government", US Army Electronic Proving Ground, Fort Huchuca, Arizona.

3. TM 11-5985-262-15, "Antenna AS-1729/VRC", Headquarters Department of the Army, Mar 1969.

4. D. S. Paunovic and B. D. Popovic, "Broadband RC-Loaded Microwave Cylindrical Antenna with approximately Real Input Admittance", The Radio and Electronic Engineer, Vol. 47, No. 5, May 1977, pp 225-228.

5. B. D. Popovic, "Theory of Cylindrical Antennas with Arbitrary Impedance Loading", Proceedings of the IEE, Vol. 118, No. 10, October 1971, pp 1327-1332.

6. B. D. Popovic, "Theory of Cylindrical Antennas with Lumped Impedance Loading", The Radio and Electronic Engineer, Vol. 43, No. 4, April 1973, pp 243-248.

7. T. T. Wu and R. W. P. King, "The Cylindrical Antenna with Non-reflecting Resistive Loading", IEEE Transactions On Antennas and Propagation, Vol. AP-13, No. 3, May 1965, pp 369-373.

8. B. L. J. Rao, J. E. Ferris, and W. E. Zimmerman, "Broadband Characteristics of Cylindrical Antennas with Exponentially Tapered Capacitive Loading", IEEE Transactions on Antennas and Propagation, Vol. AP-17, No. 2, March 1969, pp 145-151.

9. B. D. Popovic, M. B. Dragovic, and A. R. Djordjevic, "Optimal Broadband Cylindrical Antenna with One and Two Lumped Capacitive Loadings", Electronics Letters, 6 March 1975, Vol. 11, No. 5, pp 99-100.

10. R. F. Baum, "A Contribution to the Approximation Problem", Proceedings of the IRE, Vol. 36, No. 7, July 1948, pp 863-869.

11. R. G. Brown, R. A. Sharpe, W. L. Hughes, and R. E. Post, LINES, WAVES, AND ANTENNAS, New York, The Ronald Press Co., 1973.

12. H. J. Carlin, "A New Approach to Gain-Bandwidth Problems", IEEE Transactions on Circuits and Systems, Vol. CAS-24, No. 4, April 1977, pp 170-175.

13. Wai-Kai Chen, "Explicit Formulas for the Synthesis of Optimum Broad-Band Impedance - Matching Networks", IEEE Transactions on Circuits and Systems, Vol. CAS-24, No. 4, April 1977, pp 157-169.

14. R. M. Fano, "Theoretical Limitations on the Broadband Matching of Arbitrary Impedances", Journal of the Franklin Institute, Vol. 249, No. 1, January 1950.

15. E. A. Guillemin, SYNTHESIS OF PASSIVE NETWORKS, New York, John Wiley and Sons, Inc., 1957.

16. E. Hallen, ELECTROMAGNETIC THEORY, New York, John Wiley and Sons, Inc., 1962.

17. R. F. Harrington, TIME-HARMONIC ELECTROMAGNETIC FIELDS, New York, McGraw-Hill Book Co., Inc., 1961.

18. C. W. Harrison, "Monopole with Inductive Loading", IEEE Transactions on Antennas and Propagation", Vol AP-11, No. 4, July 1963, pp 394-400.

19. W. H. Hoyt, ENGINEERING ELECTROMAGNETICS, New York, McGraw-Hill Book Co., Inc., 1958.

20. E. C. Jordan, ELECTROMAGNETIC WAVES AND RADIATING SYSTEMS, Englewood Cliffs, N.J., Prentice-Hall, Inc., 1950.

21. R. W. P. King, ELECTROMAGNETIC ENGINEERING, New York, McGraw-Hill Book Co., Inc., 1945.

22. R. W. P. King and T. T. Wu, "The Cylindrical Antenna with Arbitrary Driving Point", IEE Transactions on Antennas and Propagation, Vol. AP-13, No. 5, September 1965, pp 710-718.

23. R. W. P. King, THE THEORY OF LINEAR ANTENNAS, Cambridge, Mass., Harvard University Press, 1956.

24. J. D. Kraus, ANTENNAS, New York, McGraw-Hill Book Co., Inc., 1950.

25. G. L. Matthae, "Synthesis of Tchebycheff Impedance - Matching Networks, Filters, and Interstages", IRE Transactions on Circuit Theory, Vol. CT-3, No. 3, September 1956, pp 163-172.

26. B. D. Popvic, M. B. Dragovic, and D. S. Paunovic, "Broadband Cylindrical Antenna with Continuous Resistive and Concentrated Capacitive Loadings", Electronic Letters, 11 December 1975, Vol. 11, No.25/26, pp 611-613.

27. S. Ramo and J. R. Whinnery, FIELDS AND WAVES IN MODERN RADIO, New York, John Wiley and Sons, Inc., 1953.

28. S. Ramo, J. R. Whinnery, and T. Van Duzer, FIELDS AND WAVES IN COMMUNICATION ELECTRONICS, New York, John Wiley and Sons, Inc., 1965.

29. H. Ruston and J. Bordogna, ELECTRIC NETWORKS: FUNCTIONS, FILTERS, ANALYSIS, New York, McGraw-Hill Book Co., Inc., 1966.

30. S. A. Schelkunoff and H. T. Friis, ANTENNAS THEORY AND PRACTICE, New York, John Wiley and Sons, Inc., 1952.

31. L. C. Shen, T. T. Wu and R. W. P. King, "A Simple Formula of Current in Dipole Antennas", IEEE Transactions on Antennas and Propagation, Vol. AP-16, No. 5, September 1968, pp 542-547.

32. J. E. Storer, PASSIVE NETWORK SYNTHESIS, New York, McGraw-Hill Co., Inc., 1957.

33. T. T. Wu and R. W. P. King, "Driving Point and Input Admittance of Linear Antenna" Journal of Applied Physics, Vol. 30, No. 1, January 1959, pp 74-76.

34. D. C. Youla, "A New Theory of Broad-band Matching", IEEE Transactions On Circuit Theory, Vol. CT-11, No. 1, March 1964, pp 30-50.

35. D. C. Youla, "A Tutorial Exposition of some Key Network - Theoretic Idea Underlying Classical Insertion - Loss Filter Design", Proceedings of the IEEE Vol. 59, No. 5, May 1971, pp 760-799.

36. "Reference Data for Engineers", Sixth Edition, Howard W. Sams and Co., Inc., pp11-4,11-6.

37. M. E. VanValkenburg, NETWORK ANALYSIS, Prentice Hall, Inc., 1955.

38. B. Cave, "Constrained Optimal Design", Optimal Systems Research, Inc.